

UNCLASSIFIED

AD NUMBER

AD919595

LIMITATION CHANGES

TO:

Approved for public release; distribution is unlimited.

FROM:

Distribution authorized to U.S. Gov't. agencies only; Test and Evaluation; MAY 1974. Other requests shall be referred to Air Force Armament Lab., Eglin AFB, FL 32542.

AUTHORITY

AFATL ltr 20 Sep 1976

THIS PAGE IS UNCLASSIFIED

cy. 2



**SEPARATION AND CARRIAGE LOADS CHARACTERISTICS OF
THREE GUIDED BOMBS FROM THE A-7D AIRCRAFT AT
MACH NUMBERS FROM 0.70 TO 1.05**

E. G. Allee, Jr. and M. R. Cunningham
ARO, Inc.

PROPULSION WIND TUNNEL FACILITY
ARNOLD ENGINEERING DEVELOPMENT CENTER
AIR FORCE SYSTEMS COMMAND
ARNOLD AIR FORCE STATION, TENNESSEE 37389

May 1974

Final Report for Period December 19-26, 1973

This document has been approved for public release

its distribution is unlimited per AFATL Mr. 20 Sep 1976

~~Distribution limited to U.S. Government agencies only; this report contains information on test and evaluation of military hardware; May 1974; other requests for this document must be referred to Air Force Armament Laboratory (DLJA), Eglin AFB, FL 32542.~~

Property of U. S. Air Force
AEDC LIBRARY
F40600-74-C-0001

Prepared for

AIR FORCE ARMAMENT LABORATORY (DLJA)
EGLIN AFB, FL 32542

NOTICES

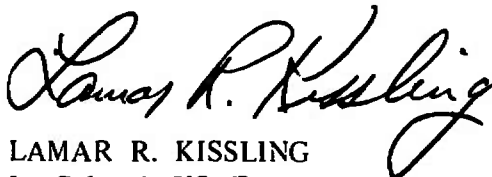
When U. S. Government drawings specifications, or other data are used for any purpose other than a definitely related Government procurement operation, the Government thereby incurs no responsibility nor any obligation whatsoever, and the fact that the Government may have formulated, furnished, or in any way supplied the said drawings, specifications, or other data, is not to be regarded by implication or otherwise, or in any manner licensing the holder or any other person or corporation, or conveying any rights or permission to manufacture, use, or sell any patented invention that may in any way be related thereto.

Qualified users may obtain copies of this report from the Defense Documentation Center.

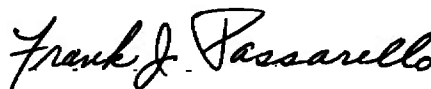
References to named commercial products in this report are not to be considered in any sense as an endorsement of the product by the United States Air Force or the Government.

APPROVAL STATEMENT

This technical report has been reviewed and is approved.



LAMAR R. KISSLING
Lt Colonel, USAF
Chief Air Force Test Director, PWT
Directorate of Test



FRANK J. PASSARELLO
Colonel, USAF
Director of Test

UNCLASSIFIED

SECURITY CLASSIFICATION OF THIS PAGE (When Data Entered)

REPORT DOCUMENTATION PAGE		READ INSTRUCTIONS BEFORE COMPLETING FORM
1. REPORT NUMBER AEDC-TR-74-45 AFATL-TR-74-81	2. GOVT ACCESSION NO.	3. RECIPIENT'S CATALOG NUMBER
4. TITLE (and Subtitle) SEPARATION AND CARRIAGE LOADS CHARACTER- ISTICS OF THREE GUIDED BOMBS FROM THE A-7D AIRCRAFT AT MACH NUMBERS FROM 0.70 TO 1.05		5. TYPE OF REPORT & PERIOD COVERED Final Report, Dec. 19 - 26, 1973
		6. PERFORMING ORG. REPORT NUMBER
7. AUTHOR(s) E. G. Allee, Jr. and M. R. Cunningham, ARO, Inc.		8. CONTRACT OR GRANT NUMBER(s)
9. PERFORMING ORGANIZATION NAME AND ADDRESS Arnold Engineering Development Center Arnold Air Force Station, TN 37389		10. PROGRAM ELEMENT, PROJECT, TASK AREA & WORK UNIT NUMBERS Program Element 27241F Project No. 3169
11. CONTROLLING OFFICE NAME AND ADDRESS Air Force Armament Laboratory (DLJA) Eglin AFB, FL 32542		12. REPORT DATE May 1974
		13. NUMBER OF PAGES 80
14. MONITORING AGENCY NAME & ADDRESS (if different from Controlling Office)		15. SECURITY CLASS. (of this report) UNCLASSIFIED
		15a. DECLASSIFICATION/DOWNGRADING SCHEDULE N/A
16. DISTRIBUTION STATEMENT (of this Report) Distribution limited to U.S. Government agencies only; this report contains information on test and evaluation of military hardware; May 1974; other requests for this document must be referred to Air Force Armament Laboratory (DLJA), Eglin AFB, FL 32542.		
17. DISTRIBUTION STATEMENT (of the abstract entered in Block 20, if different from Report)		
18. SUPPLEMENTARY NOTES Available in DDC.		
19. KEY WORDS (Continue on reverse side if necessary and identify by block number) A-7D aircraft trajectories carriage loads external stores MK-82LGB separation MK-84LGB MK-84EOGB		
20. ABSTRACT (Continue on reverse side if necessary and identify by block number) Wind tunnel tests were conducted in the Aerodynamic Wind Tunnel (4T) to investigate the separation characteristics of the Improved MK-82LGB and MK-84LGB from the wing pylons and racks of the A-7D aircraft. Carriage loads data were also acquired on the MK-82LGB and the MK-84EOGB. Trajectory data were obtained at Mach numbers from 0.78 to 0.95 at a simulated altitude of 7000 ft. Simulated dive angles were 0 and 70 deg during this phase of the test. With		

UNCLASSIFIED

SECURITY CLASSIFICATION OF THIS PAGE(When Data Entered)

20, Continued

one exception, all stores separated without store-to-aircraft contact. Store-to-store contact occurred when the MK-82LGB was launched from a fully loaded TER. Carriage loads data were taken over a Mach number range from 0.70 to 1.05 at angles of attack from -2 to 12 deg and yaw angles from -2 to 2 deg.

AFSC
Arnold AFB Tex

UNCLASSIFIED

SECURITY CLASSIFICATION OF THIS PAGE(When Data Entered)

PREFACE

The work reported herein was done by the Arnold Engineering Development Center (AEDC) for the Air Force Armament Laboratory (AFATL/DLJA), Air Force Systems Command (AFSC), under Program Element 27241F, Project 3169. AFATL Project Monitor was Mr. Bob Arnold. The test results presented were obtained by ARO, Inc. (a subsidiary of Sverdrup & Parcel and Associates, Inc.), contract operator of AEDC, AFSC, Arnold Air Force Station, Tennessee. The test was conducted under ARO Project No. PA447 and the manuscript (ARO Control No. ARO-PWT-TR-74-25) was submitted for publication on March 6, 1974.

CONTENTS

	<u>Page</u>
1.0 INTRODUCTION	5
2.0 APPARATUS	
2.1 Test Facility	5
2.2 Test Articles	6
2.3 Instrumentation	7
3.0 TEST DESCRIPTION	
3.1 Test Conditions	7
3.2 Data Acquisition	7
3.3 Corrections	9
3.4 Precision of Data	9
4.0 RESULTS AND DISCUSSION	
4.1 Trajectory Data	10
4.2 Carriage Loads Data	11

ILLUSTRATIONS

Figure

1. Isometric Drawing of a Typical Store Separation Installation and a Block Diagram of the Computer Control Loop	13
2. Schematic of the Tunnel Test Section Showing Model Location	14
3. Sketch of A-7D Aircraft Model	15
4. Details and Dimensions of the A-7D Wing Pylon Models	16
5. Details and Dimensions of the TER Models	17
6. Details and Dimensions of the MER Models	18
7. Details and Dimensions of the MK-84EOGB	19
8. Dimensional Sketch of the MK-84LGB	20
9. Dimensional Sketch of the MK-82LGB	21
10. Model Photographs	22
11. Identification of TER and MER Store Stations and Orientations	26
12. Test Configuration Identification	27
13. Typical Installation Photographs	29
14. Sketch Illustrating a Store Approaching the Touch Wire at the Carriage Position (Model Inverted)	31
15. Trajectories for the MK-84LGB, Configurations 2 and 3	32

<u>Figure</u>	<u>Page</u>
16. Trajectories for the MK-82LGB, Configuration 4	35
17. Trajectories for the MK-82LGB, Configuration 5	37
18. Trajectories for the MK-82LGB, Configuration 6	40
19. Trajectories for the MK-82LGB, Configuration 7	43
20. Trajectories for the MK-82LGB, Configuration 8	46
21. Trajectories for the MK-82LGB, Configuration 9	50
22. MK-82LGB Launched with Partially Deployed Fins, Configurations 4L and 5R	53
23. MK-82LGB Launched with Fixed Canards, Configuration 6R	55
24. Carriage Loads Data for the MK-84EOGB, Configuration 1L	58
25. Carriage Loads Data for the MK-82LGB, Configuration 10	59
26. Carriage Loads Data for the MK-82LGB, Configuration 11	61
27. Carriage Loads Data for the MK-82LGB, Configuration 12	63

TABLES

1. Full-Scale Store Parameters Used in the Trajectory Calculations	73
2. Axial-Force Coefficient Values for the MK-82LGB Trajectories	74
3. Full-Scale Position and Coefficient Uncertainties	74
4. Repeatability of Loads Data for Configuration 11L	75
 NOMENCLATURE	 76

1.0 INTRODUCTION

In an effort to increase the number of stores that can be carried, the MK-82LGB and MK-84LGB (laser-guided bombs) were fitted with fins which could retract into cuffs. Captive trajectory and carriage loads tests were run on the 0.05-scale models of these stores to ascertain the effect of these changes on the carriage loads and store separation characteristics. The test was conducted in the Aerodynamic Wind Tunnel (4T) of the Propulsion Wind Tunnel Facility (PWT).

The test program consisted of two parts, (1) captive trajectory testing and (2) store airloads. The flight conditions that were simulated for the trajectory portion of the test included Mach numbers from 0.78 to 0.95, a simulated altitude of 7000 ft, and parent aircraft angles of attack from 2.0 to 3.4 deg. For the carriage loads portion of the test, the simulated flight conditions were Mach numbers of 0.70, 0.90, and 1.05, a parent-aircraft angle-of-attack range from -2 to 12 deg, and parent-aircraft yaw angles from -2 to 2 deg. Carriage loads data were also obtained for one configuration of the MK-84EOGB. For these data parent-aircraft angle of attack was varied from 0 to 6 deg at Mach numbers from 0.70 to 0.95.

2.0 APPARATUS

2.1 TEST FACILITY

Tunnel 4T is a closed-loop, continuous flow, variable density tunnel in which the Mach number can be varied from 0.1 to 1.3. At all Mach numbers, the stagnation pressure can be varied from 300 to 3700 psfa. The test section is 4 ft square and 12.5 ft long with perforated, variable porosity (0.5- to 10-percent open) walls. It is completely enclosed in a plenum chamber from which the air can be evacuated, allowing part of the tunnel airflow to be removed through the perforated walls of the test section.

For store separation testing, two separate and independent support systems are used to support the models. The parent aircraft model is inverted in the test section and supported by an offset sting attached to the main pitch sector. The store model is supported by the captive trajectory support (CTS), which extends down from the tunnel top wall and provides store movement (six degrees of freedom) independent of the parent-aircraft model. An isometric drawing of a typical store separation installation is shown in Fig. 1.

Also shown in Fig. 1 is a block diagram of the computer control loop used during captive trajectory testing. The analog system and the digital computer work as an integrated unit and, utilizing required input information, control the store movement during a trajectory. Store positioning is accomplished by use of six individual d-c electric motors. Maximum translational travel of the CTS is ± 15 in. from the tunnel centerline in the lateral and vertical directions and 36 in. in the axial direction. Maximum angular displacements are ± 45 deg in pitch and yaw and ± 360 deg in roll. A more complete description of the test facility can be found in the Test Facilities Handbook.¹ A schematic showing the test section details and the location of the models in the tunnel is presented in Fig. 2.

2.2 TEST ARTICLES

The test articles used consisted of 0.05-scale models of the stores and the A-7D aircraft (including pylons, racks, and dummy stores). The A-7D aircraft model used is geometrically similar to the full-scale aircraft except for slight modifications necessary for tunnel installation. A sketch giving the basic details and dimensions of the A-7D aircraft model is presented in Fig. 3. Details and dimensions of the wing pylon models are given in Fig. 4. When the pylons are mounted on the parent aircraft, the pylon surfaces for store and rack mounting are inclined nose down 3 deg with respect to the aircraft waterline. Shown in Figs. 5 and 6 are the details and dimensions of the triple ejection rack (TER) and the multiple ejection rack (MER), respectively. The racks were mounted on the wing pylons to match the corresponding 30-in. suspension points (see Figs. 4, 5, and 6). Dimensional sketches of the MK-84EOGB, MK-84LGB, and MK-82LGB are presented in Figs. 7, 8, and 9, respectively. Photographs of these models are presented in Fig. 10.

The launch trajectory and store airloads investigations on the MK-82LGB and the MK-84LGB were conducted using models with the fins in the folded position. Selected trajectories were continued after 0.200 sec with the fins deployed 20 deg on the MK-82LGB and 27.5 deg on the MK-84LGB. Under actual flight conditions, the canards are free to float ± 10 deg until activated by the guidance package at some time after store release. In order to simulate this condition, both the metric and dummy models of the MK-82LGB and MK-84LGB were run with the canards removed. A few runs were made with the canards in place and fixed at zero deflection to ascertain the effect on the trajectories should the canards lock prior to activation by the store guidance.

¹Test Facilities Handbook (Ninth Edition). "Propulsion Wind Tunnel Facility, Vol. 4." Arnold Engineering Development Center, July 1971.

The MER/TER numbering sequence, initial store roll, and aircraft weapons loading configurations are presented in Figs. 11 and 12. Photographs of a typical installation are presented in Fig. 13.

2.3 INSTRUMENTATION

Two internal, strain-gage, balances were used during the test. A 0.4-in.-diam, six-component balance was used for tests with the MK-84EOGB and MK-84LGB stores, and a 0.16-in.-diam, five-component balance was used for tests with the MK-82LGB store. The balances were installed on a 3-in. offset sting which was mounted on the CTS. Translational and angular positions were obtained from the CTS analog outputs. The parent-aircraft angle of attack was set using an absolute angle-of-attack indicator which was located in the A-7D model fuselage. The pylons and racks were instrumented with touch wires to provide a position indication when the store model was in its carriage position. The CTS system was also electrically connected to automatically stop the CTS and main pitch sector movements if the store model or CTS rig contacted the aircraft model, aircraft support sting, or the test section walls.

3.0 TEST DESCRIPTION

3.1 TEST CONDITIONS

Separation trajectory data were obtained at Mach numbers from 0.73 to 0.95. Tunnel dynamic pressure was held constant at 500 psf, and tunnel stagnation temperature was maintained near 100°F.

Tunnel conditions were held constant at the desired Mach number and stagnation pressure while data for each trajectory were obtained. The trajectories were terminated when the store or sting contacted the parent-aircraft model or when a CTS limit was reached.

Carriage loads data were acquired at Mach numbers from 0.70 to 1.05. Tunnel dynamic pressure and stagnation temperature were the same for both portions of the test.

3.2 DATA ACQUISITION

3.2.1 Trajectory Data Acquisition

To obtain a trajectory, test conditions were established in the tunnel and the parent model was positioned at the desired angle of attack. The store model was then oriented

to a position corresponding to the store carriage location. After the store was set at the desired initial position, operational control of the CTS was switched to the digital computer, which controlled the store movement during the trajectory through commands to the CTS analog system (see block diagram, Fig. 1). Data from the wind tunnel, consisting of measured model forces and moments, wind tunnel operating conditions, and CTS rig positions, were input to the digital computer for use in the full-scale trajectory calculations.

The digital computer was programmed to solve the six-degree-of-freedom equations to calculate the angular and linear displacements of the store relative to the parent-aircraft pylon. In general, the program involves using the last two successive measured values of each static aerodynamic coefficient to predict the magnitude of the coefficients over the next time interval of the trajectory. These predicted values are used to calculate the new position and attitude of the store at the end of the time interval. The CTS is then commanded to move the store model to this new position, and the aerodynamic loads are measured. If these new measurements agree with the predicted values, the process is continued over another time interval of the same magnitude. If the measured and predicted values do not agree within the desired precision, the calculation is redone over a time interval one-half the previous value. This process is repeated until a complete trajectory has been obtained.

In applying the wind tunnel data to the calculations of the full-scale store trajectories, the measured forces and moments are reduced to coefficient form and then applied with proper full-scale store dimensions and flight dynamic pressure. Dynamic pressure was calculated using a flight velocity equal to the free-stream velocity component plus the components of store velocity relative to the aircraft, and a density corresponding to the simulated altitude.

The initial portion of each launch trajectory incorporated simulated ejector forces in addition to the measured aerodynamic forces acting on the store. The ejector forces for the stores are presented in Table 1. The ejector force was considered to act perpendicular to the (rack or pylon) mounting surface. The locations of the applied ejector forces and other full-scale store parameters used in the trajectory calculations are also listed in Table 1.

Since the five-component balance used with the MK-82LGB did not have the capability of measuring axial forces, values of the axial-force coefficient as provided by AFATL were input into the data reduction program as constants for each trajectory. These values are listed in Table 2.

3.2.2 Store Airloads Data Acquisition

To obtain the store airloads data, test conditions were established in the tunnel, and the parent aircraft was manually positioned at the desired initial angle of attack. The store model was then automatically moved by the CTS to a position parallel to its carriage position but displaced by a preselected offset distance in Y and/or Z from the touch point (see Fig. 14). The computer then commanded the CTS rig to move the store onto the touch position. Store movement was in increments of 0.30 in. When the store contacted the touch wire, it was commanded to move off of touch in the reverse direction in steps one-half the size of the increment used in approaching the touch position. When the computer no longer sensed the touch signal, it stopped the CTS rig movement and recorded the force and moment data at that position (Fig. 14). The store model was then automatically moved clear of the parent model, and the next data point was initiated by manually moving the parent aircraft to the next selected angle of attack.

3.3 CORRECTIONS

Balance, sting, and support deflections caused by the aerodynamic loads on the store models were accounted for in the data reduction program to calculate the true store model angles and positions. Corrections were also made for model weight tares to calculate the net aerodynamic forces on the store model.

3.4 PRECISION OF DATA

The trajectory data are subject to error from several sources including tunnel conditions, balance measurements, extrapolation tolerances allowed in predicting coefficients, computer inputs, and CTS positioning control. The maximum error in the CTS position control was ± 0.05 in. for the translational settings, ± 0.15 deg for the angular displacement settings in pitch and yaw, and ± 1.0 deg in roll. Extrapolation tolerances were ± 0.10 for each of the aerodynamic coefficients. Based on a 95-percent confidence level, the maximum uncertainties in the full-scale position data caused by the balance precision limitations are presented in Table 3. The estimated uncertainty in setting Mach number was no greater than ± 0.003 , and the uncertainty in parent-model angle of attack was estimated to be no greater than ± 0.1 deg.

The uncertainties in aerodynamic coefficients for the carriage loads data were calculated assuming negligible bias and a 95-percent confidence level. Typical results are also presented in Table 3.

4.0 RESULTS AND DISCUSSION

4.1 TRAJECTORY DATA

Captive trajectory data were obtained on the improved versions of both the MK-82LGB and MK-84LGB. Trajectory data are presented in Figs. 15 through 23 as functions of full-scale trajectory time with both angular and linear displacements given relative to the pylon axis system. Positive X, Y, and Z displacements as seen by the pilot are forward, to the right, and down, respectively. Positive changes in θ , ψ , and ϕ (from the same vantage point) are nose up, nose right, and clockwise, respectively. Trajectories were terminated when a CTS travel limit was reached, when the store or CTS rig contacted some part of the parent aircraft or its support structure, or when it was determined that the trajectory had continued a sufficient time for the store to clear the aircraft and/or for the fins to deploy to their partially open state. Store positions and velocities at a time of 0.20 sec after release were used as the initial conditions for trajectory continuations with the fins partially deployed. These trajectories were continued until the store was clear of the parent aircraft. Flagged symbols are used to indicate those portions of the trajectories which were acquired with deployed fins. Configuration numbers correspond to those shown in Fig. 12 with the suffix R or L being used to indicate separations from the right or left wing. Ejector forces depended on the store launched and on whether that store was ejected from a pylon or a MER or TER (see Table 1).

Trajectories obtained with the MK-84LGB are presented in Fig. 15. In general, the separations were well behaved with no contact between the store and the parent aircraft. The initial pitching and yawing motions of the store were damped by the deployment of the fins. With the exception of Configuration 2L (Fig. 15a), fin deployment had little effect on the rolling motion of the store. For that configuration at $M_\infty = 0.78$, the roll rate increased after the fins were deployed.

The MK-82LGB trajectory data are presented in Figs. 16 through 23. Again the initial pitching and yawing motions of the store were damped by deployment of the fins. The effect of fin deployment on store roll was small, with some evidence of an increase in roll rate on certain configurations (see Figs. 18b and 20c). Analysis of the ejector force moment induced on the store would indicate that the ejectors of the MER/TER would induce an initial positive moment whereas the pylon ejectors create an initial negative pitching moment. Launches from the MER did exhibit an initial positive pitching motion (see Figs. 20 and 21); however, launches from both the pylon and the TER had an initial negative pitching motion (see Figs. 16 through 19). The magnitude of this motion varied

with Mach number and configuration. In general, the initial store motion in the pitch and yaw planes seemed to be less when the store was launched from the MER than from the TER. There also seemed to be a greater tendency for these motions to damp out without fin deployment when the store was launched from a MER position. These data indicate that there is a much stronger aerodynamic flow pattern about the TER than about the MER.

The only contact between the store and the parent aircraft occurred for Configuration 7L (Figs. 19a and b). For this configuration, the initial yawing and pitching moments of the store resulted in contact between the fins of the launched store and the fins of the store mounted on the inboard TER station (Station 3) at all Mach numbers and at both dive angles at which data were acquired.

Certain configurations were run at dive angles of both 0 and 70 deg. These data are presented together by configuration number with the dive angle indicated at the top of the figure. In general, the differences in trajectories between the two dive angles were small. Limited data were acquired with the MK-82LGB launched off of a pylon with the fins partially deployed prior to release. These data are presented in Fig. 22.

Configuration 6R was rerun with the canards in place to determine the effect on the trajectories if the store were launched with the canards "locked" at zero deflection instead of being free to float. The resulting trajectories are presented in Fig. 23 along with the canards-off data. The store with canards exhibited a more rapid initial pitching and yawing motion than did the store with canards removed.

4.2 CARRIAGE LOADS DATA

Carriage loads data were acquired for the MK-84EOGB and the MK-82LGB. These data are presented in Figs. 24 through 27. Note that the angle of attack against which these data are plotted is the parent-aircraft angle of attack. The angle of attack of the store was 3 deg less than the angle of the parent aircraft (see Fig. 4).

Aerodynamic coefficients of the MK-84EOGB are presented in Fig. 24. Changes in all coefficients with Mach number and angle of attack were generally small, with the exception of a significant shift in all coefficients between $M_\infty = 0.90$ and $M_\infty = 0.95$.

Data obtained from the MK-82LGB, Configurations 10 and 11, are presented in Figs. 25 and 26, respectively. The major changes noted were in the variations of side-force, yawing-moment, and rolling-moment coefficients with angle of attack. During the

acquisition of the carriage loads data, two data points were taken at each angle of attack. The repeatability of these data points was affected by the uncertainties of the balance and CTS rig settings as well as the stability of the airflow about the store at a given station. With the exception of Configuration 11L, the carriage loads data repeatability on a given configuration was very good. Configuration 11L, however, exhibited significant changes in the repeat points of the side-force, yawing-moment, and rolling-moment coefficients. A tabulation of these data is presented in Table 4. It is probable that the presence of stores on all three stations of the TER resulted in a highly turbulent flow pattern in the vicinity of the store on which the loads were obtained. It should be noted that Configuration 11L was identical to Configuration 7L of the trajectory data for which the store on TER Station 1 contacted the adjacent store upon release (see Fig. 19).

Carriage loads data were obtained at yaw angles of 0 and ± 2 deg for Configuration 12. These data are presented in Fig. 27.

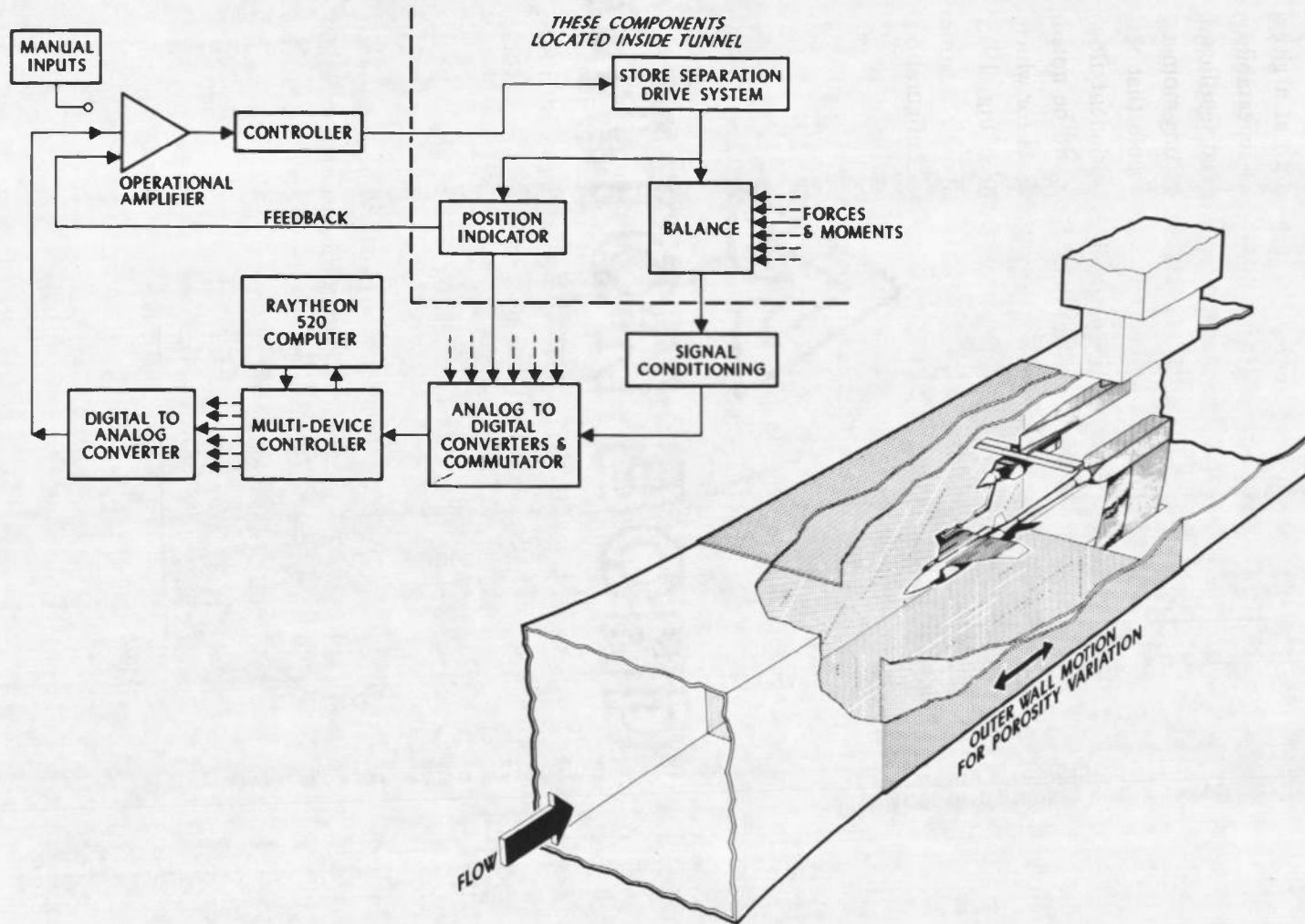


Figure 1. Isometric drawing of a typical store separation installation and a block diagram of the computer control loop.

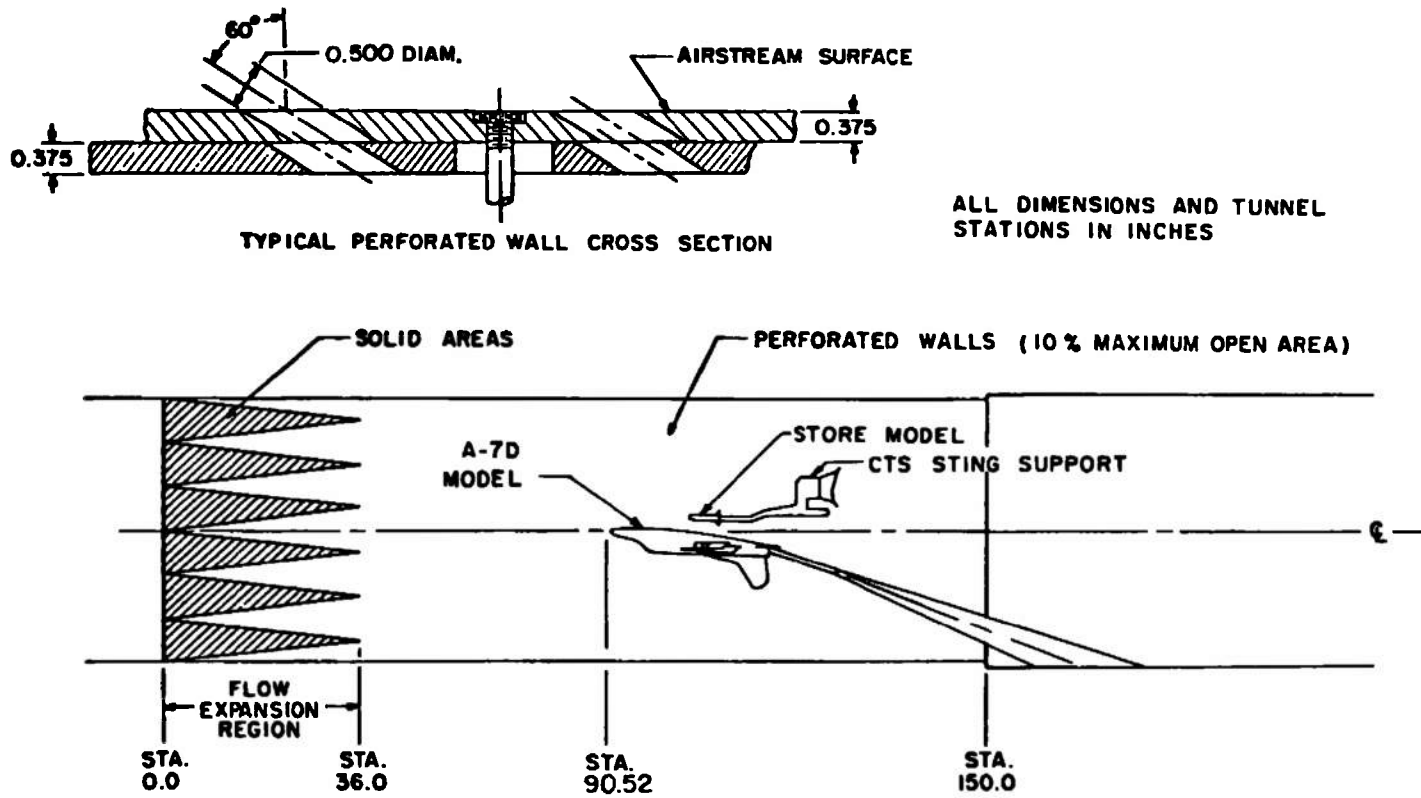


Figure 2. Schematic of the tunnel test section showing model location.

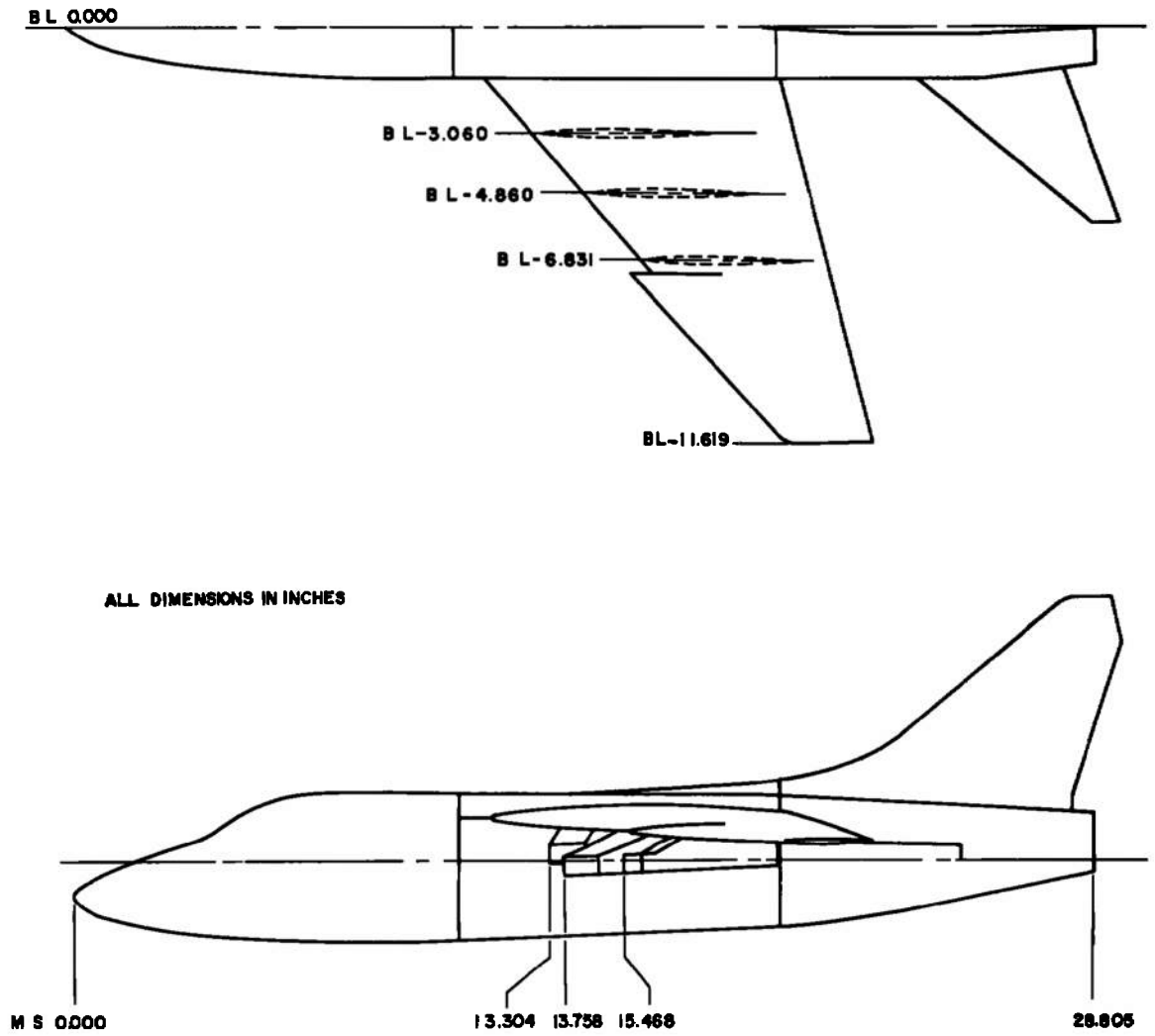
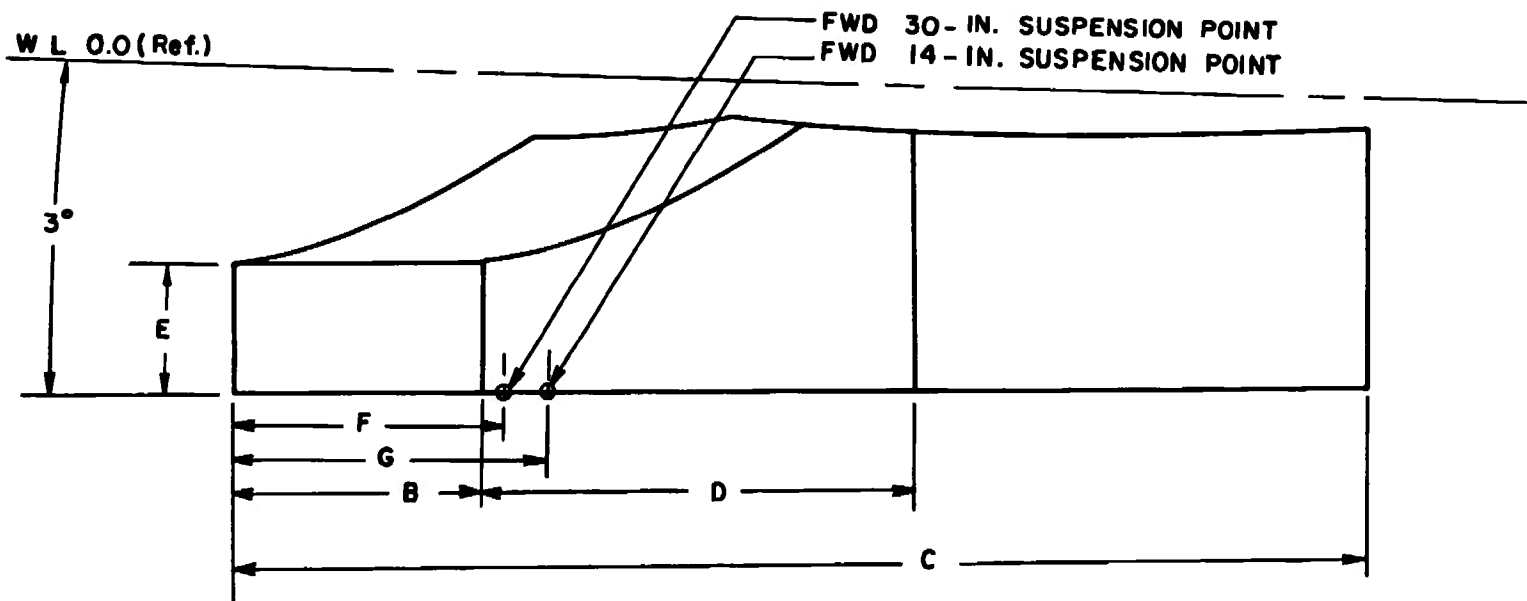


Figure 3. Sketch of A-7D aircraft model.



ALL DIMENSIONS IN INCHES

	INBOARD	CENTER	OUTBOARD
B	1.030	1.030	0.515
C	4.580	4.850	4.437
D	1.630	1.905	2.008
E	0.575	0.575	0.513
F	0.950	0.950	0.750
G	1.350	1.350	1.150

Figure 4. Details and dimensions of the A-7D wing pylon models.

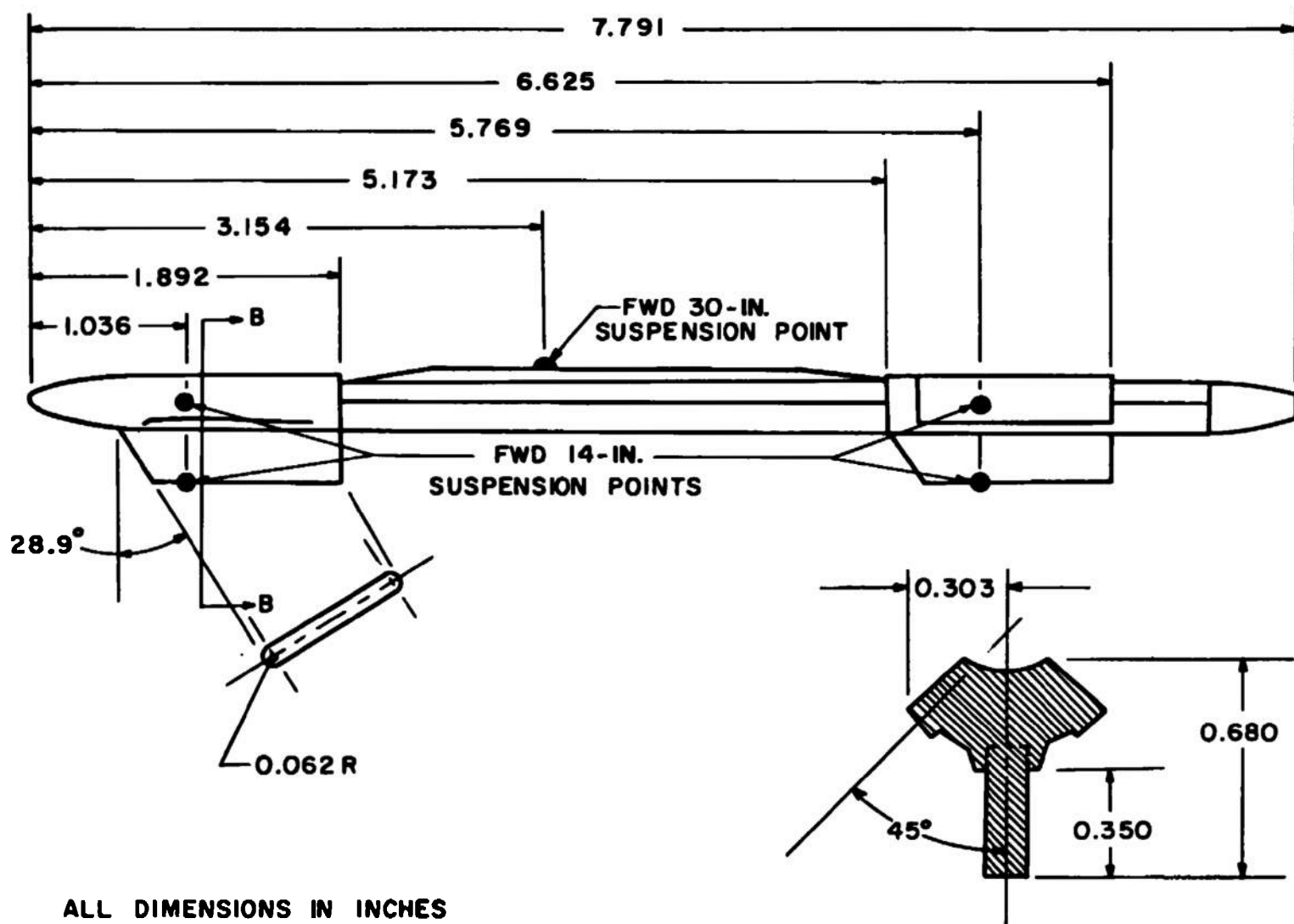


Figure 5. Details and dimensions of the TER models.

18

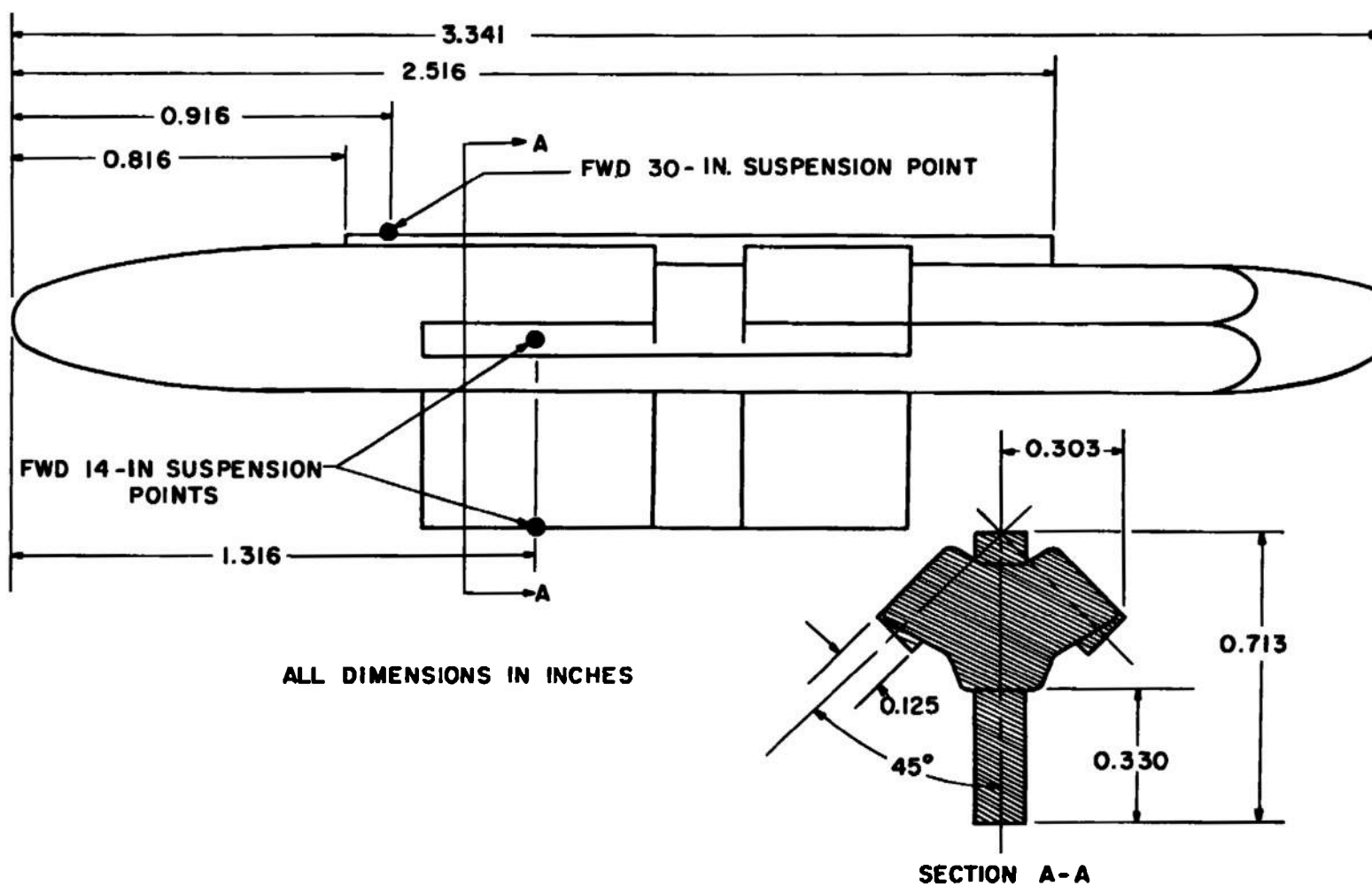
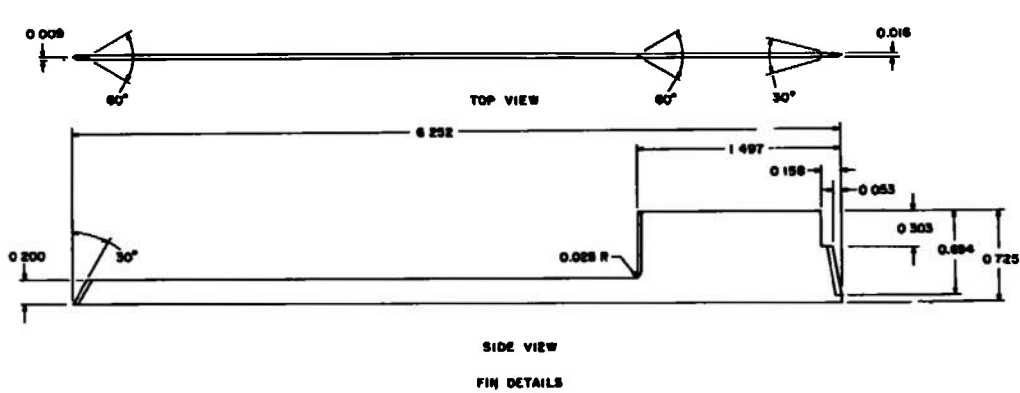


Figure 6. Details and dimensions of the MER models.



X, in	R _i , in
2.273	0.364
2.385	0.376
2.535	0.396
2.733	0.412
2.985	0.426
3.185	0.438
3.385	0.448
3.580	0.450
4.000	0.450
4.250	0.450
4.500	0.450
4.684	0.450
4.684	0.448
5.084	0.444
5.284	0.437
5.484	0.428
5.684	0.416
5.684	0.401
5.616	0.400

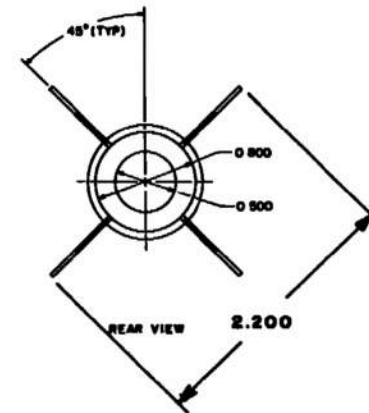
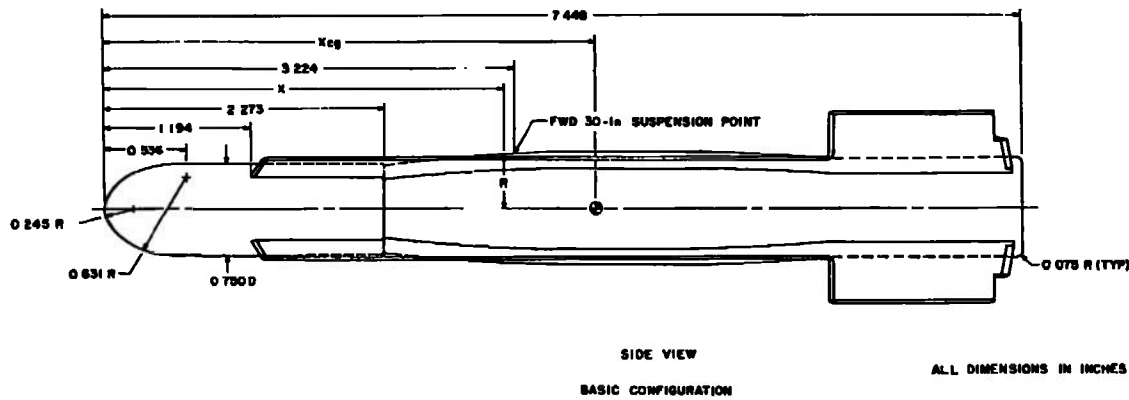
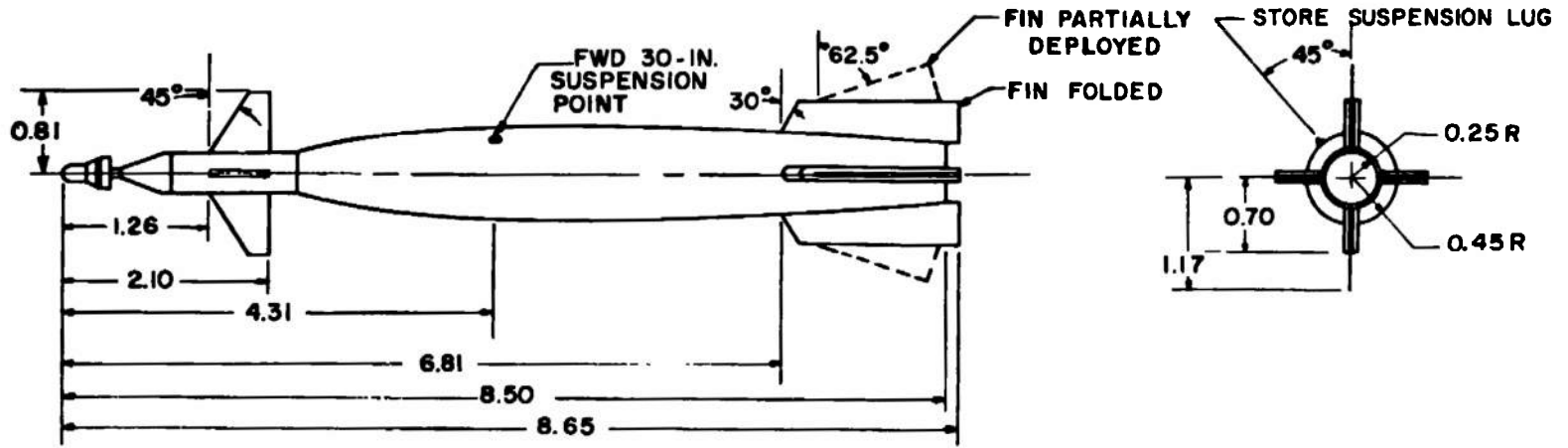


Figure 7. Details and dimensions of the MK-84EOGB.



MODEL SHOWN ROLLED -45°
 ALL DIMENSIONS IN INCHES

Figure 8. Dimensional sketch of the MK-84LGB.

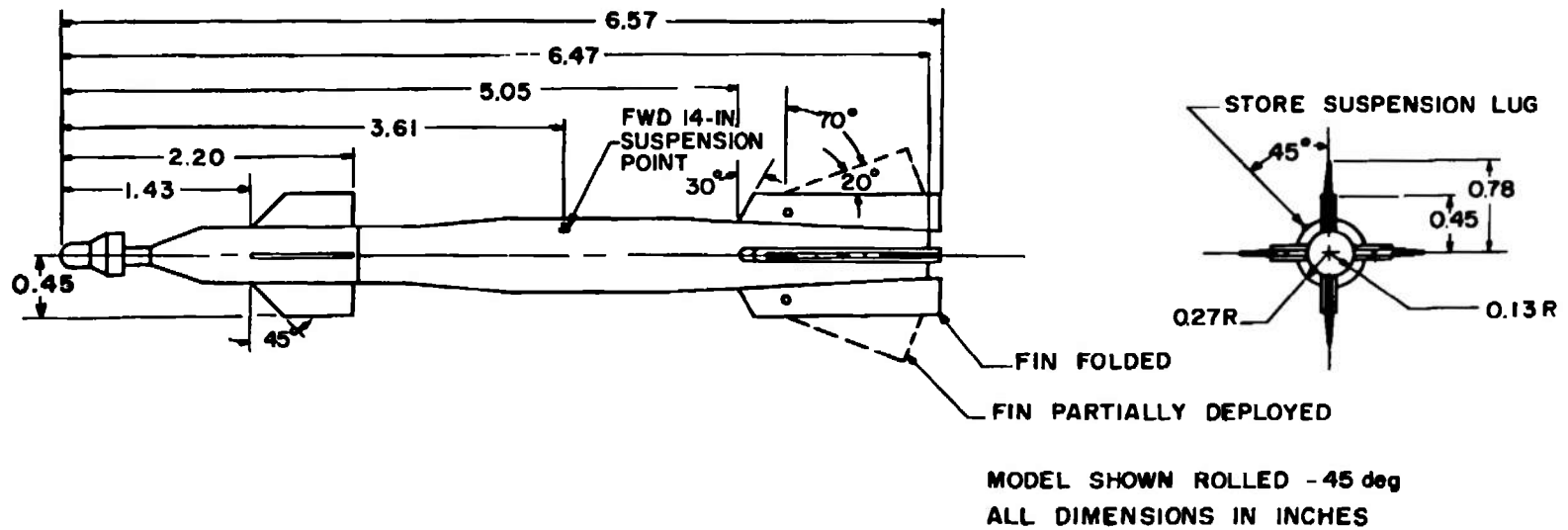
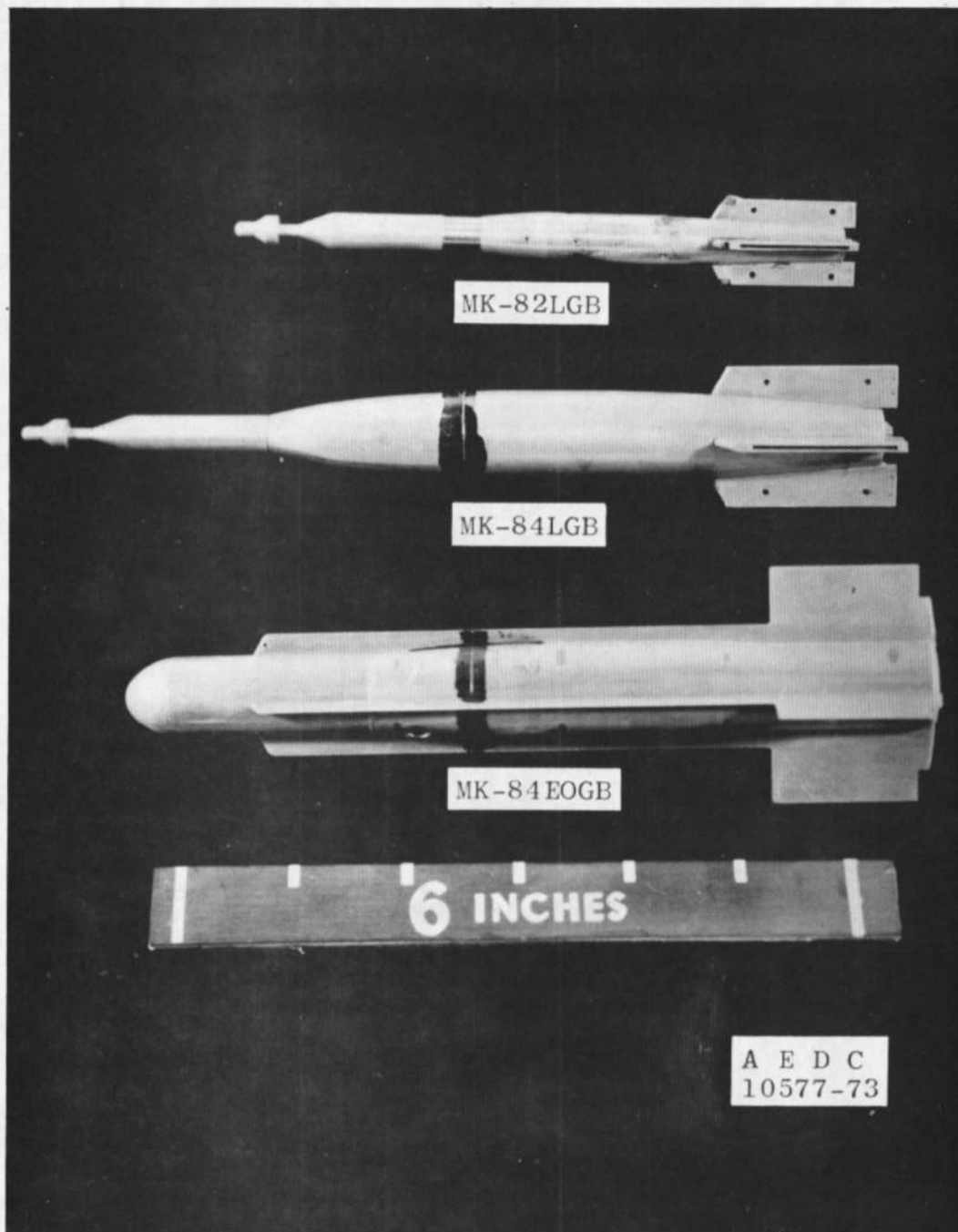
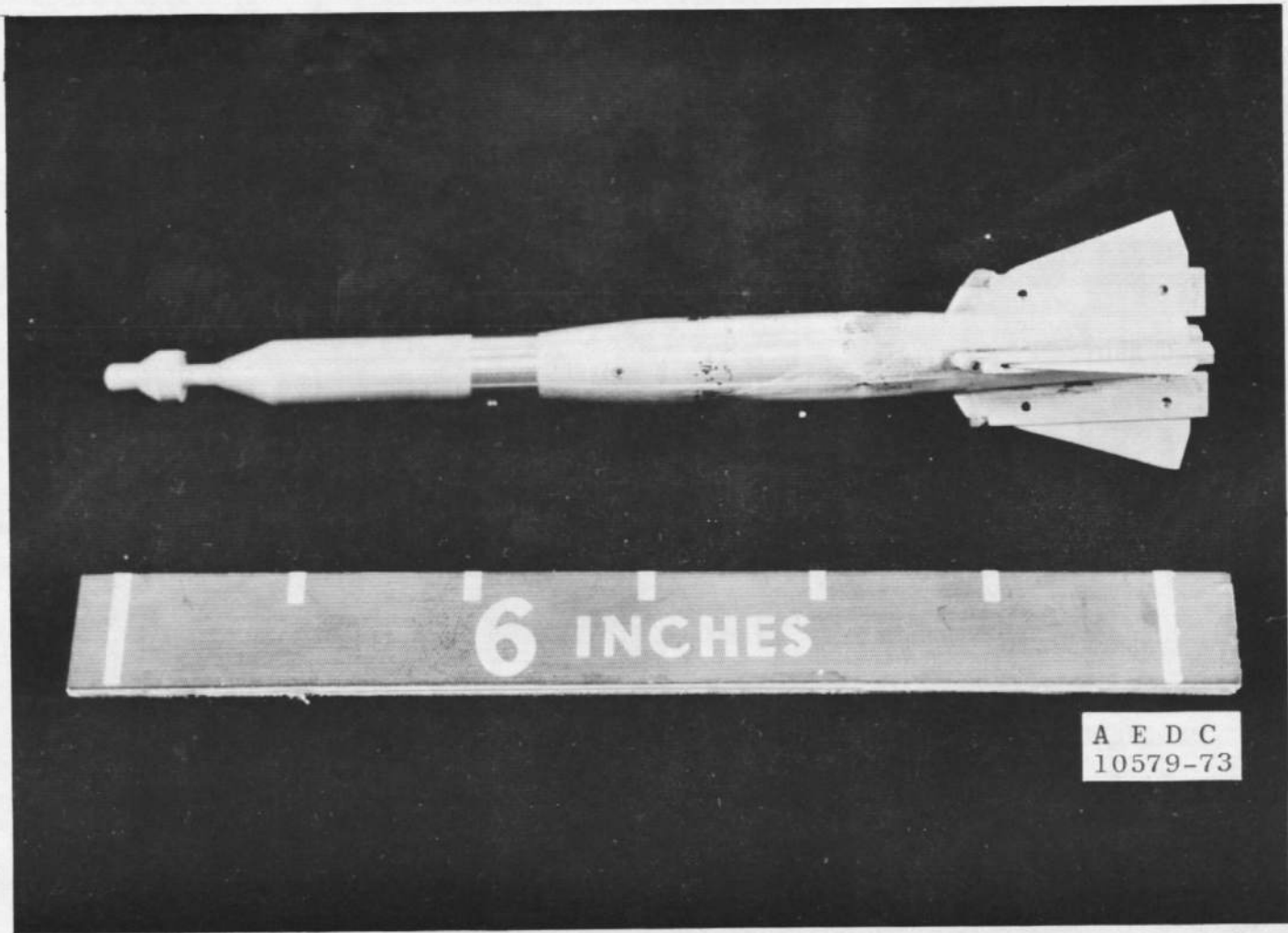


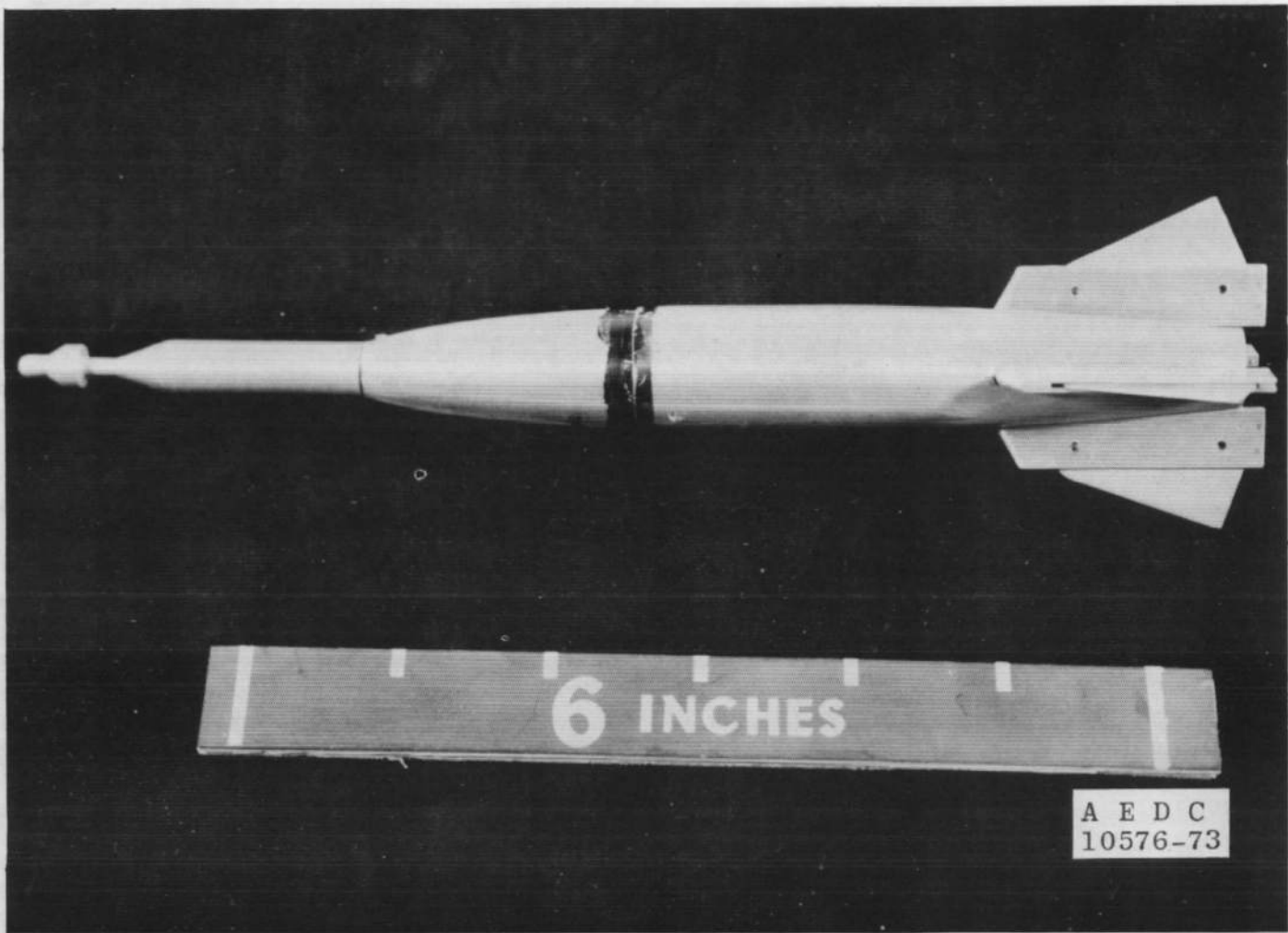
Figure 9. Dimensional sketch of the MK-83LGB.



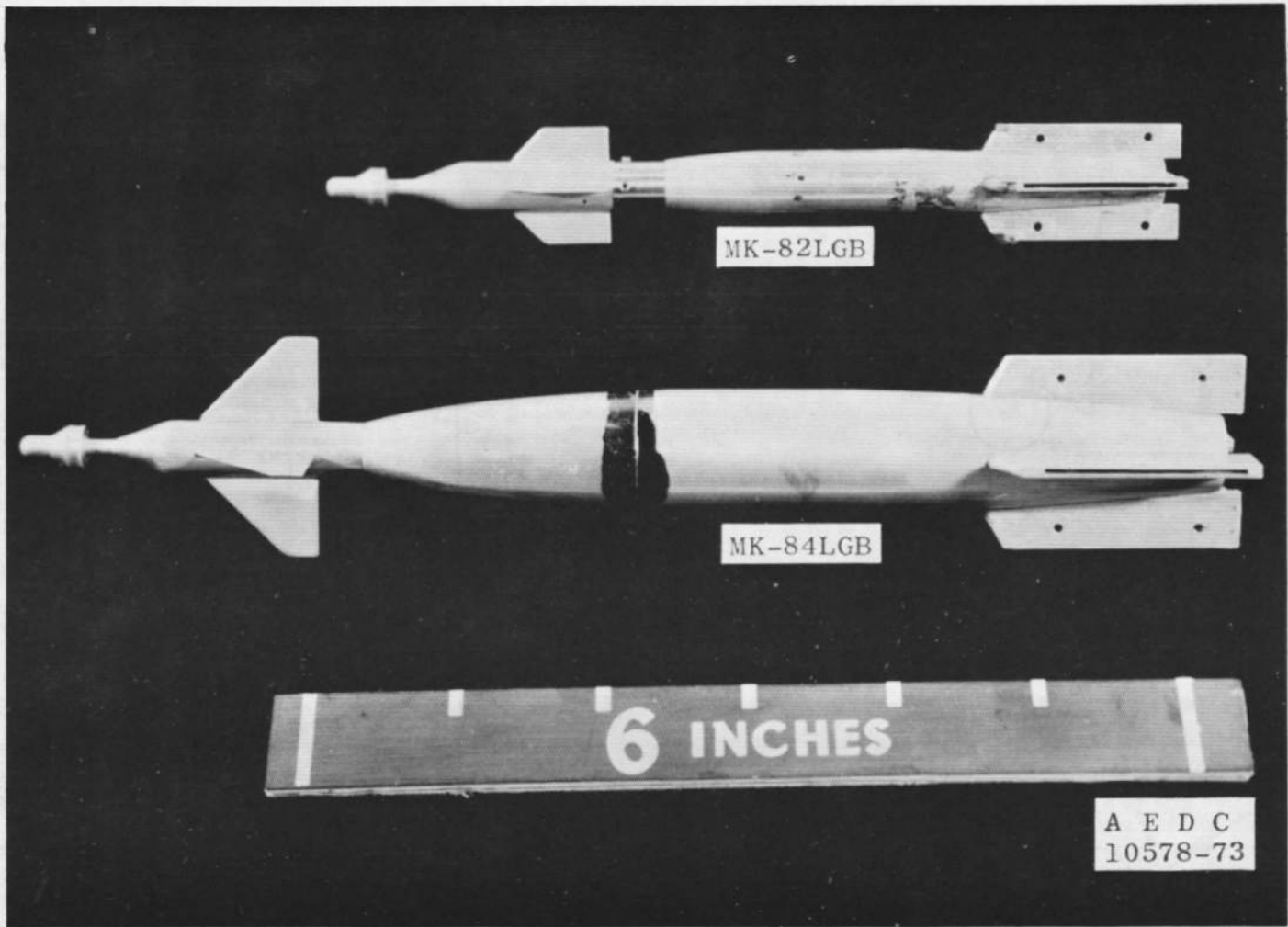
a. MK-82LGB, MK-84LGB, MK-84EOGB
Figure 10. Model photographs.



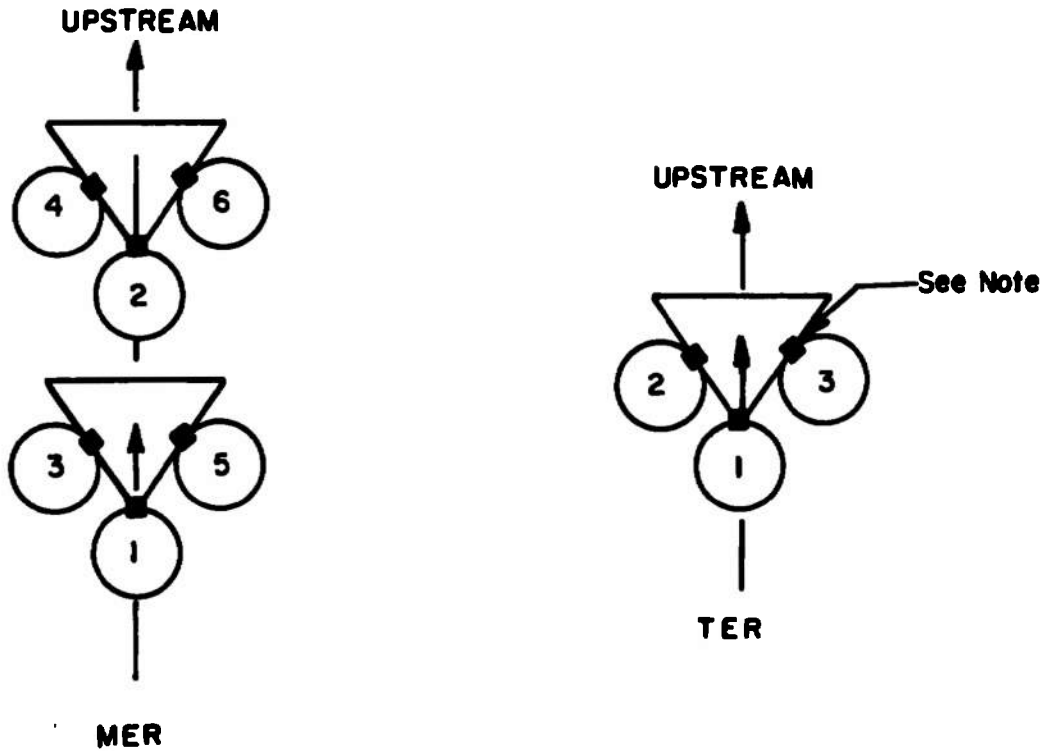
b. MK-82LGB with fins partially deployed
Figure 10. Continued.



c. MK-84LGB with fins partially deployed
Figure 10. Continued.



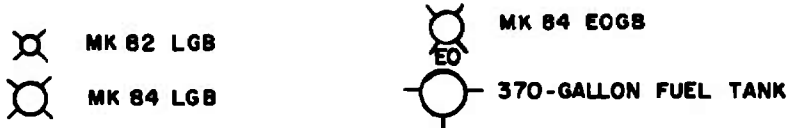
d. MK-82LGB and MK-84LGB with fixed canards
Figure 10. Concluded.









































NOTE: The square indicates the orientation of the suspension lugs

TYPE RACK	STATION	ROLL ORIENTATION, deg
MER ↓	1	0
	2	0
	3	45
	4	45
	5	-45
	6	-45
TER ↓	1	0
	2	45
	3	-45

Figure 11. Identification of TER and MER store stations and orientations.

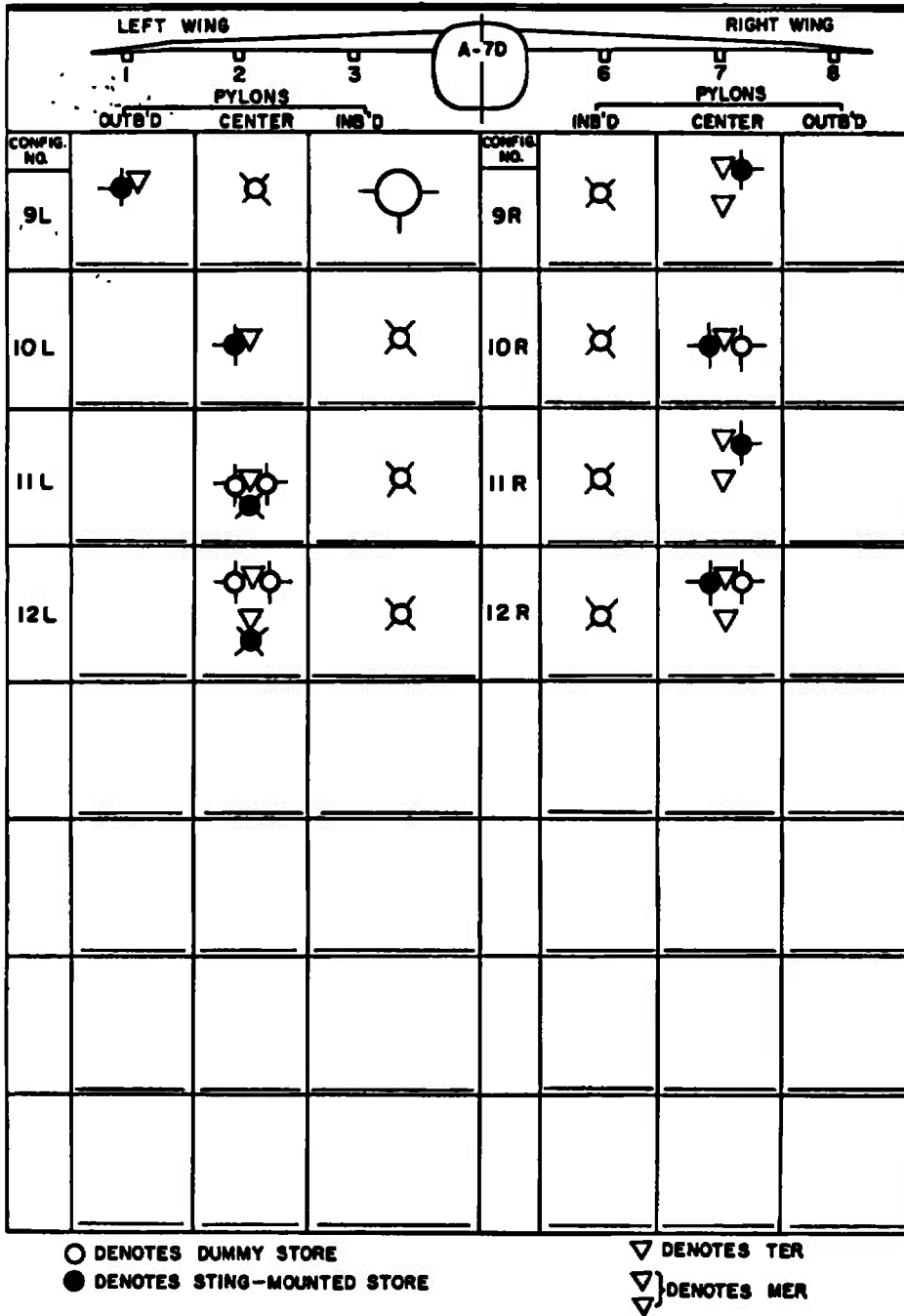


LEFT WING				RIGHT WING			
PYLONS				PYLONS			
OUTB'D		CENTER		INS'D		OUTB'D	
CONFIG. NO.				CONFIG. NO.			
1L				1R			
2L				2R			
3L				3R			
4L				4R			
5L		 		5R			
6L		 		6R			
7L		  		7R			
8L		   		8R		  	

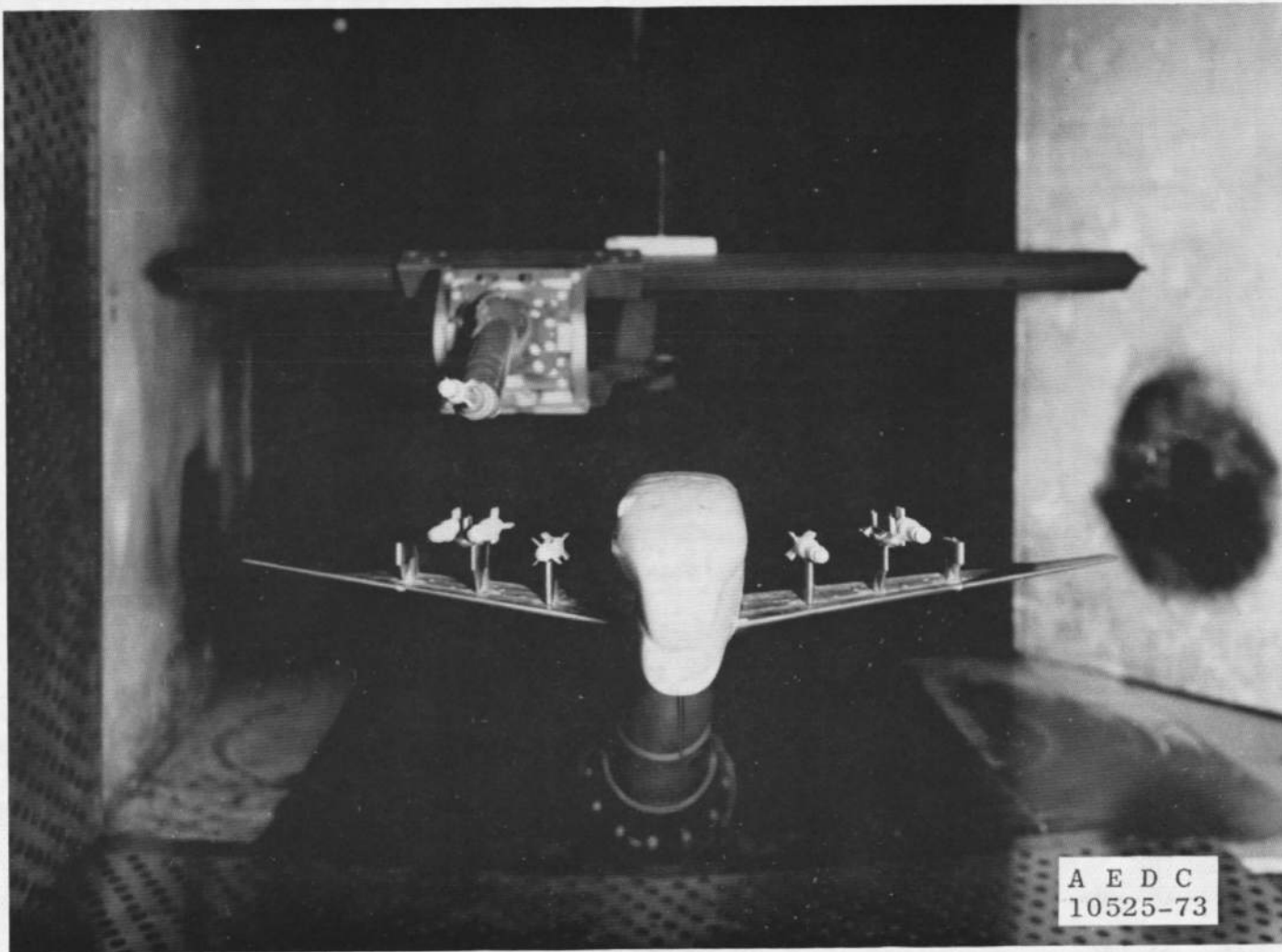
 DENOTES DUMMY STORE
 DENOTES STING-MOUNTED STORE

 DENOTES TER
 DENOTES MER

a. Configurations 1 through 8
 Figure 12. Test configuration identification.

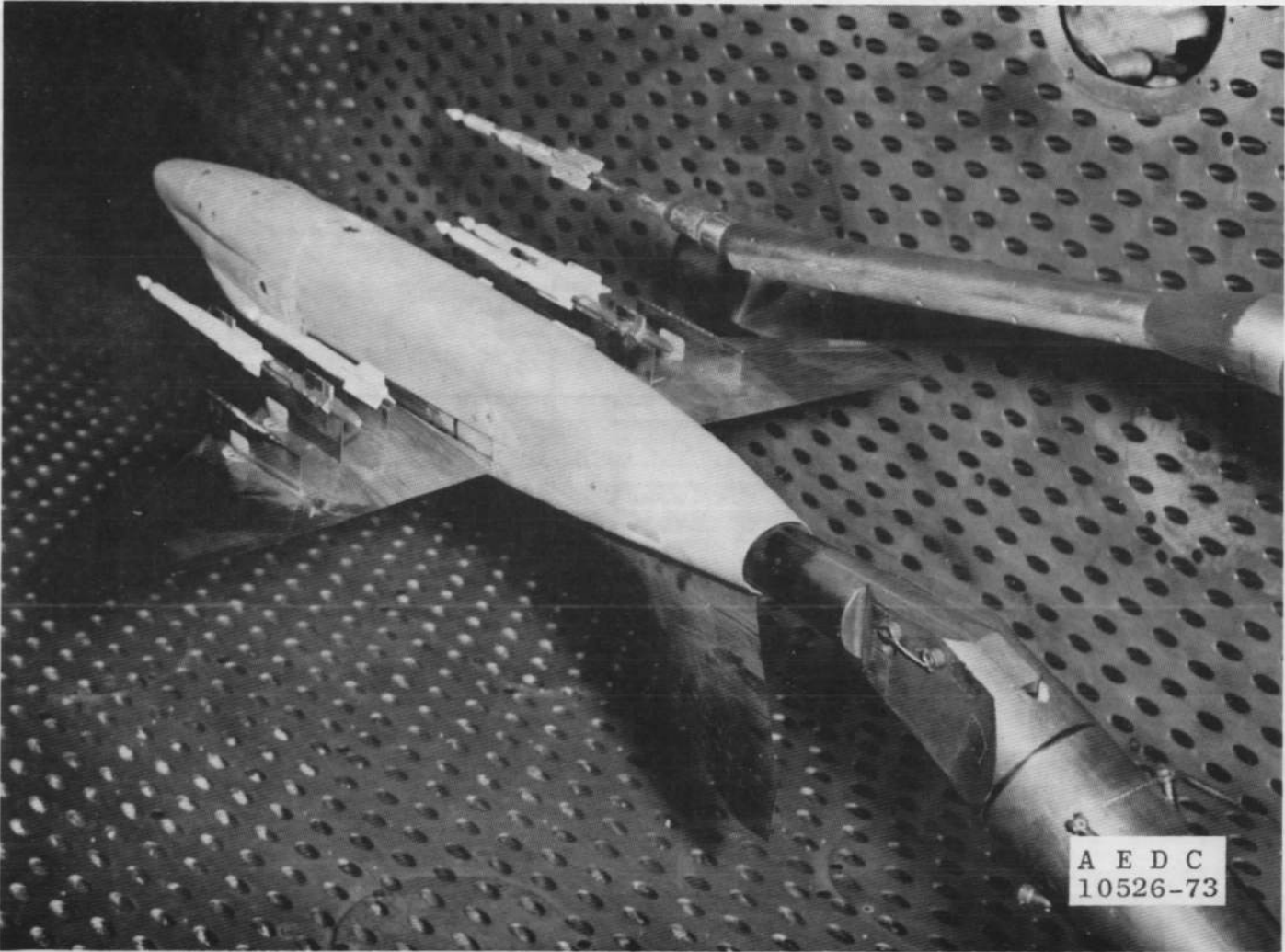


b. Configurations 9 through 12
 Figure 12. Concluded.



a. Front view

Figure 13. Typical installation photographs.



b. Aft view
Figure 13. Concluded.

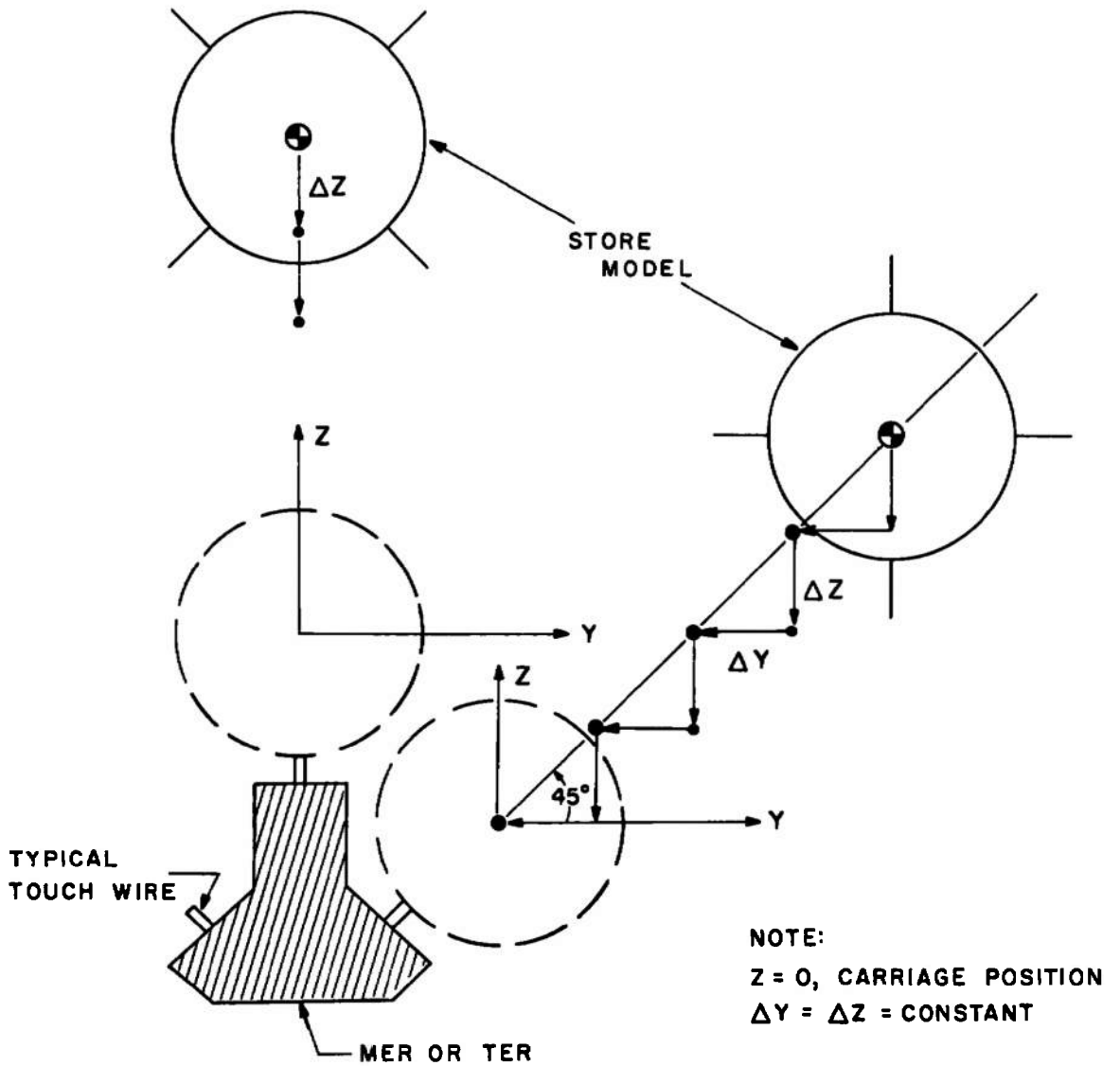
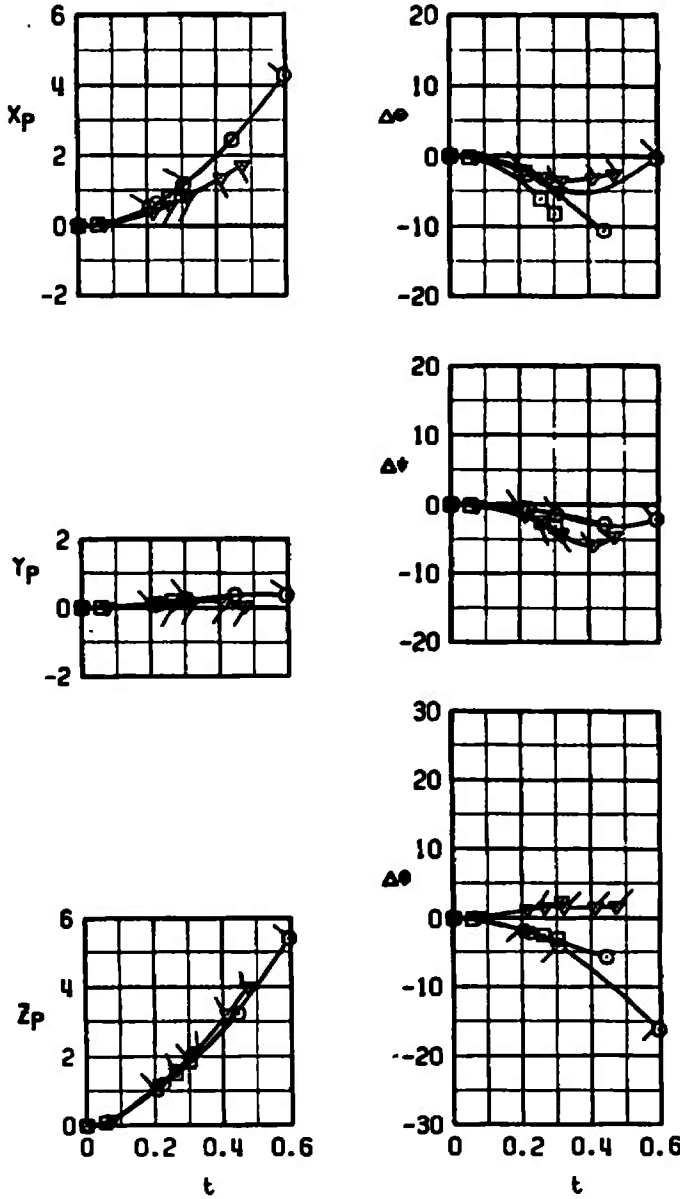


Figure 14. Sketch illustrating a store approaching the touch wire at the carriage position (model inverted).

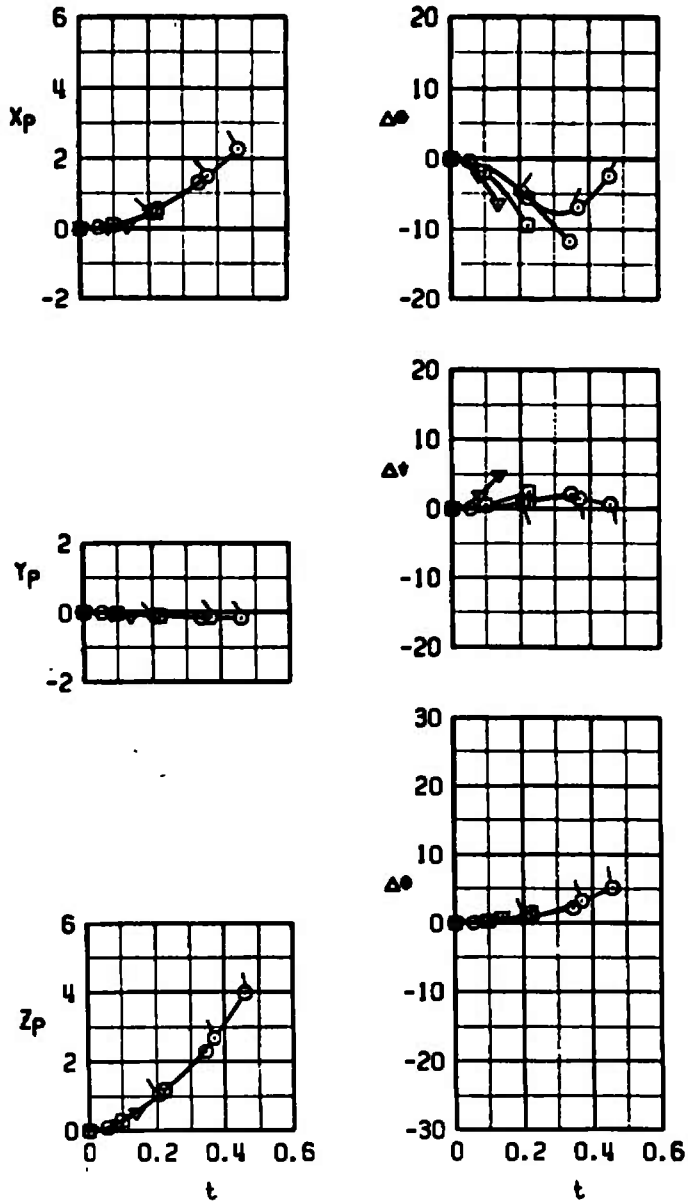
SYMBOL	M_∞	α	DIVE
○	0.78	2.2	70
⊙	0.78	2.2	70
□	0.86	2.1	70
△	0.95	2.0	70
▽	0.95	2.0	70



a. Configuration 2L, dive = 70 deg

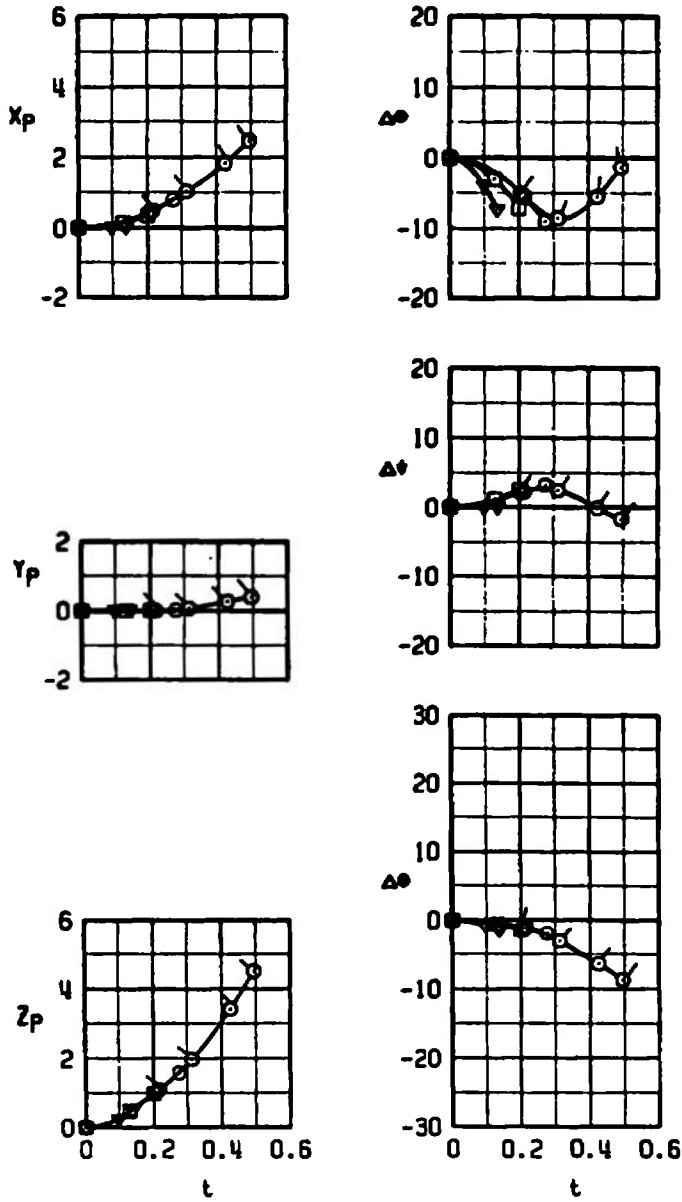
Figure 15. Trajectories for the MK-84LGB, Configurations 2 and 3.

SYMBOL	M_∞	α	DIVE
○	0.78	2.2	70
◐	0.78	2.2	70
◑	0.86	2.1	70
▼	0.95	2.0	70



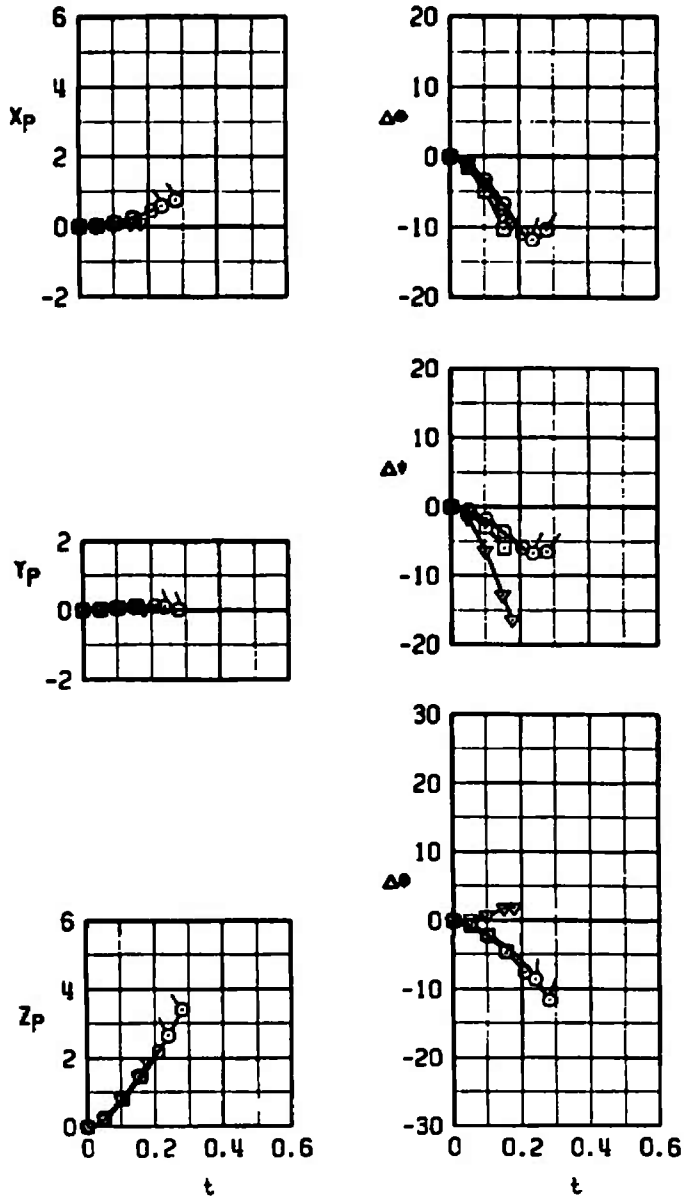
b. Configuration 2R, dive = 70 deg
Figure 15. Continued.

SYMBOL	M_∞	α	DIVE
○	0.78	2.2	70
⊙	0.78	2.2	70
□	0.86	2.1	70
▽	0.95	2.0	70



c. Configuration 3L, dive = 70 deg
 Figure 15. Concluded.

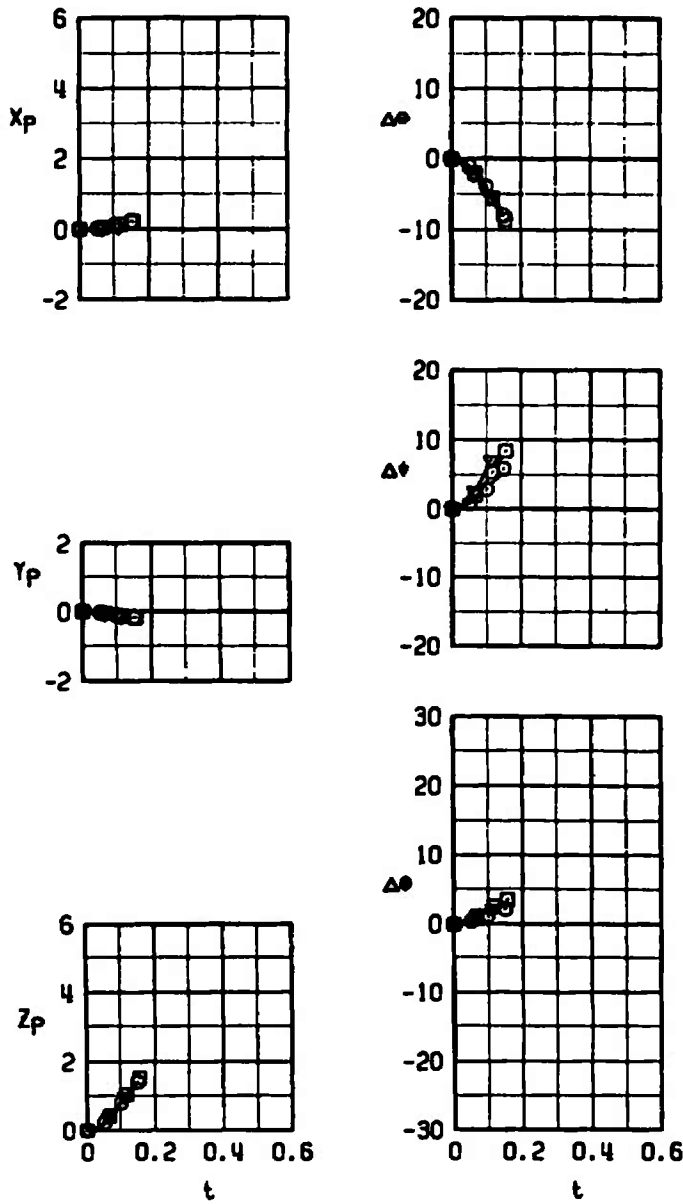
SYMBOL	M_∞	α	DIVE
○	0.78	2.2	70
◌	0.78	2.2	70
◻	0.86	2.1	70
◿	0.95	2.0	70



a. Configuration 4L, dive = 70 deg

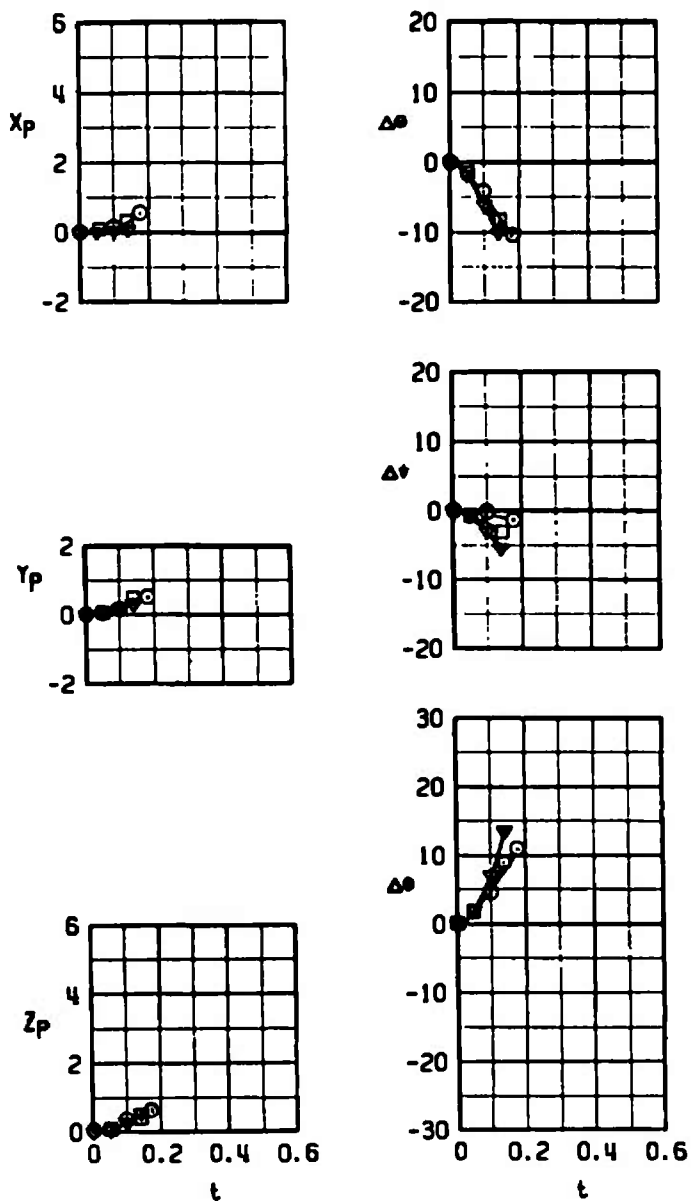
Figure 16. Trajectories for the MK-82LGB, Configuration 4.

SYMBOL	M_∞	α	DIVE
○	0.78	2.2	70
□	0.86	2.1	70
▽	0.95	2.0	70



b. Configuration 4R, dive = 70 deg
 Figure 16. Concluded.

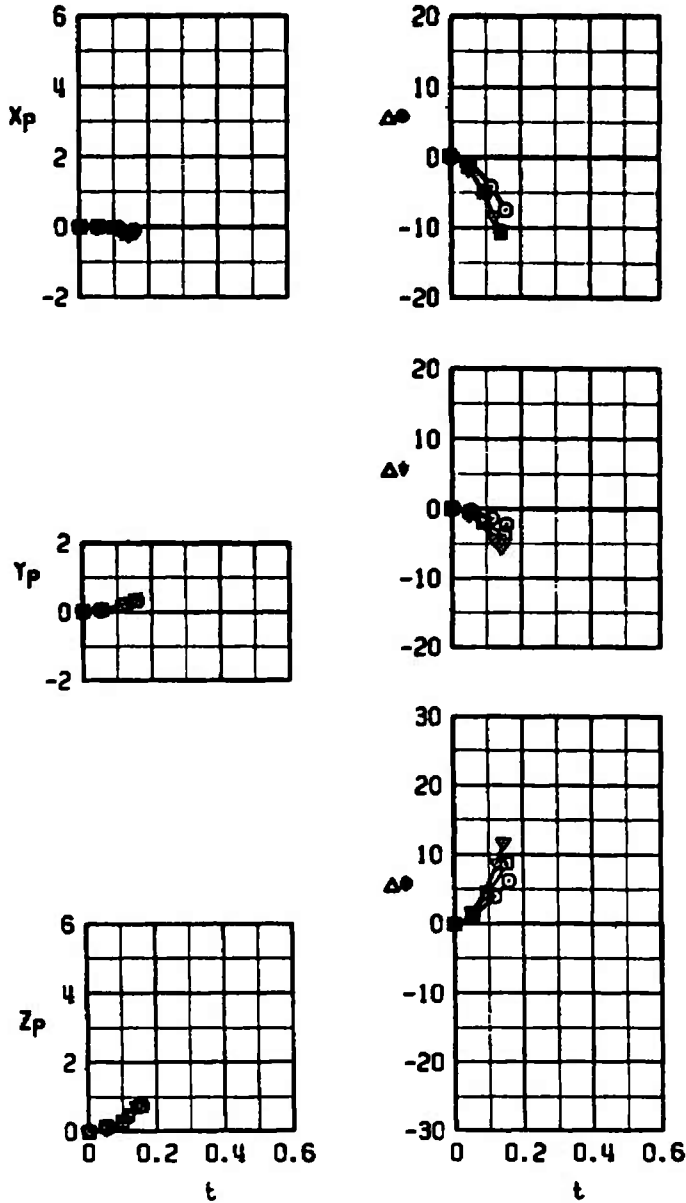
SYMBOL	M_L	α	DIVE
○	0.78	2.2	70
□	0.85	2.1	70
▽	0.95	2.0	70



a. Configuration 5L, dive = 70 deg

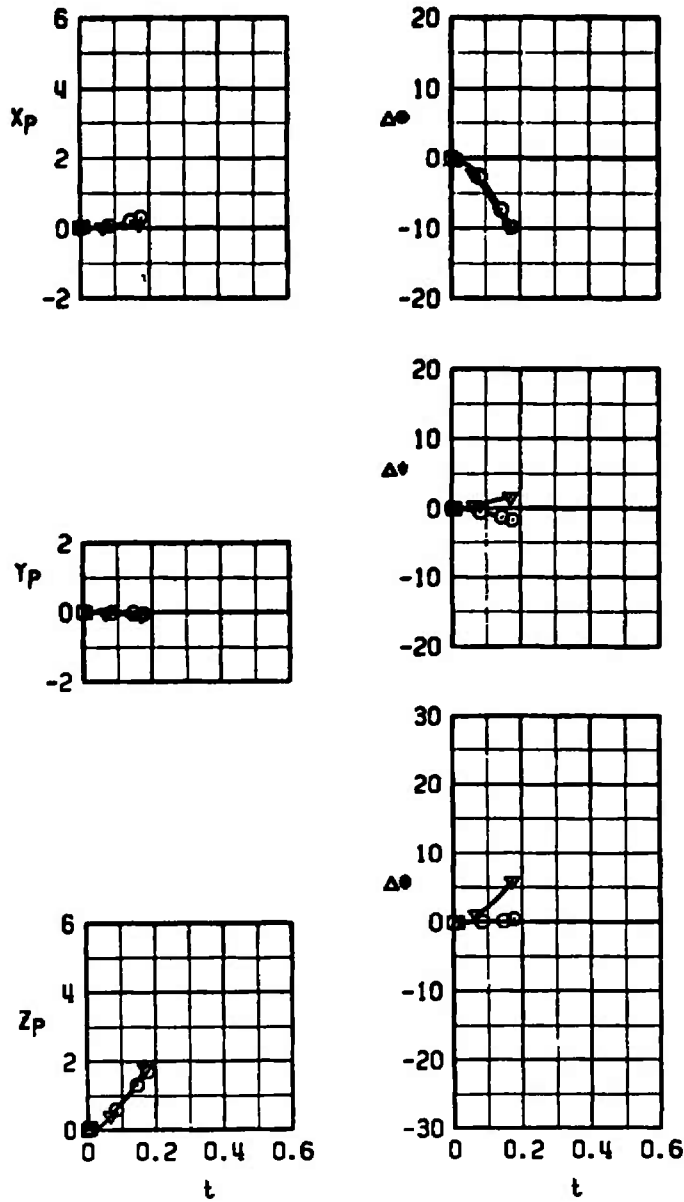
Figure 17. Trajectories for the MK-82LGB, Configuration 5.

SYMBOL	M_∞	α	DIVE
○	0.78	3.4	0
□	0.86	3.0	0
▼	0.95	2.5	0



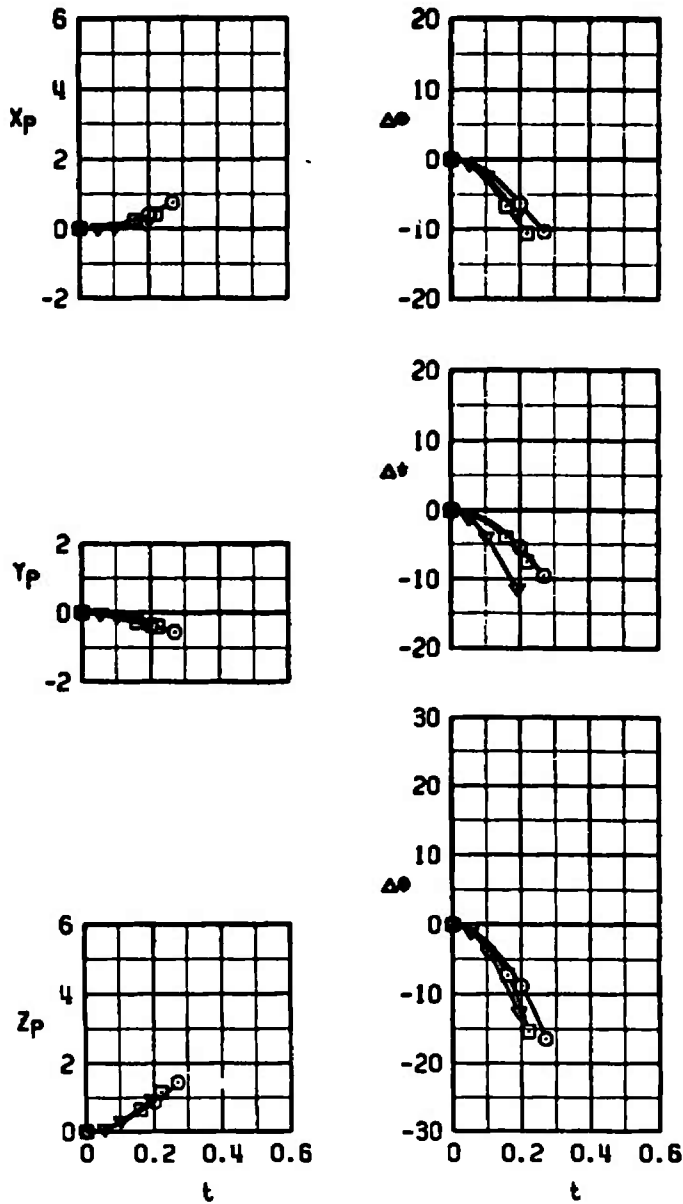
b. Configuration 5L, dive = 0
Figure 17. Continued.

SYMBOL	H_L	α	DIVE
○	0.78	2.2	70
□	0.86	2.1	70
▼	0.95	2.0	70



c. Configuration 5R, dive = 70 deg
 Figure 17. Concluded.

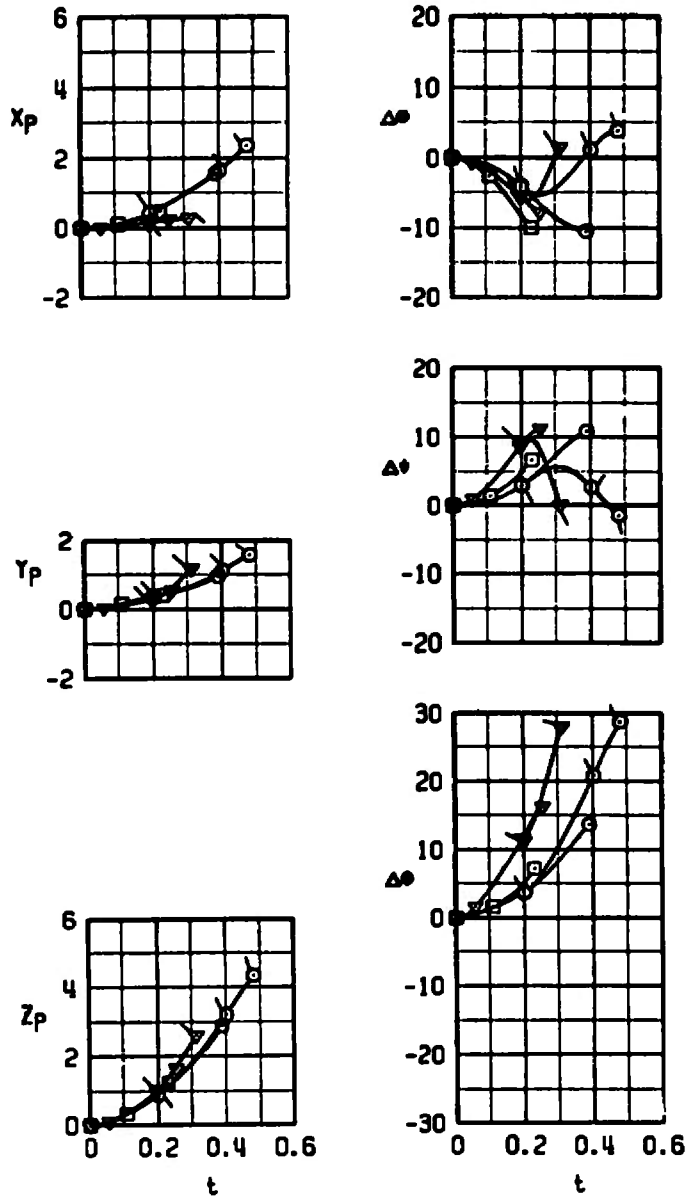
SYMBOL	M_∞	α	DIVE
○	0.78	3.4	70
□	0.86	3.4	70
▼	0.95	2.0	70



a. Configuration 6L, dive = 70 deg

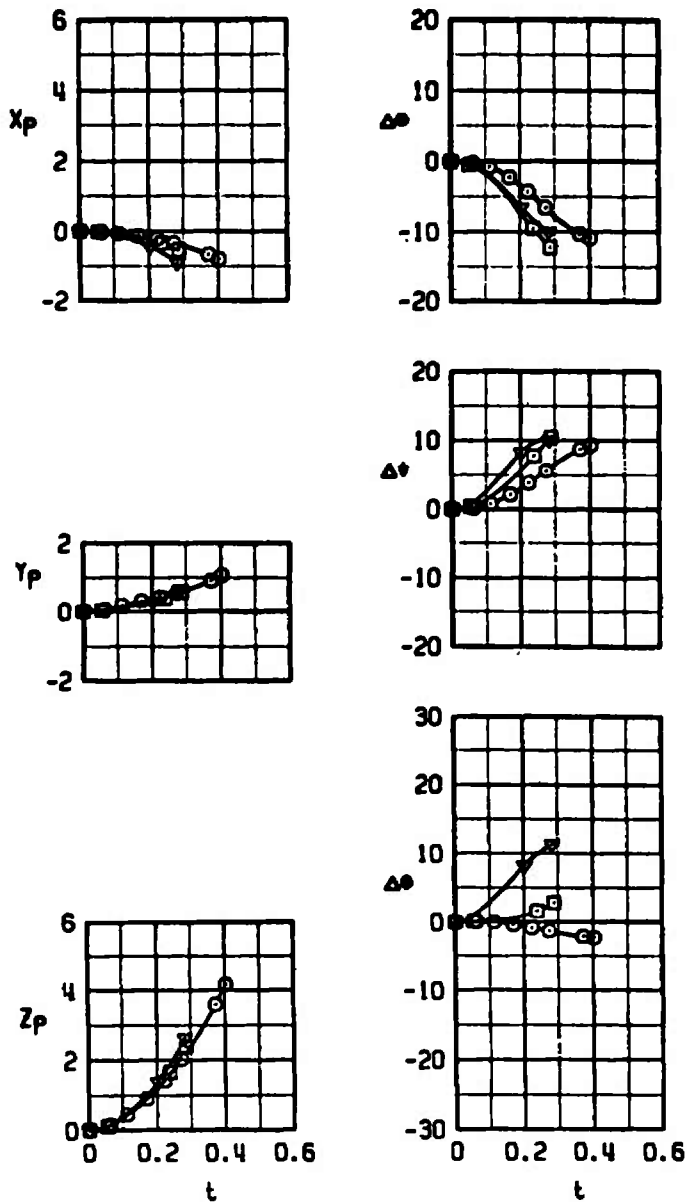
Figure 18. Trajectories for the MK-82LGB, Configuration 6.

SYMBOL	M_∞	Q	DIVE
○	0.78	2.2	70
⊙	0.78	2.2	70
□	0.86	2.1	70
▽	0.95	2.0	70
▼	0.95	2.0	70



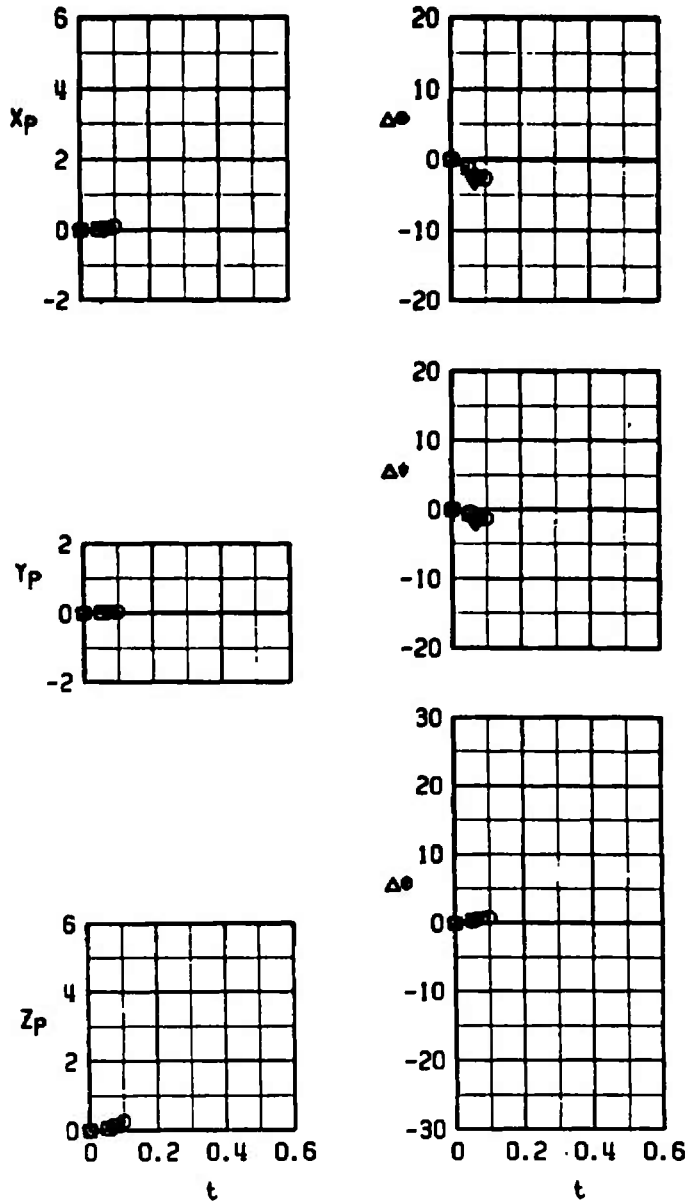
b. Configuration 6R, dive = 70 deg
 Figure 18. Continued.

SYMBOL	M_∞	α	DIVE
○	0.78	3.4	0
□	0.86	3.4	0
▽	0.95	3.4	0



c. Configuration 6R, dive = 0
 Figure 18. Concluded.

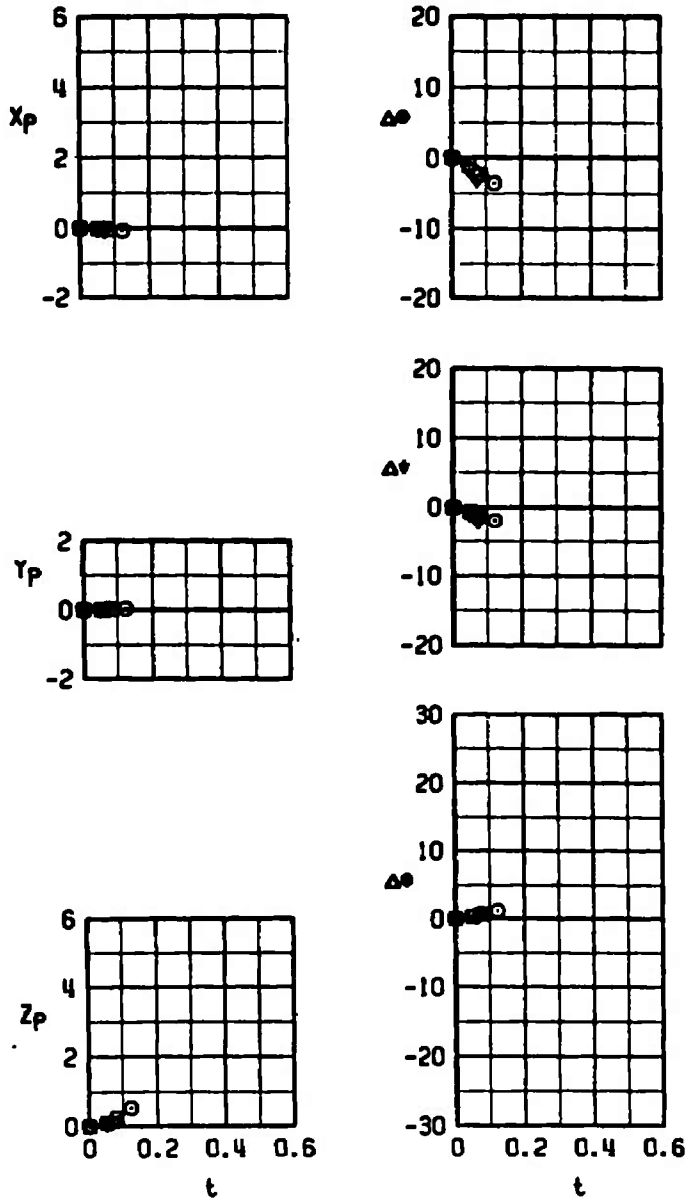
SYMBOL	M_L	α	DIVE
○	0.78	2.2	70 STORE CONTACT
□	0.86	2.1	70 STORE CONTACT
▼	0.95	2.0	70 STORE CONTACT



a. Configuration 7L, dive = 70 deg

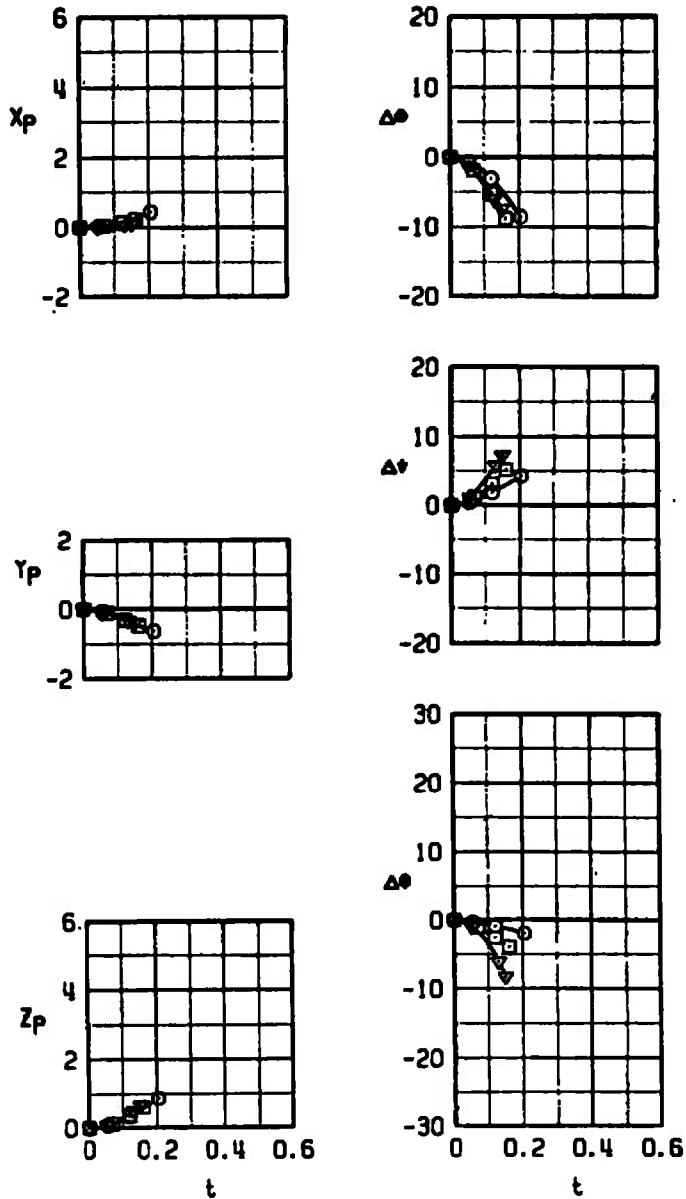
Figure 19. Trajectories for the MK-82LGB, Configuration 7.

SYMBOL	N_c	Q	DIVE	STORE CONTACT
○	0.78	3.4	0	STORE CONTACT
□	0.86	3.0	0	STORE CONTACT
▼	0.95	2.5	0	STORE CONTACT



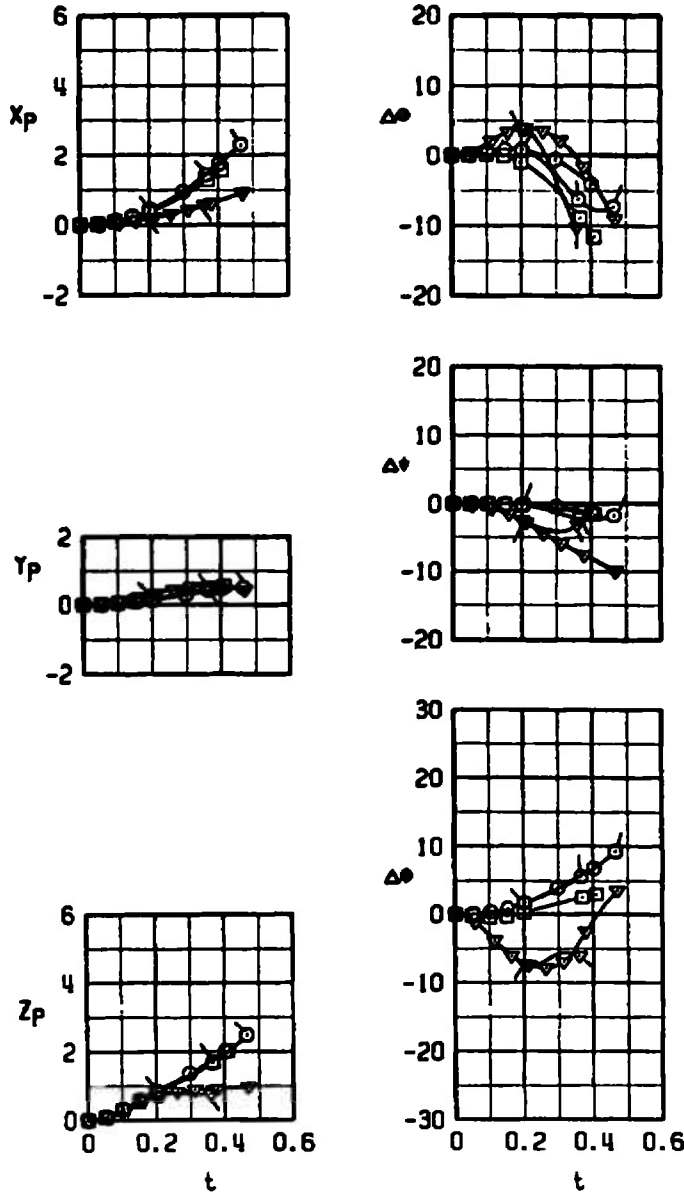
b. Configuration 7L, dive = 0
 Figure 19. Continued.

SYMBOL	M_L	α	DIVE
○	0.78	2.2	70
□	0.86	2.1	70
▽	0.95	2.0	70



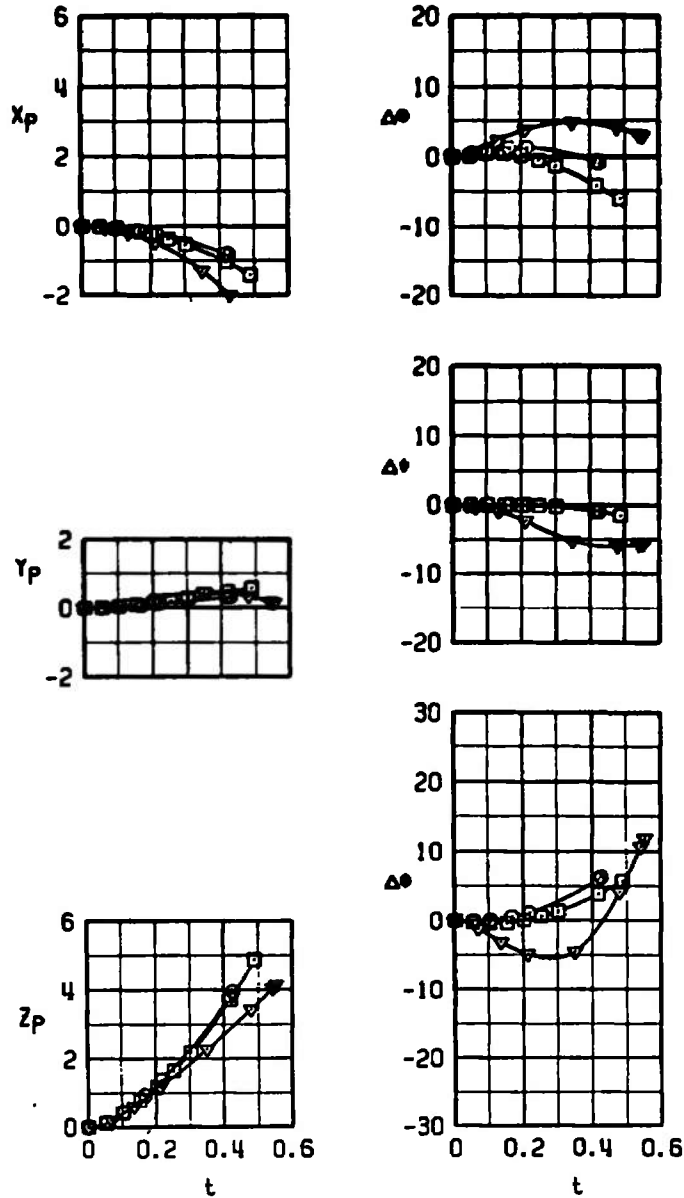
c. Configuration 7R, dive = 70 deg
Figure 19. Concluded.

SYMBOL	M_∞	α	DIVE
○	0.78	2.2	70
◐	0.78	2.2	70
◑	0.86	2.1	70
◒	0.95	2.0	70
◓	0.95	2.0	70



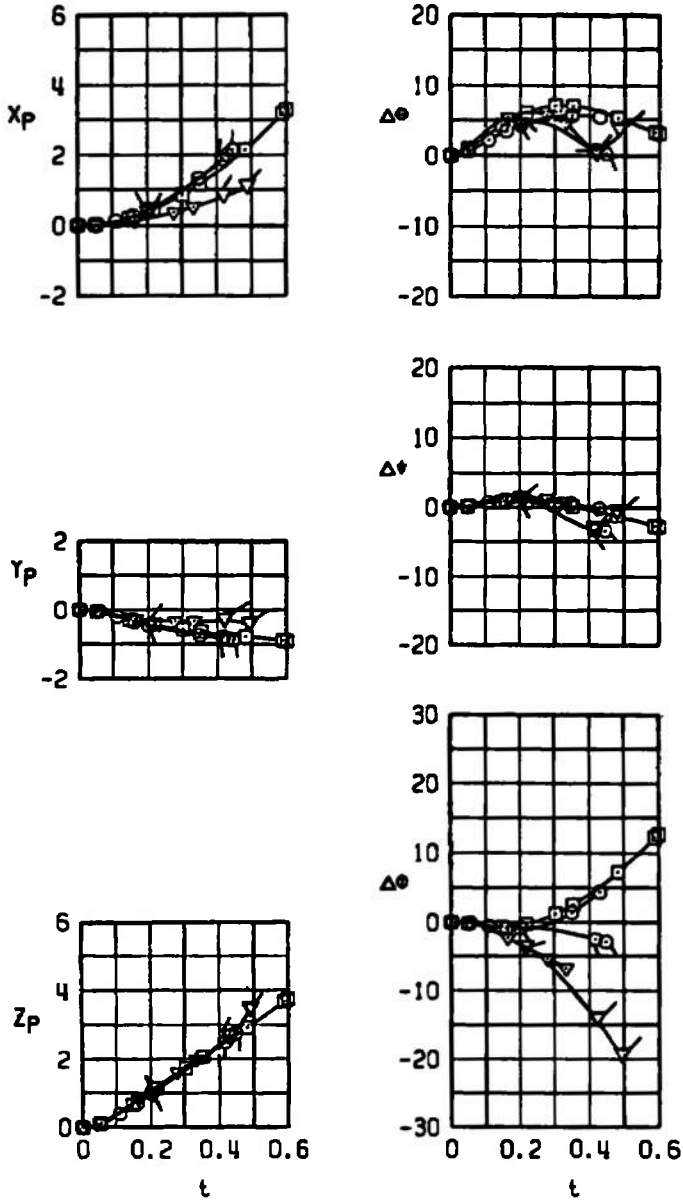
a. Configuration 8L, dive = 70 deg
 Figure 20. Trajectories for the MK-82LGB, Configuration 8.

SYMBOL	M_∞	α	DIVE
○	0.78	3.4	0
□	0.86	3.0	0
▼	0.95	2.5	0



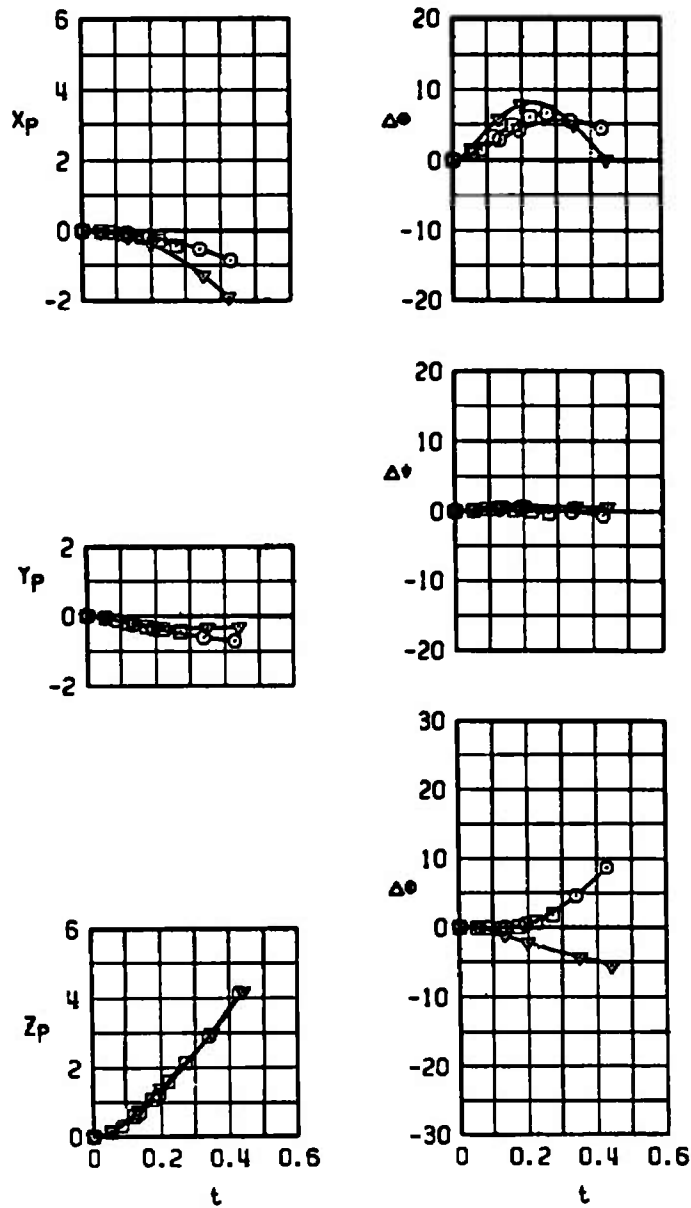
b. Configuration 8L, dive = 0
Figure 20. Continued.

SYMBOL	M_∞	α_p	DIVE
○	0.78	2.2	70
○	0.78	2.2	70
□	0.86	3.0	70
△	0.95	2.0	70
△	0.95	2.0	70



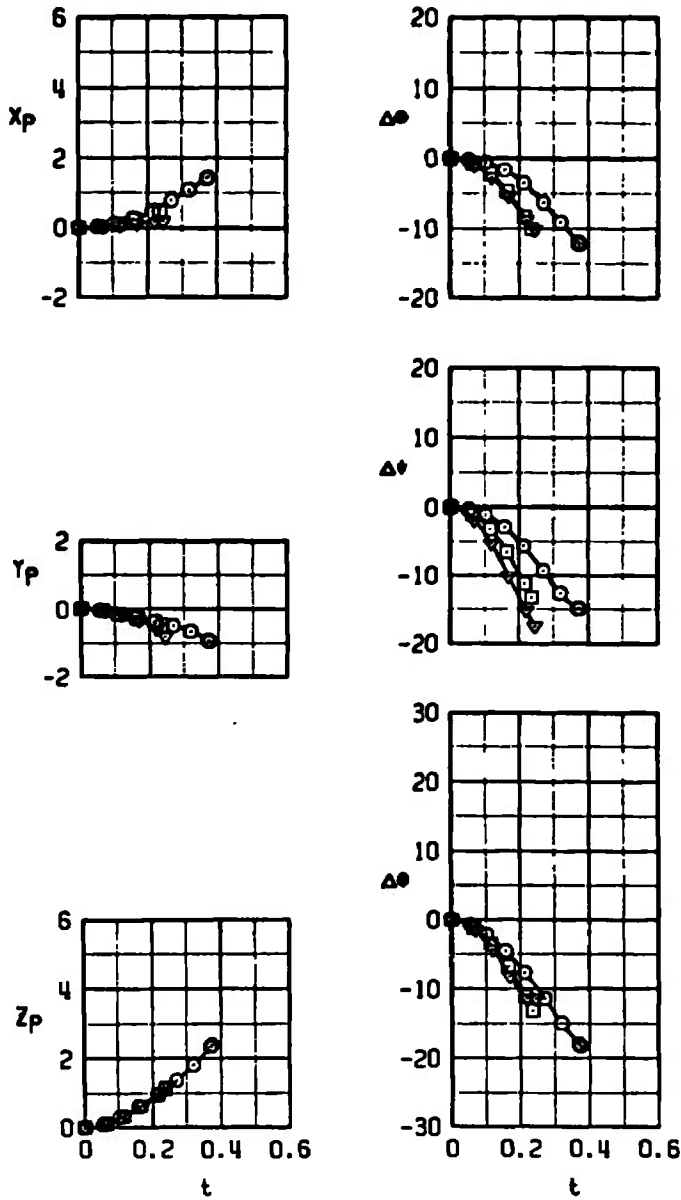
c. Configuration 8R, dive = 70 deg
Figure 20. Continued.

SYMBOL	M_∞	α_p	DIVE
○	0.78	3.4	0
□	0.86	3.0	0
▽	0.95	2.5	0



d. Configuration 8R, dive = 0
 Figure 20. Concluded.

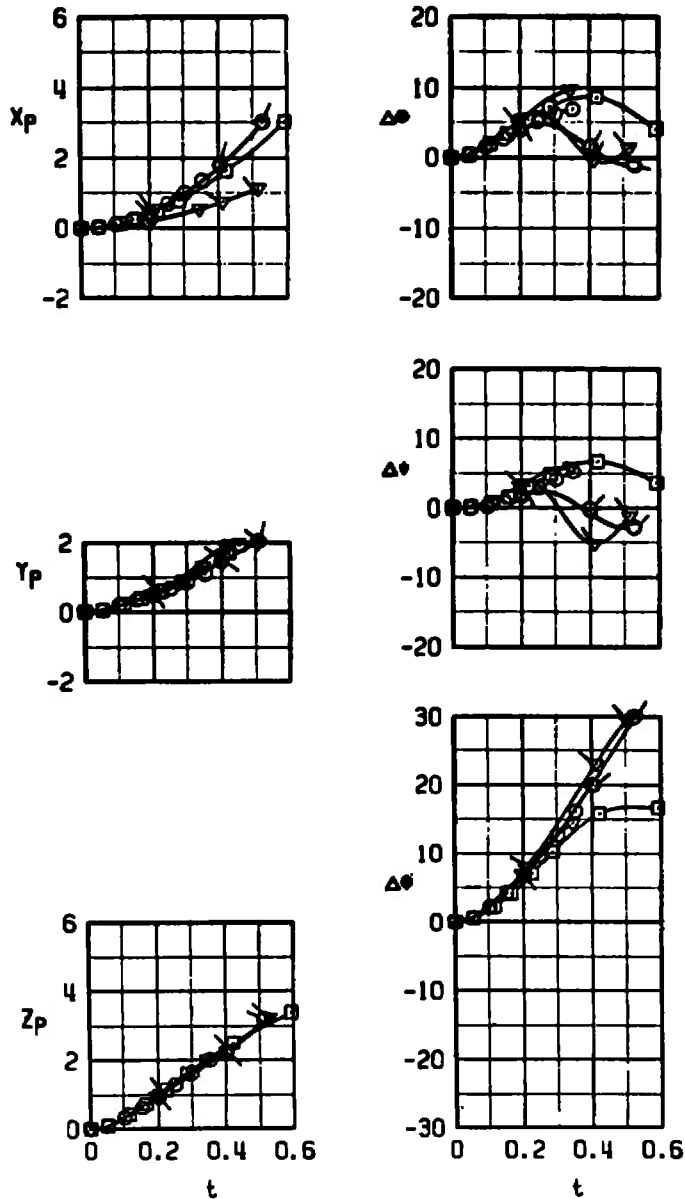
SYMBOL	M_∞	α	DIVE
○	0.78	2.2	70
□	0.86	2.1	70
▼	0.95	2.0	70



a. Configuration 9L, dive = 70 deg

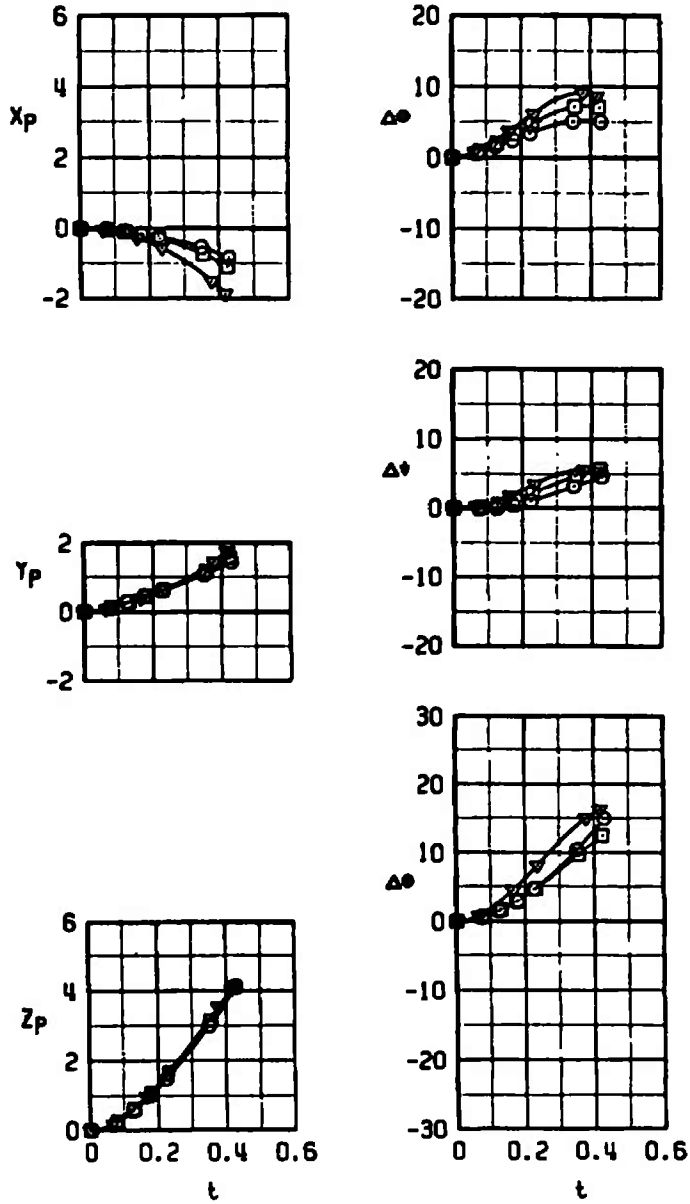
Figure 21. Trajectories for the MK-82LGB, Configuration 9.

SYMBOL	M _L	α	DIVE
○	0.78	2.2	70
○	0.78	2.2	70
□	0.86	2.1	70
△	0.95	2.0	70
▽	0.95	2.0	70



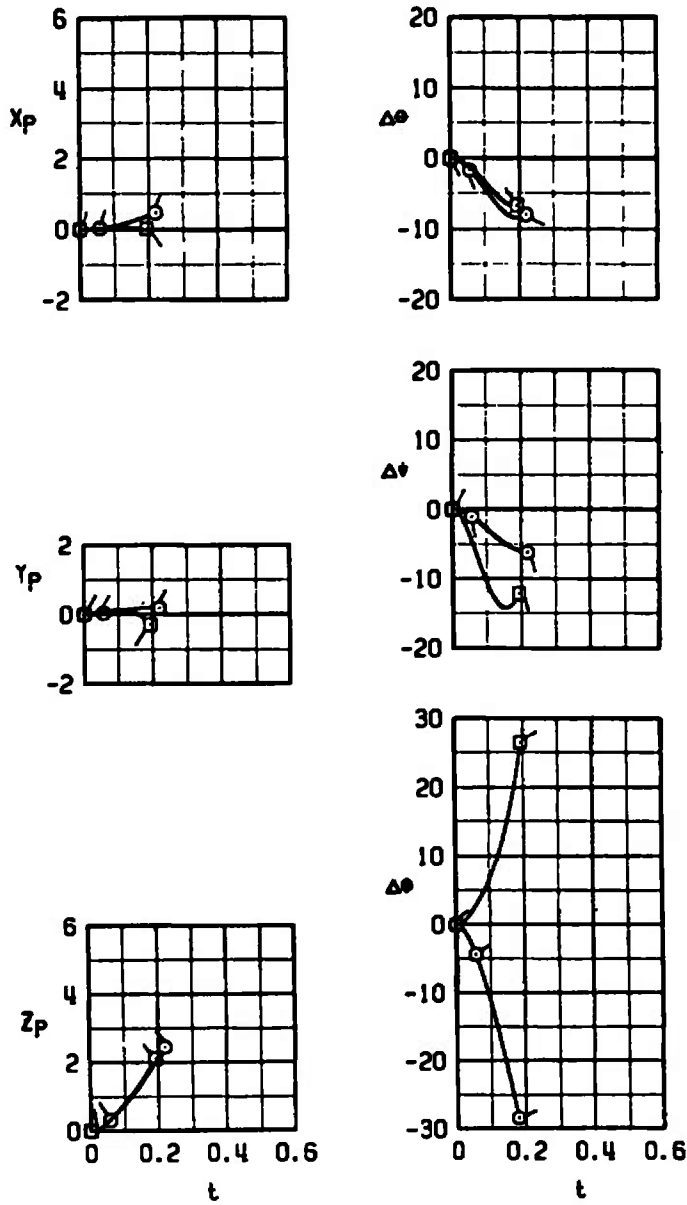
b. Configuration 9R, dive = 70 deg
Figure 21. Continued.

SYMBOL	M_∞	α	DIVE
○	0.78	3.4	0
□	0.86	3.0	0
▽	0.95	2.5	0



c. Configuration 9R, dive = 0
 Figure 21. Concluded.

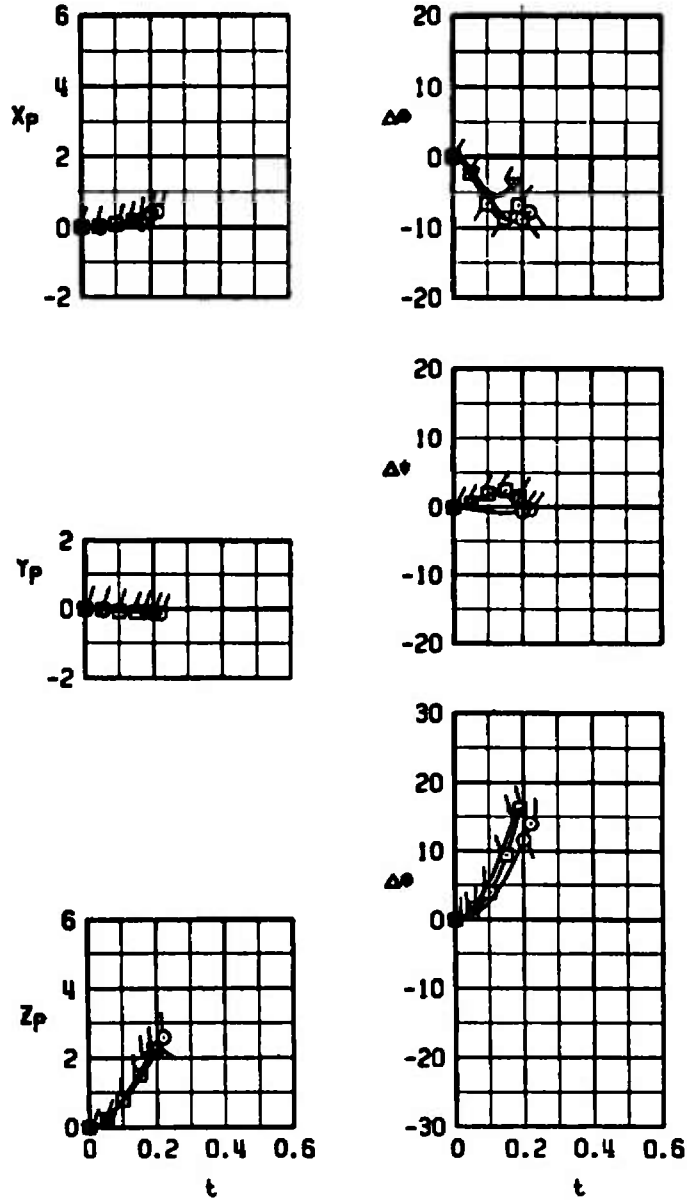
SYMBOL	M_L	α	DIVE
○	0.78	2.2	70
□	0.95	2.0	70



a. Configuration 4L, dive = 70 deg

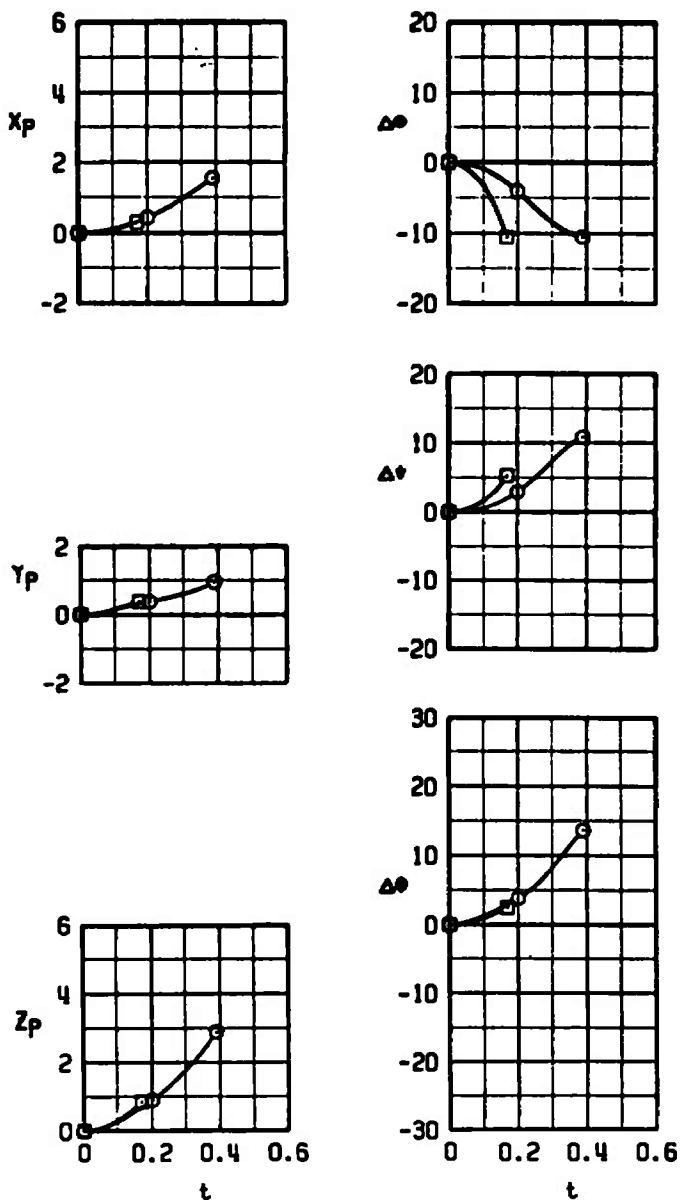
Figure 22. MK-82LGB launched with partially deployed fins, Configurations 4L and 5R.

SYMBOL	M_∞	α	DIVE
∇	0.78	2.2	70
\square	0.86	2.1	70
\circ	0.95	2.0	70



b. Configuration 5R, dive = 70 deg
Figure 22. Concluded.

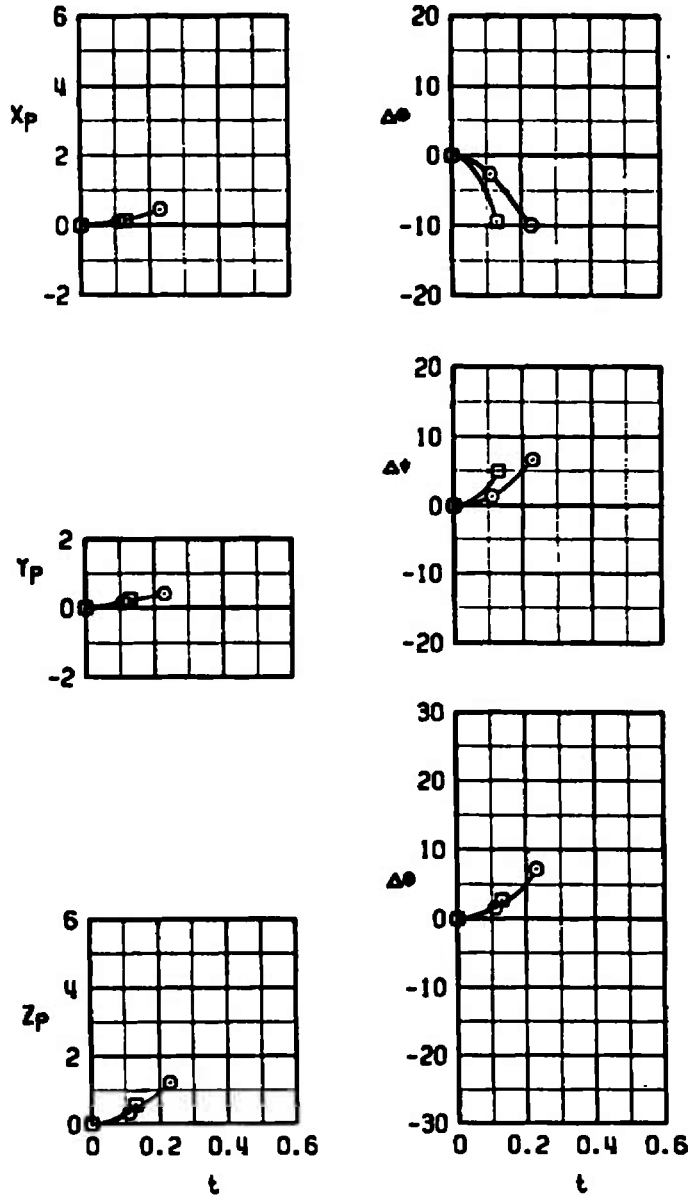
SYMBOL	M_∞	α	DIVE	CANARDS
○	0.78	2.2	70	OFF
□	0.78	2.2	70	ON



a. $M_\infty = 0.78$

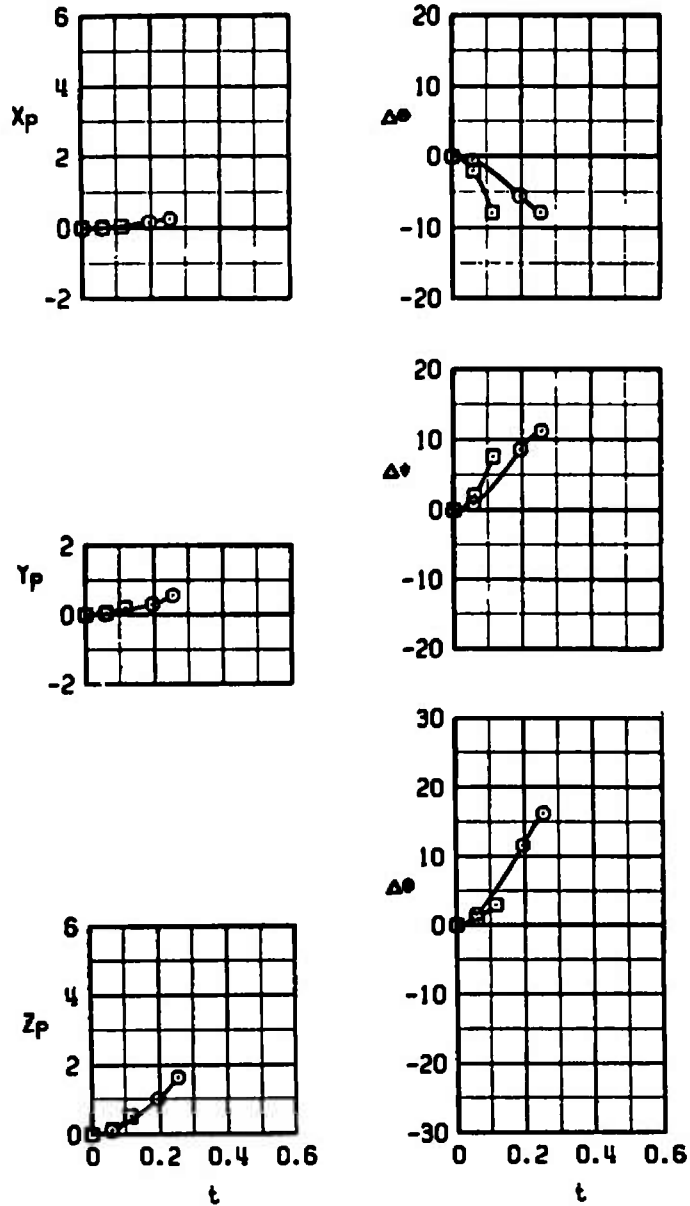
Figure 23. MK-82LGB launched with fixed canards, Configuration 6R.

SYMBOL	M_∞	α	DIVE	CANARDS
○	0.86	2.1	70	OFF
□	0.86	2.1	70	ON



b. $M_\infty = 0.86$
 Figure 23. Continued.

SYMBOL	M_∞	α	DIVE	CANARDS
○	0.95	2.0	70	OFF
□	0.95	2.0	70	ON



c. $M_\infty = 0.95$
 Figure 23. Concluded.

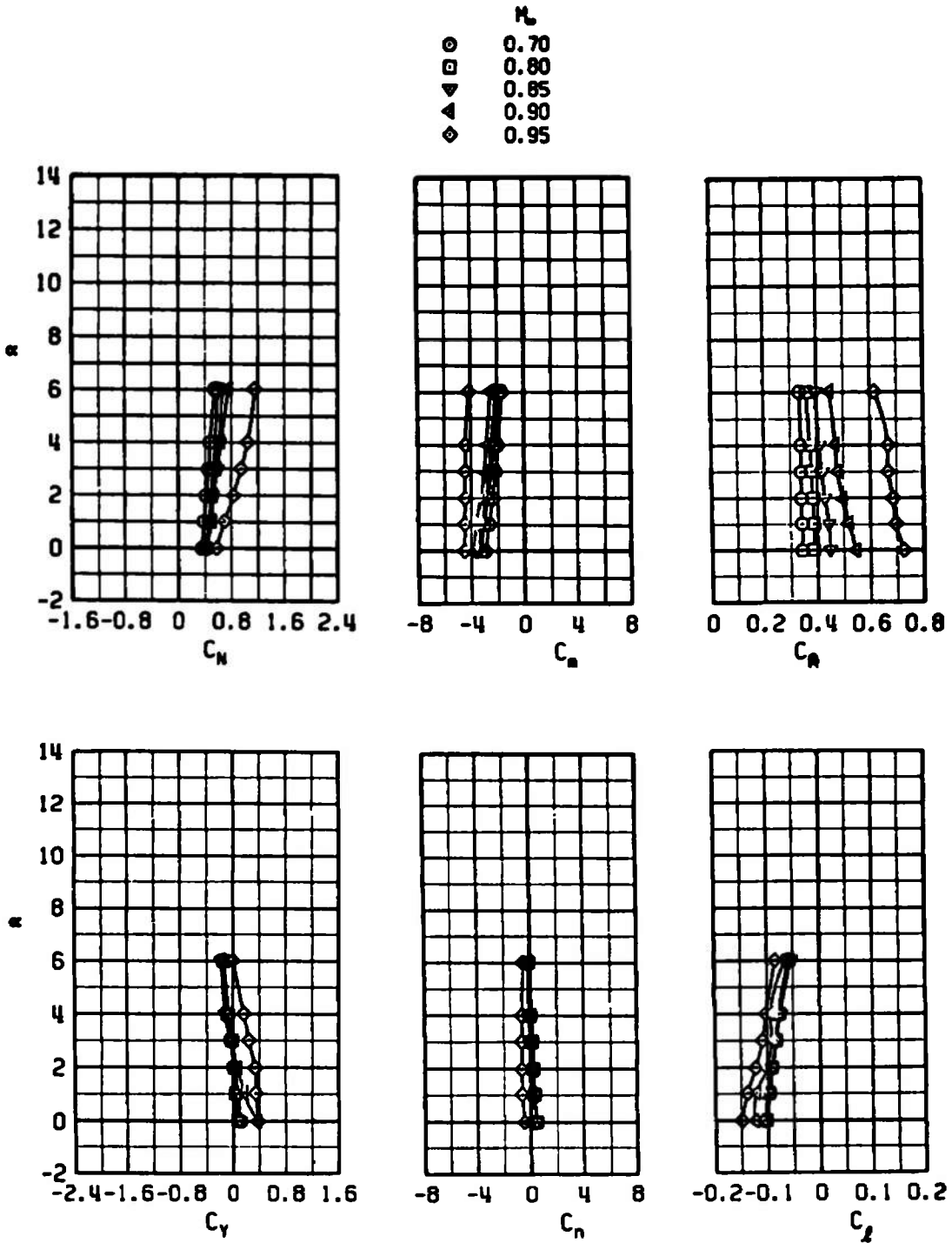
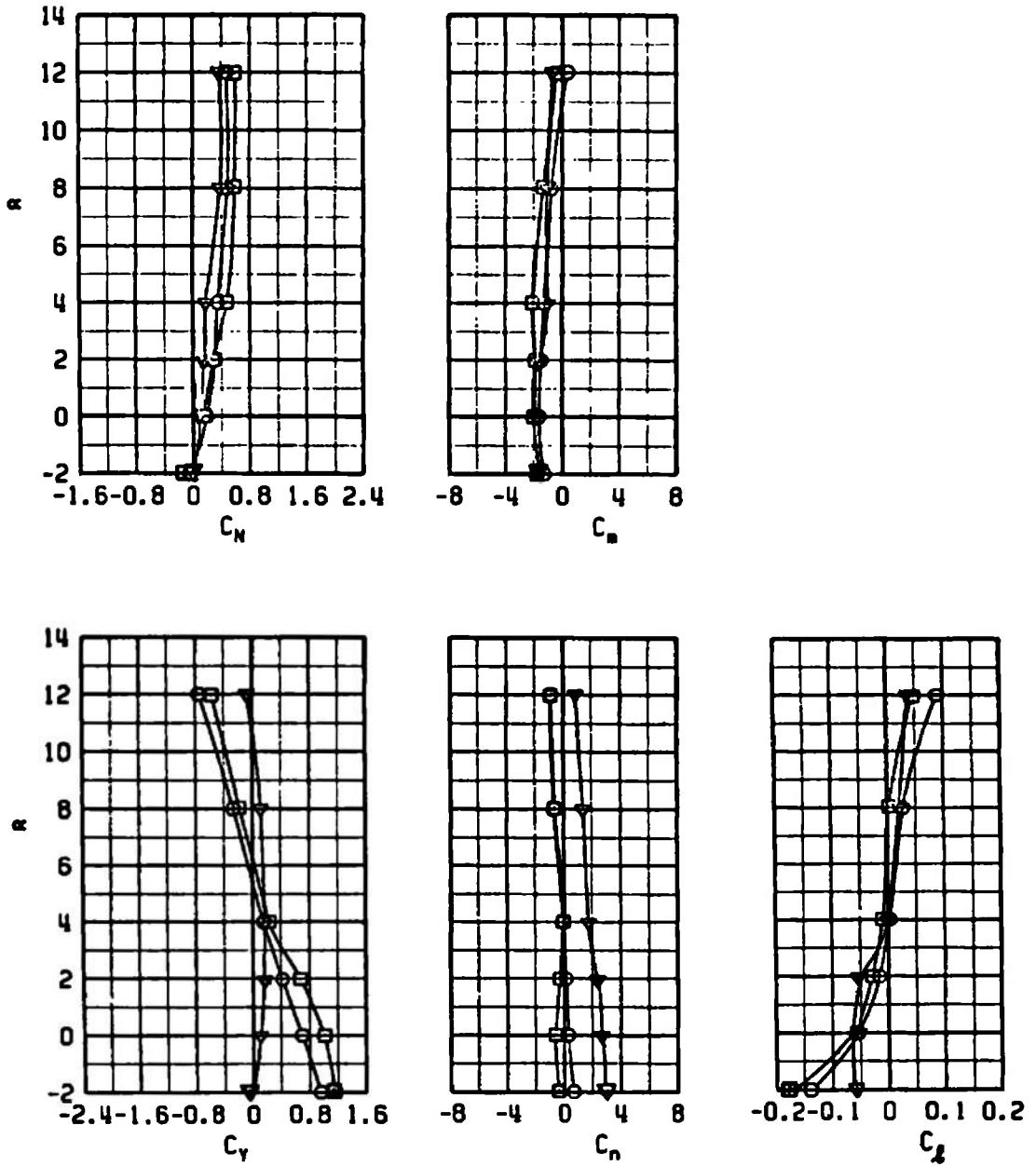


Figure 24. Carriage loads data for the MK-84EOGB, Configuration 1L.

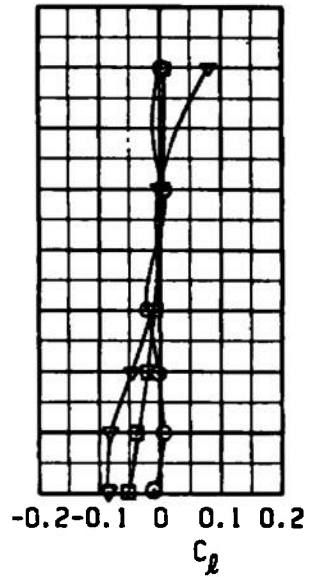
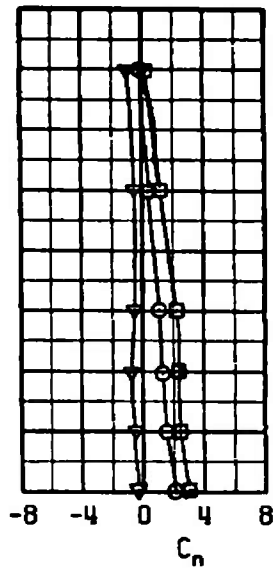
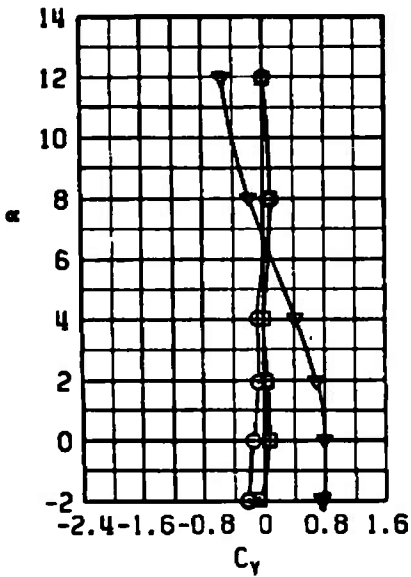
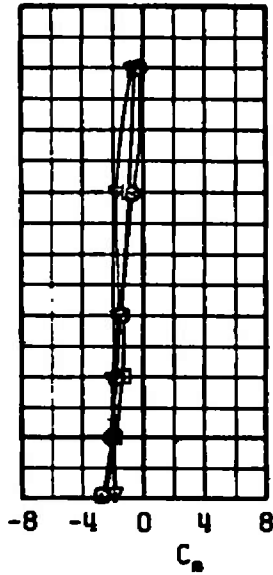
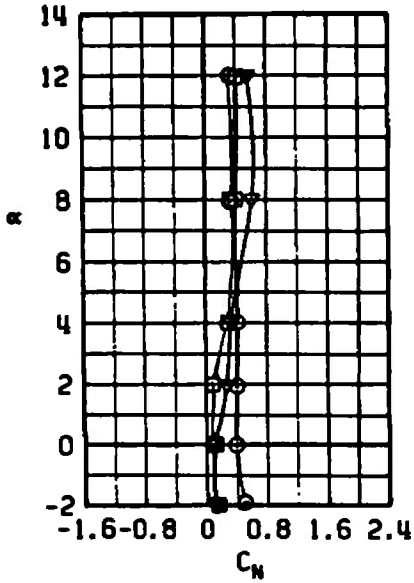
M_L
 ○ 0.70
 □ 0.90
 ▼ 1.05



a. Configuration 10L

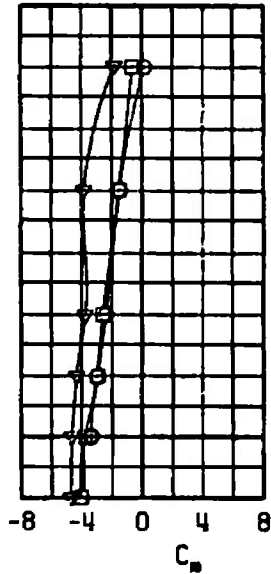
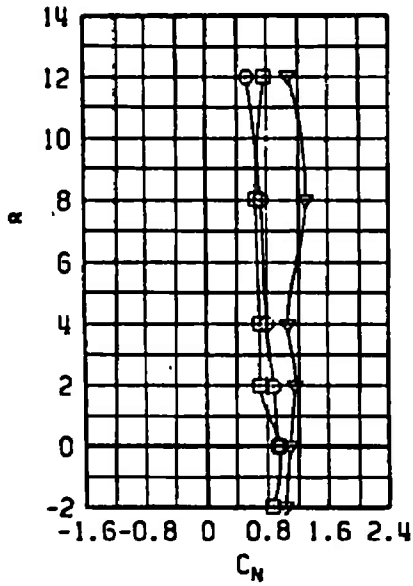
Figure 25. Carriage loads data for the MK-82LGB, Configuration 10.

M_∞
 ○ 0.70
 □ 0.90
 ▼ 1.05

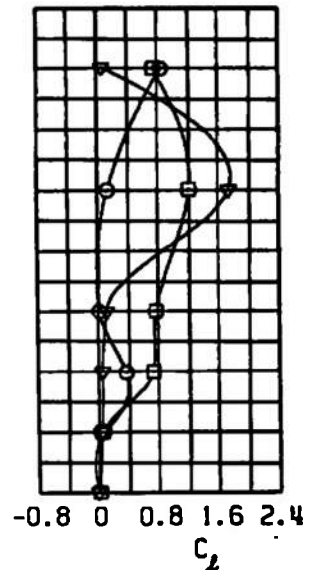
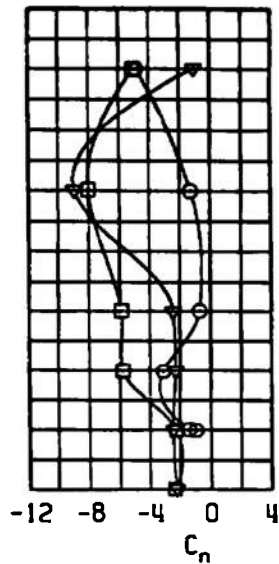
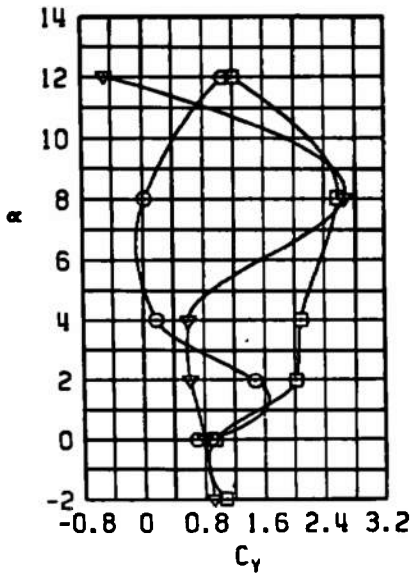


b. Configuration 10R
 Figure 25. Concluded.

M_∞
 ○ 0.70
 □ 0.90
 ▽ 1.05



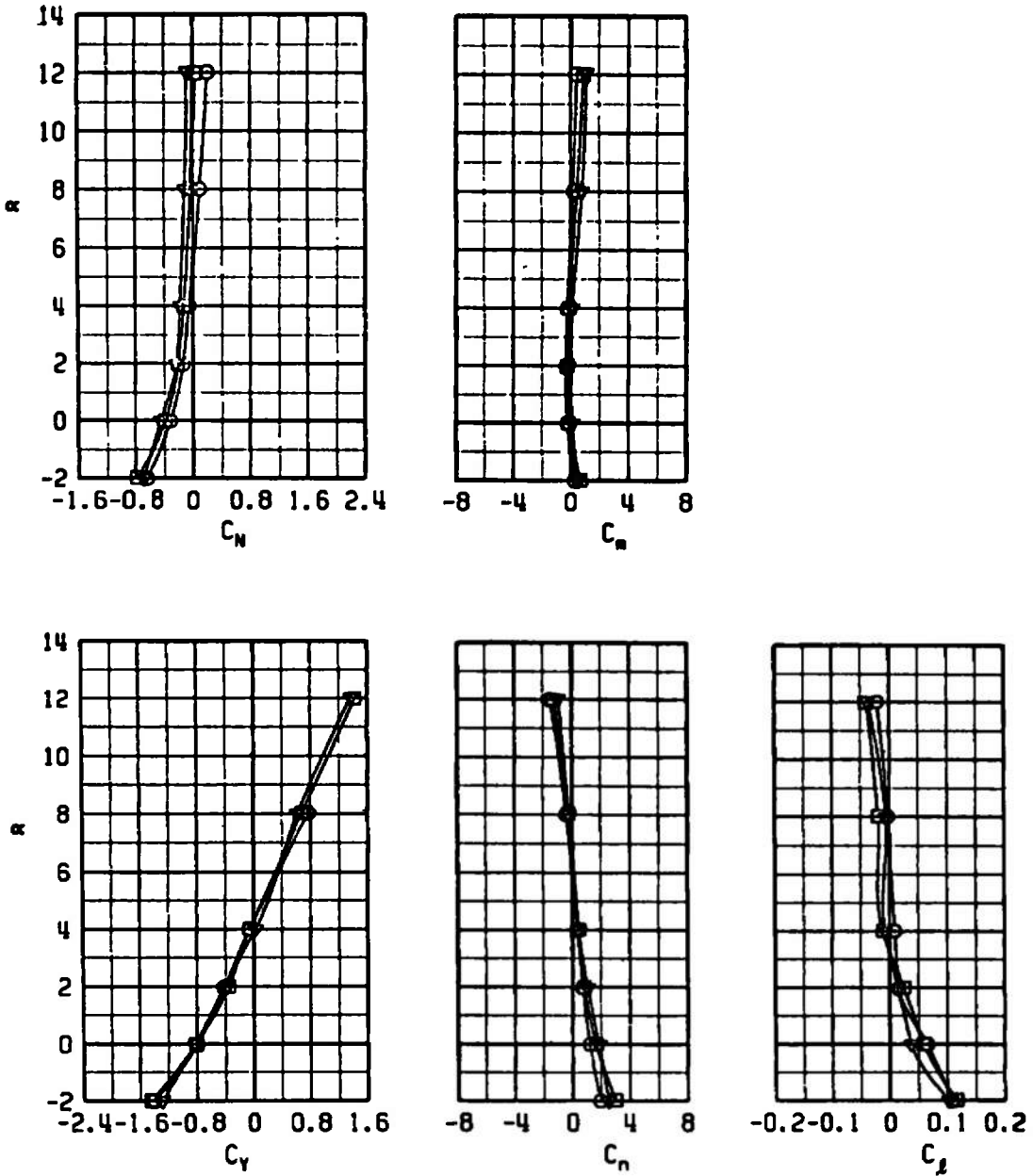
NOTE: Scale change on C_f vs Q plot for this figure only.



a. Configuration 11L

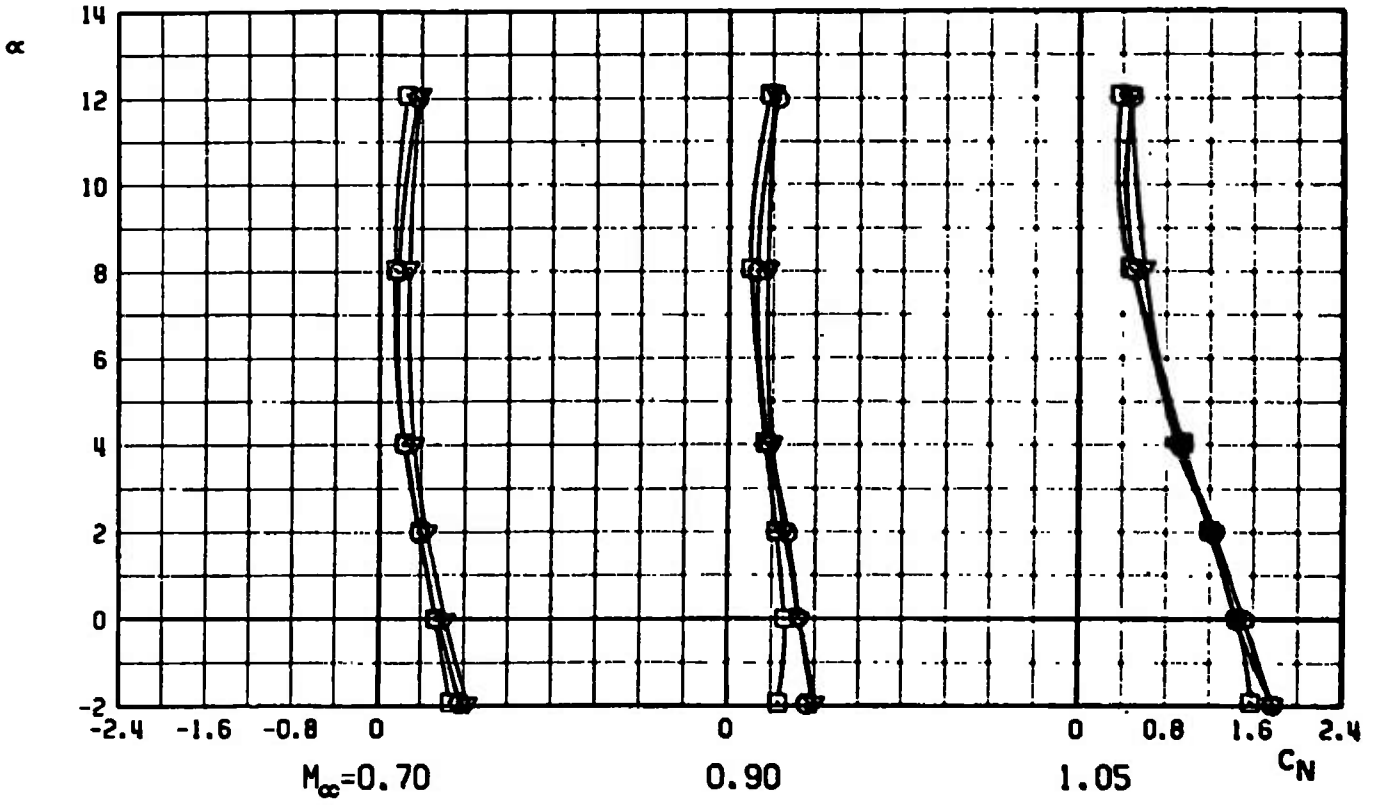
Figure 26. Carriage loads data for the MK-82LGB, Configuration 11:

M_∞
 ○ 0.70
 □ 0.90
 ▼ 1.05



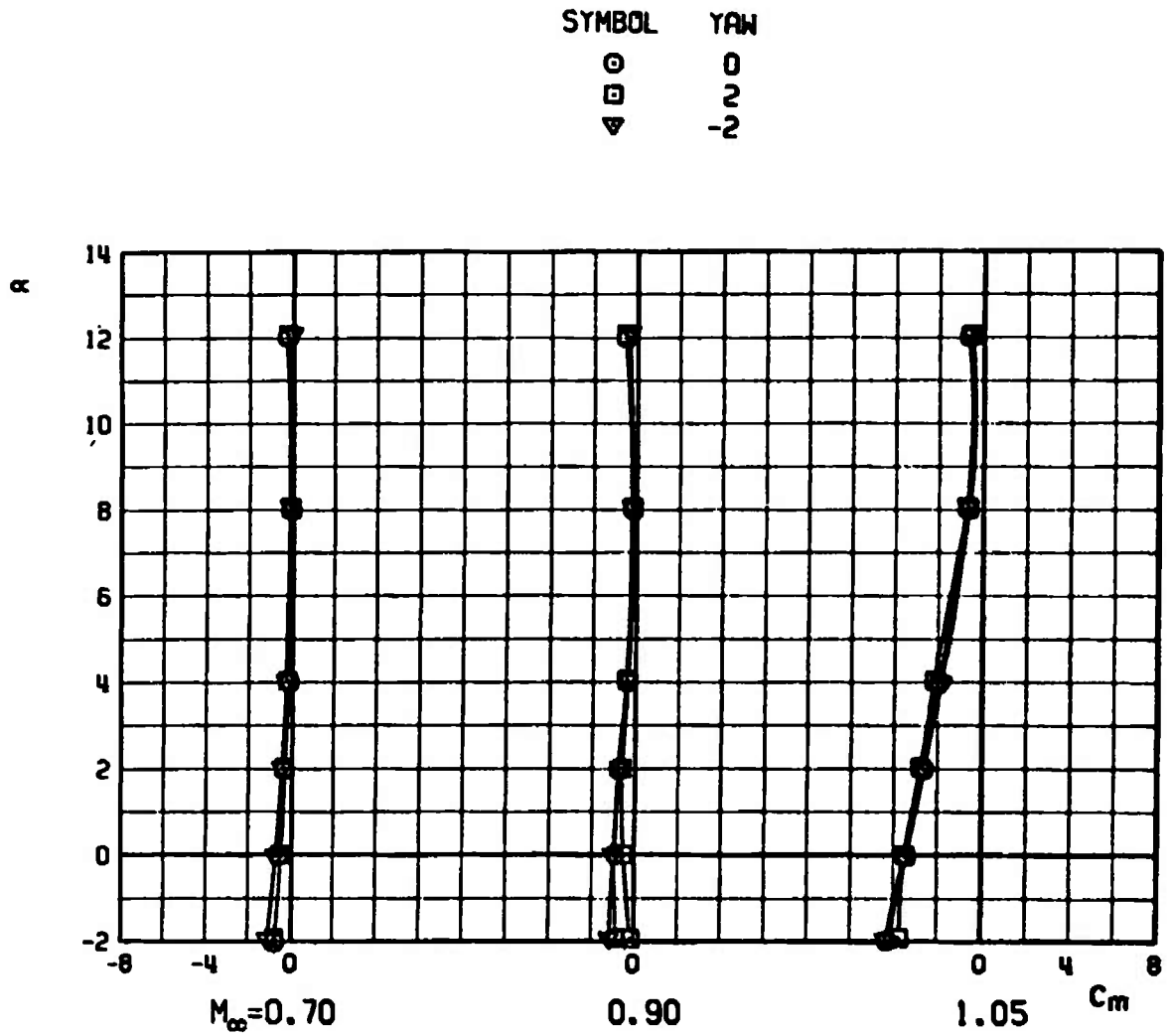
b. Configuration 11R
 Figure 26. Concluded.

SYMBOL	YAW
○	0
□	2
▽	-2



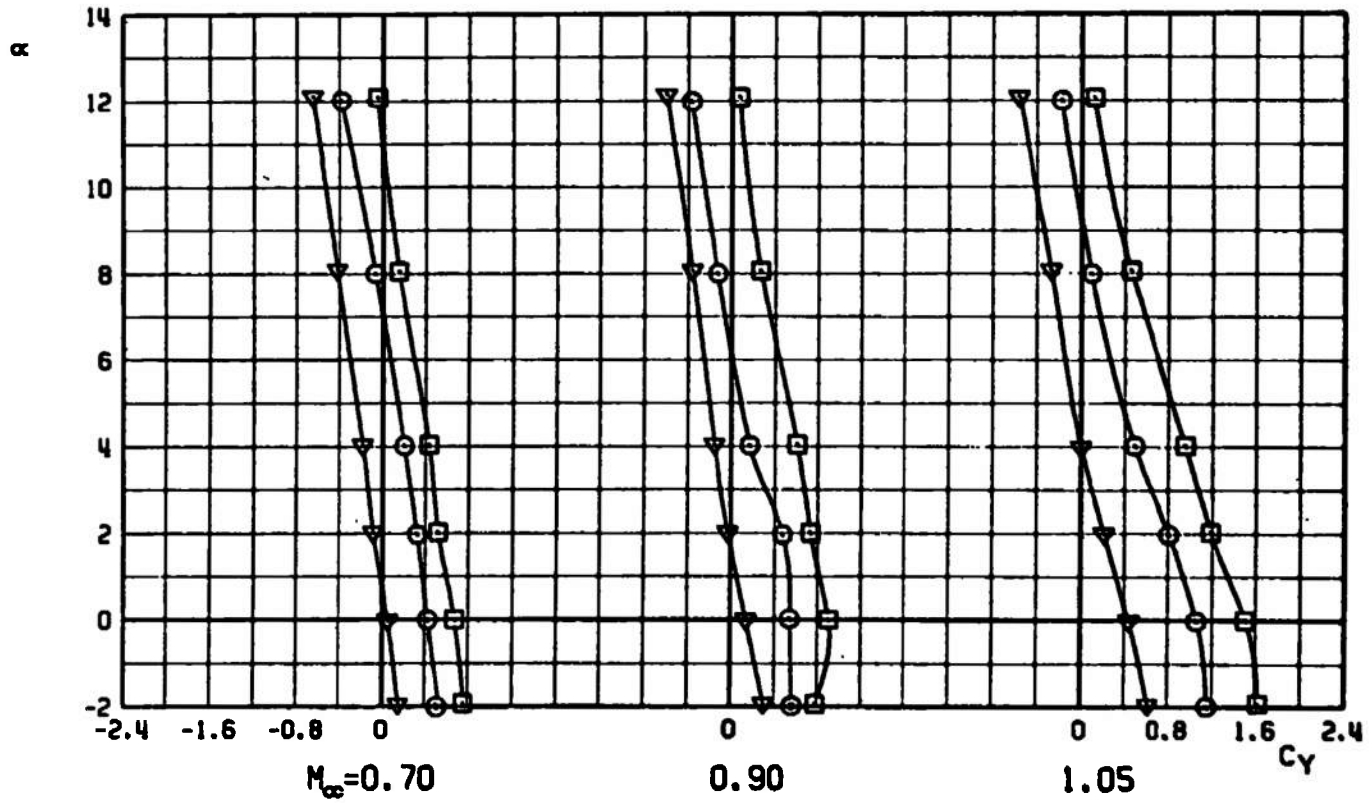
a. Configuration 12L, C_N versus α

Figure 27. Carriage loads data for the MK-82LGB, Configuration 12.



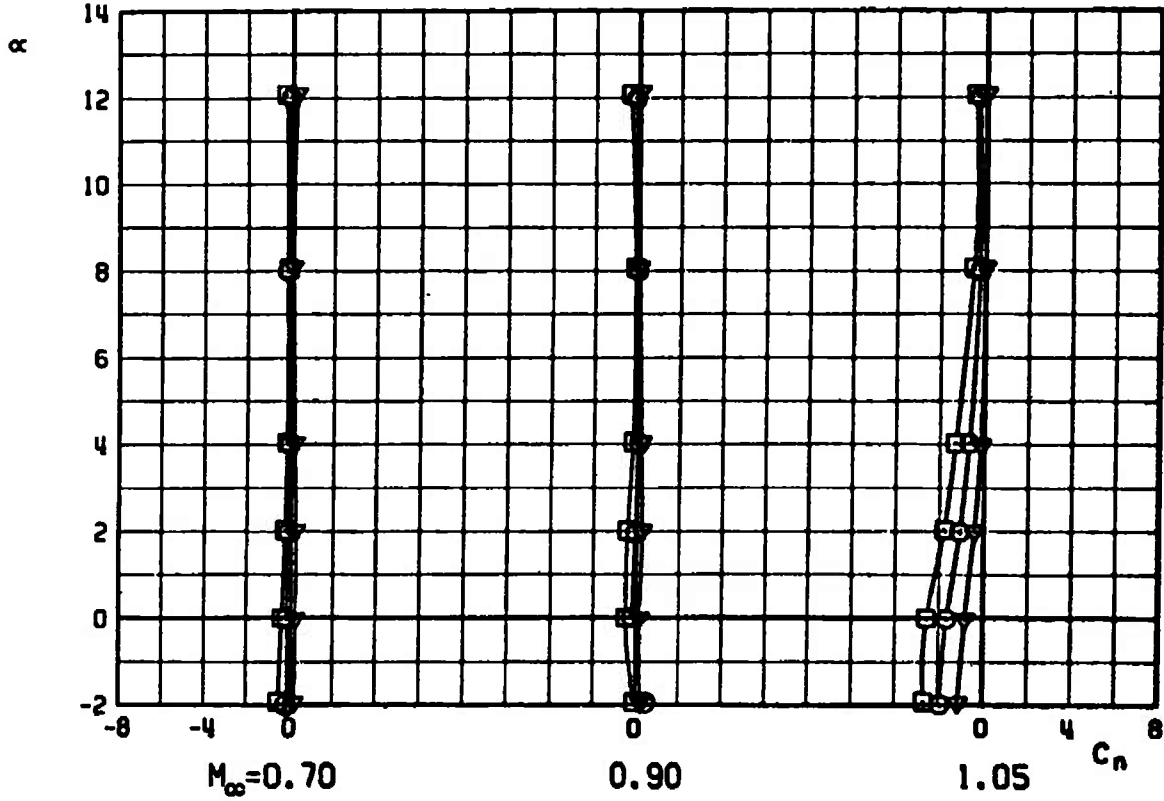
b. Configuration 12L, C_m versus α
 Figure 27. Continued.

SYMBOL	YAW
○	0
□	2
▽	4

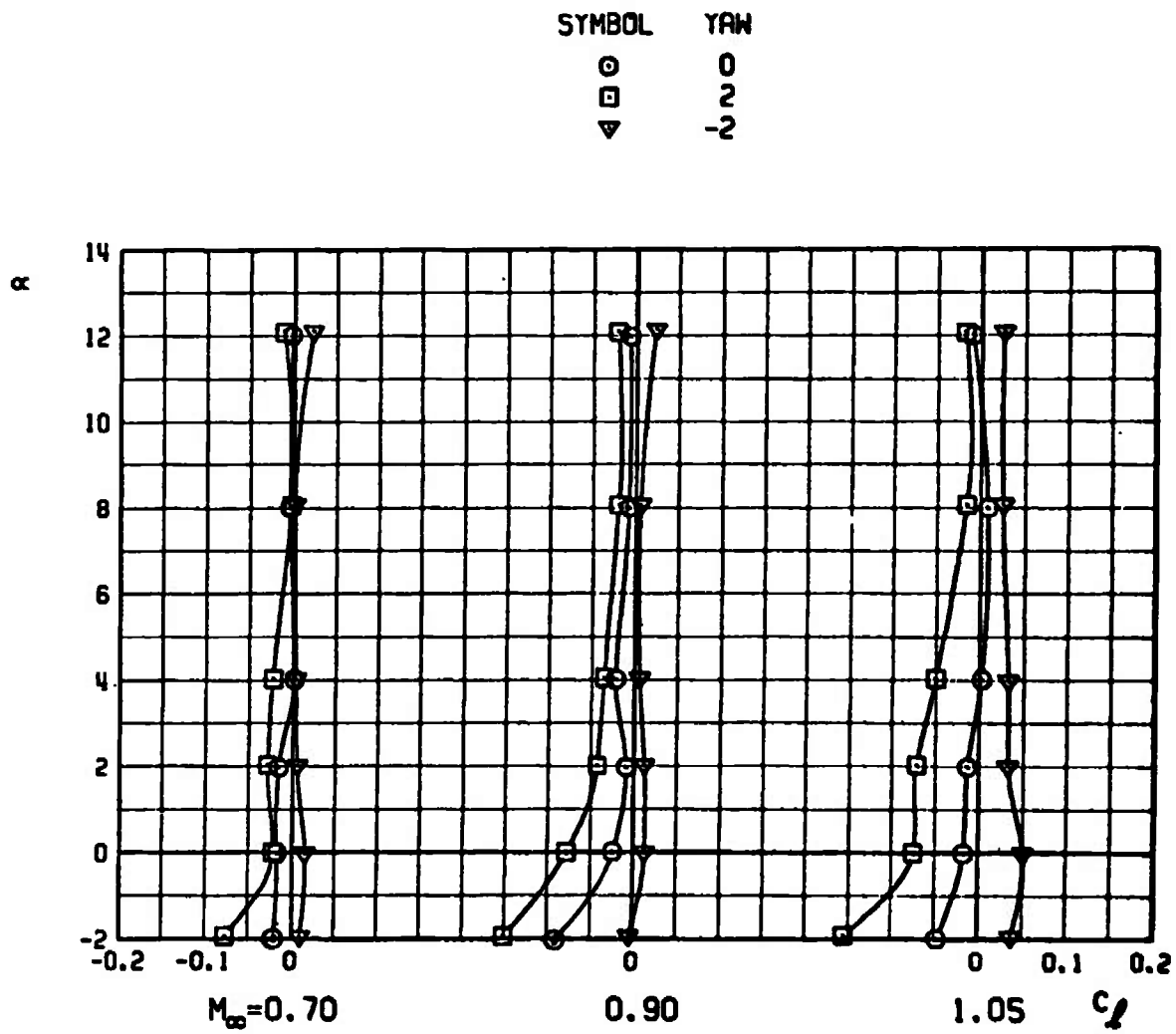


c. Configuration 12L, C_Y versus α
Figure 27. Continued.

SYMBOL	YAW
○	0
□	2
△	-2

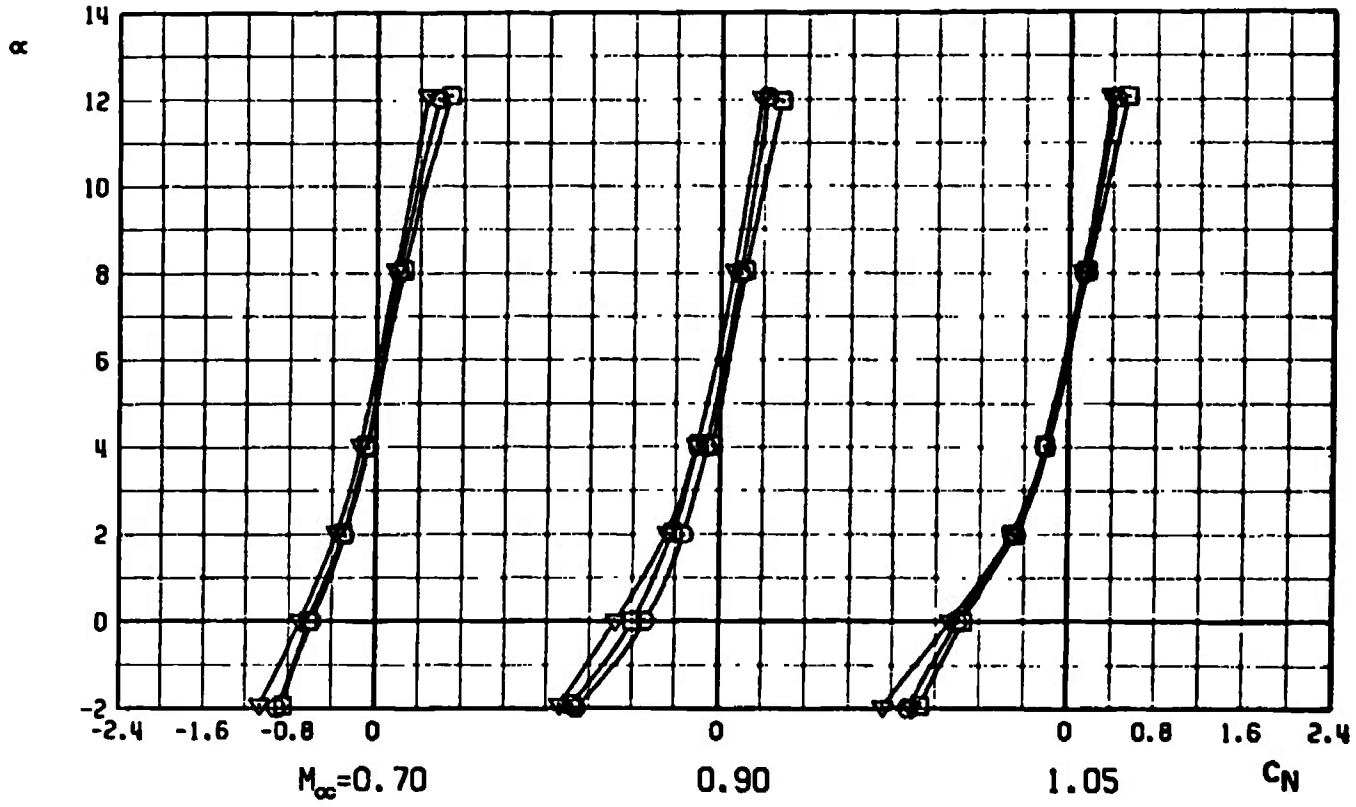


d. Configuration 12L, C_n versus α
 Figure 27. Continued.



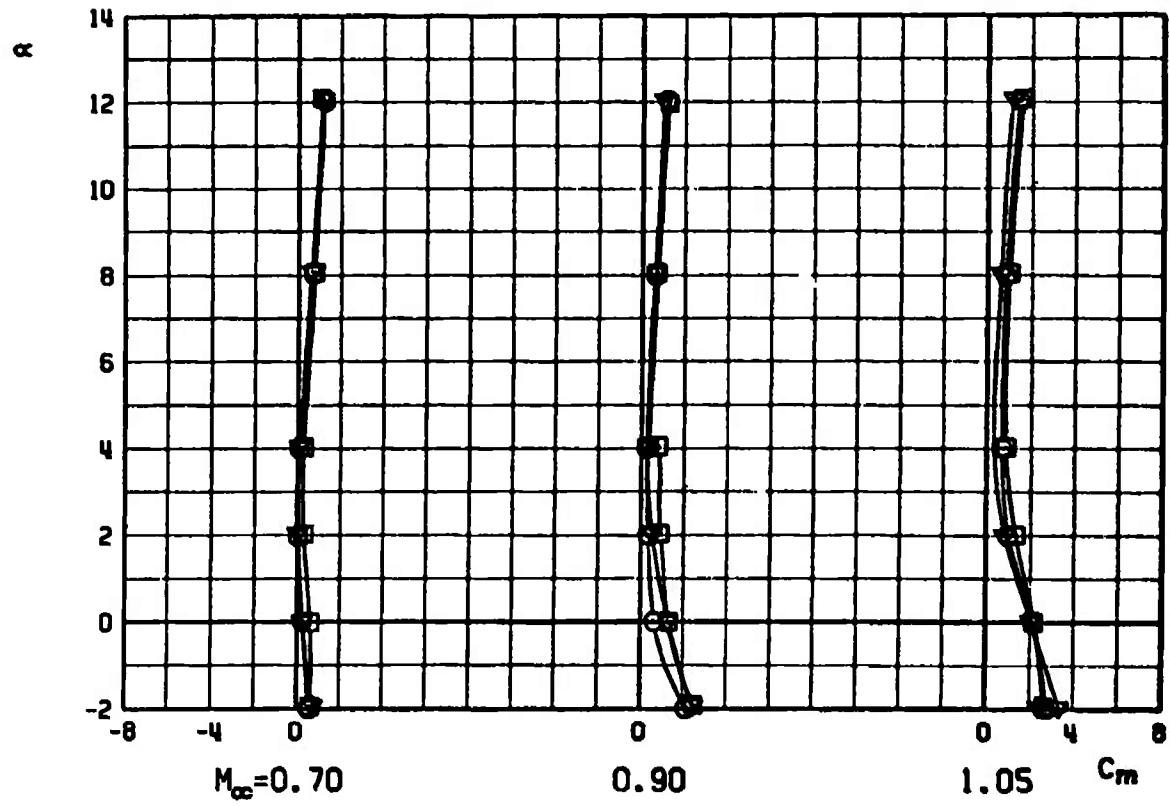
e. Configuration 12L, C_l versus α
Figure 27. Continued.

SYMBOL	YAW
○	0
□	2
△	-2



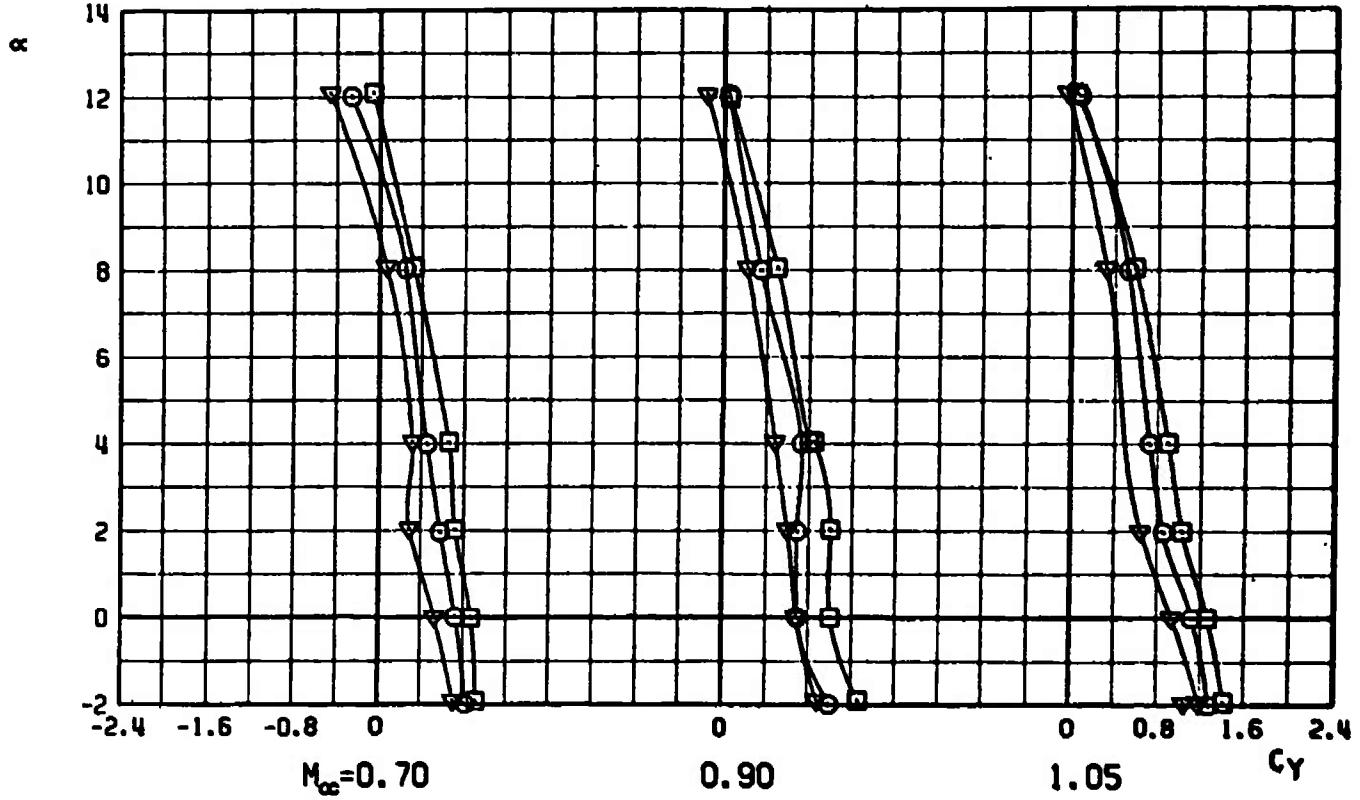
f. Configuration 12R, C_N versus α
Figure 27. Continued.

SYMBOL	YAW
○	0
□	2
▼	-2



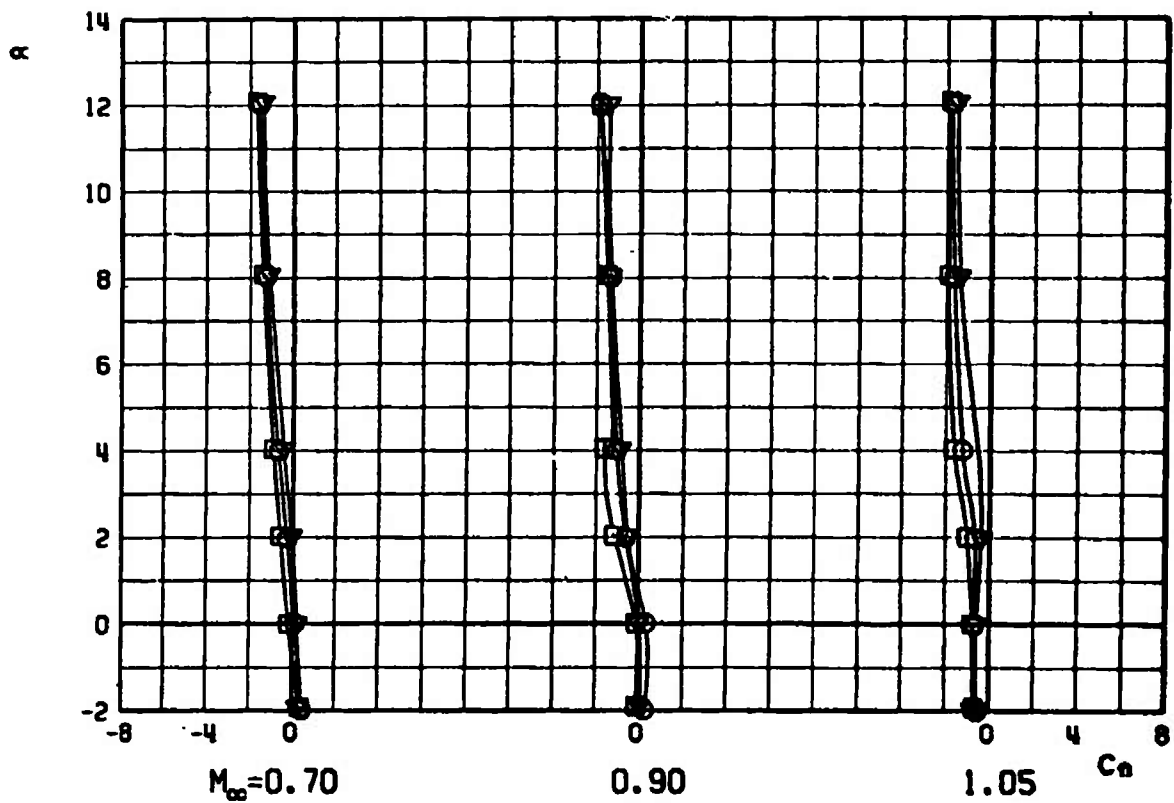
g. Configuration 12R, C_m versus α
Figure 27. Continued.

SYMBOL	YAW
○	0
□	2
△	2



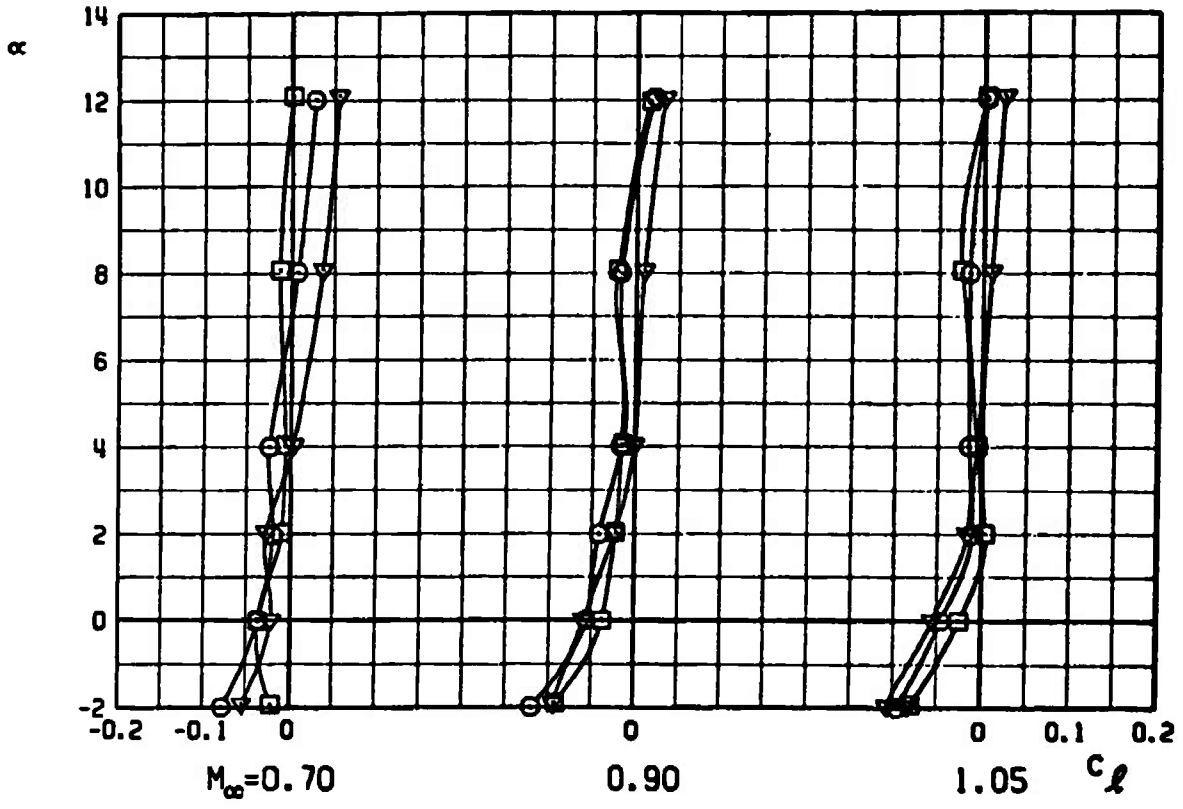
h. Configuration 12R, C_Y versus α
 Figure 27. Continued.

SYMBOL	YAW
○	0
□	2
△	-2



i. Configuration 12R, C_n versus α
Figure 27. Continued.

SYMBOL	YAW
○	0
□	2
△	-2



j. Configuration 12R, C_l versus α
 Figure 27. Concluded.

Table 1. Full-Scale Store Parameters Used in the Trajectory Calculations

Store Parameter	MK-84EOGB	MK-84LGB		MK-82LGB	
		Folded Fins	Deployed Fins	Folded Fins	Deployed Fins
X_{cg}	6.6083	8.1916	8.1916	6.425	6.425
S	1.766	1.766	1.766	0.629	0.629
b	1.500	1.500	1.500	0.895	0.895
\bar{m}	N/A	63.447	63.447	18.758	18.758
I_{xx}	↓	24	24	2	2
I_{yy}	↓	406	406	78	78
I_{zz}	↓	406	406	78	78
$C_{\ell p}$	↓	-0.71	-2.2	-1.50	-6.3
C_{mq}	↓	-100	-240	-185	-430
C_{nr}	↓	-100	-240	-185	-430
FZ_1 (MER/TER)	↓	---	N/A	1150	N/A
FZ_1 (MAU-12)	↓	2010	↓	2100	↓
FZ_2 (MAU-12)	↓	1700	↓	1390	↓
X_L (MER/TER)	↓	---	↓	-0.317	↓
X_{L1} (MAU-12)	↓	0.592	↓	0.692	↓
X_{L2} (MAU-12)	↓	-1.075	↓	-0.975	↓

Table 2. Axial-Force Coefficient Values for the MK-82LGB Trajectories

M_∞	C_A
0.73	0.370
0.77	0.375
0.78	0.376
0.80	0.380
0.81	0.387
0.85	0.406
0.86	0.410
0.88	0.423
0.90	0.440
0.93	0.505
0.94	0.550
0.95	0.600

Table 3. Full-Scale Position and Coefficient Uncertainties

Maximum Full-Scale Position Uncertainties								
Store	M_∞	t, sec	ΔX_p , ft	ΔY_p , ft	ΔZ_p , ft	$\Delta \theta$, deg	$\Delta \psi$, deg	$\Delta \phi$, deg
MK-84LGB	0.78	0.4	± 0.02	± 0.01	± 0.02	± 0.3	± 0.2	± 0.7
↓	0.86	↓	± 0.03	± 0.01	± 0.02	± 0.3	± 0.2	± 0.9
↓	0.95	↓	± 0.03	± 0.01	± 0.02	± 0.4	± 0.2	± 1.1
MK-82LGB	0.78	0.4	---	± 0.03	± 0.05	± 0.5	± 0.4	± 19.1
↓	0.86	↓	---	± 0.03	± 0.07	± 0.6	± 0.5	± 23.3
↓	0.94	↓	---	± 0.04	± 0.08	± 0.7	± 0.14	± 28.4

Aerodynamic Coefficient Uncertainties (Carriage Loads)							
Store	M_∞	ΔC_N	ΔC_Y	ΔC_A	ΔC_l	ΔC_m	ΔC_n
MK-84EOGB	0.70	± 0.011	± 0.005	± 0.014	± 0.002	± 0.024	± 0.009
↓	0.80	± 0.011	± 0.006	± 0.014	± 0.002	± 0.027	± 0.009
↓	0.95	± 0.011	± 0.006	± 0.015	± 0.002	± 0.026	± 0.009
MK-82LGB	0.70	± 0.030	± 0.016	---	± 0.023	± 0.042	± 0.025
↓	0.90	± 0.030	± 0.016	---	± 0.022	± 0.041	± 0.025
↓	1.05	± 0.029	± 0.016	---	± 0.023	± 0.041	± 0.025

Table 4. Repeatability of Loads Data for Configuration 11L

$M_{\infty} = 0.70$						
α	C_Y		C_n		C_l	
-2.01	9.6680-01	7.5500-01	-1.1700+00	-9.6160-01	5.8820-03	-5.7240-03
0.01	6.9510-01	6.0430-01	-9.8390-01	-9.9580-01	1.7300-02	6.6230-03
0.03	8.8390-01	5.8450-01	-1.4600+00	-1.0140+00	6.5670-02	1.6210-02
1.97	1.4820+00	4.8660-01	-3.1270+00	-1.2210+00	3.6450-01	7.4280-02
4.02	1.6450-01	2.8510-01	-7.2340-01	-1.1880+00	1.7820-02	4.8490-02
8.02	1.9310-02	1.0350-01	-1.2930+00	-1.4410+00	1.2960-01	7.9690-02
12.00	1.0630+00	6.2820-01	-4.8860+00	-3.3740+00	8.4610-01	5.5800-01
$M_{\infty} = 0.90$						
-1.99	1.0700+00	1.0350+00	-2.3690+00	-2.4130+00	7.4190-03	1.0390-02
0.01	9.3340-01	8.3270-01	-2.2930+00	-2.2250+00	-4.5630-02	2.5370-02
1.99	2.0210+00	1.9800+00	-5.8020+00	-4.9710+00	7.3070-01	4.5770-01
4.01	2.0900+00	5.0560-01	-5.8900+00	-2.0630+00	7.6860-01	8.7690-02
8.05	2.5840+00	1.7150+00	-8.0690+00	-5.8740+00	1.2120+00	8.3500-01
12.01	1.2020+00	8.4270-01	-5.0490+00	-4.3110+00	7.4120-01	4.0330-01
$M_{\infty} = 1.05$						
-1.99	9.0840-01	9.6940-01	-2.2470+00	-2.3840+00	-1.4640-02	5.4740-03
0.01	7.9340-01	7.7620-01	-2.4860+00	-2.4970+00	4.2180-02	4.1380-02
2.00	6.1040-01	1.0590+00	-2.3200+00	-3.3700+00	5.0230-02	2.1440-01
4.00	5.8760-01	1.9040-01	-2.4490+00	-1.8760+00	1.0600-01	4.5720-02
8.03	2.6680+00	6.6690-01	-8.9630+00	-3.6190+00	1.7370+00	4.5440-01
12.04	-5.0060-01	8.2430-01	-1.0180+00	-4.5280+00	6.1340-02	7.8290-01

75

NOMENCLATURE

BL	Aircraft buttock line from plane of symmetry, in., model scale
b	Store reference dimension, ft, full scale
C _A	Store axial-force coefficient, axial force/q _∞ S
C _ℓ	Store rolling-moment coefficient, rolling moment/q _∞ Sb
C _{ℓ_p}	Store roll-damping derivative, dC _ℓ /d(pb/2V _∞)
C _m	Store pitching-moment coefficient, referenced to the store cg, pitching moment/q _∞ Sb
C _{m_q}	Store pitch-damping derivative, dC _m /d(qb/2V _∞)
C _N	Store normal-force coefficient, normal force/q _∞ S
C _n	Store yawing-moment coefficient, referenced to the store cg, yawing moment/q _∞ Sb
C _{n_r}	Store yaw-damping derivative, dC _n /d(rb/2V _∞)
C _Y	Store side-force coefficient, side force/q _∞ S
FS	Aircraft fuselage station, in., model scale
F _Z	MER/TER ejector force, lb
F _{Z₁}	Pylon forward ejector force, lb
F _{Z₂}	Pylon aft ejector force, lb
H	Pressure altitude, ft
I _{xx}	Full-scale moment of inertia about the store X _B axis, slug-ft ²
I _{xz}	Full-scale product of inertia, X _B -Z _B axis, slug-ft ²

I_{yy}	Full-scale moment of inertia about the store Y_B axis, slug-ft ²
I_{zz}	Full-scale moment of inertia about the store Z_B axis, slug-ft ²
M_∞	Free-stream Mach number
\bar{m}	Full-scale store mass, slugs
p	Store angular velocity about the X_B axis, radians/sec
q	Store angular velocity about the Y_B axis, radians/sec
q_∞	Free-stream dynamic pressure, psf
r	Store angular velocity about the Z_B axis, radians/sec
S	Store reference area, ft ² , full scale
t	Real trajectory time from initiation of trajectory, sec
V_∞	Free-stream velocity, ft/sec
WL	Aircraft waterline from reference horizontal plane, in., model scale
X_{cg}	Full-scale cg location, ft, from nose of store
X_L	Ejector piston location relative to the store cg, positive forward of store cg, ft, full scale
X_{L1}	Forward ejector piston location relative to the store cg, positive forward of store cg, ft, full scale
X_{L2}	Aft ejector piston location relative to the store cg, positive forward of store cg, ft, full scale
X_P	Separation distance of the store cg parallel to the pylon axis system X_P direction, ft, full scale measured from the prelaunch position
Y_P	Separation distance of the store cg parallel to the pylon axis system Y_P direction, ft, full scale measured from the prelaunch position

Z_P	Separation distance of the store cg parallel to the flight axis system Z_P direction, ft, full scale measured from the prelaunch position
ZE	Ejector stroke length, ft, full scale
α	Parent-aircraft model angle of attack relative to the free-stream velocity vector, deg
$\Delta\theta$	Angle between the store longitudinal axis and its projection in the X_P - Y_P plane, positive when store nose is raised as seen by the pilot, <u>deg</u>
$\Delta\psi$	Angle between the projection of the store longitudinal axis in the X_P - Y_P plane and the X_P axis, positive when the store nose is to the right as seen by the pilot, deg
$\Delta\phi$	Change in roll angle from the vertical ϕ at launch, deg
ϕ	Angle between the projection of the store lateral axis in the Y_P - Z_P plane and the Y_P axis, positive for clockwise rotation when looking upstream, deg

FLIGHT AXIS SYSTEM COORDINATES

Directions

X_F	Parallel to the free-stream wind vector, positive direction is forward as seen by the pilot
Y_F	Perpendicular to the X_F and Z_F directions, positive direction is to the right as seen by the pilot
Z_F	In the aircraft plane of symmetry, perpendicular to the free-stream wind vector, positive direction is downward

The flight axis system origin is coincident with the aircraft cg and remains fixed with respect to the parent aircraft during store separation. The X_F , Y_F , and Z_F coordinate axes do not rotate with respect to the initial flight direction and attitude.

STORE BODY AXIS SYSTEM COORDINATES

Directions

- X_B Parallel to the store longitudinal axis, positive direction is upstream in the prelaunch position
- Y_B Perpendicular to the store longitudinal axis, and parallel to the flight axis system X_F - Y_F plane when the store is at zero roll angle, positive direction is to the right looking upstream when the store is at zero yaw and roll angles
- Z_B Perpendicular to both the X_B and Y_B axes, positive direction is downward as seen by the pilot when the store is at zero pitch and roll angles

The store body axis system origin is coincident with the store cg and moves with the store during separation from the parent airplane. The X_B , Y_B , and Z_B coordinate axes rotate with the store in pitch, yaw, and roll so that mass moments of inertia about the three axes are not time-varying quantities

PYLON AXIS SYSTEM COORDINATES

Directions

- X_P Parallel to the store longitudinal axis in the prelaunch carriage position, positive direction is forward as seen by the pilot
- Y_P Perpendicular to the X_P axis and parallel to the flight axis system X_F - Y_F plane, positive direction is to the right as seen by the pilot
- Z_P Perpendicular to both the X_P and Y_P axes, positive direction is downward

The pylon axis system origin is coincident with the store cg in the prelaunch carriage position. The axes are rotated with respect to the flight axis system by the prelaunch yaw and pitch angles of the store. Both the origin and the direction of the coordinate axes remain fixed with respect to the flight axis system throughout the trajectory.